

The
University
Of
Sheffield.

**Design and Control of Lower Limb Assistive
Exoskeleton for Hemiplegia Mobility**

by

Abdullah Khaled Alshatti

A thesis submitted to the University of Sheffield
for the degree of Doctor of Philosophy

Department of Automatic Control and Systems Engineering
The University of Sheffield
Mappin Street,
Sheffield, S1 3JD
United Kingdom

August 2019

Abstract

Mobility is one of the most vital abilities for human being that enables her/him to preserve independence while performing physical daily life activities. Currently, exoskeletons are considered as significant addition to the assistive technology, in which interest has been intensified in the last decade. There are many challenges related to assistive robotics developments such as safety, efficient power source, lightweight design and affordability.

This research aims to develop assistive exoskeleton system to support hemiplegic patient mobility. The developments involve designing humanoid and exoskeleton models in MSC. VisualNastran and implementing a control strategy in MATLAB Simulink to control the active joint trajectories of the humanoid lower limbs and exoskeleton models according to predefined joint angle position for walking, standing up and sitting down motions.

Two types of control methods are considered in this research to control the humanoid and exoskeleton models while simulating the assistance mechanism for the designated mobility task. The control methods are Proportional Integral Derivative (PID) and fuzzy-based Proportional Derivative (PD) controllers. Moreover, Spiral Dynamic Algorithm (SDA) optimisation approach is used to tune the controller's parameters. Evaluation of the developed controllers is based on a comparative assessment of the obtained simulation results and examining the dynamics of the models. The controller with optimum performance is verified by subjecting the humanoid and exoskeleton models to disturbance forces, constant loads and different speeds of motion cycles. It is demonstrated that the objectives of this research are fulfilled, and the exoskeleton is capable to provide the humanoid with the necessary assistance under different conditions.

Acknowledgments

All thanks and praises be for Allah s.w.t, for allowing me to achieve this goal, and awarded me health and strength during the course of this research.

My appreciation to my supervisor Professor M. O. Tokhi for his priceless support. It would have been difficult for me to complete this work without his motivation, time, efforts and helpful guidance throughout this research.

A special thanks to my research colleagues for their continuous help and support especially those in room 307.

Thanks to my employee ministry of defence, the government of Kuwait for sponsoring my PhD study and gave me the opportunity to be here.

My outmost appreciation to my parents, wife, sons and family for their sacrifices and moral encouragement.

Table of Contents

Abstract	i
Acknowledgments	ii
Table of Contents	iii
List of figures	vi
List of tables	ix
Abbreviations	x
Chapter 1: Introduction	1
1.1 Background and motivation	1
1.2 Hemiplegia	2
1.3 Lower limb joints	5
1.3.1 Hip.....	5
1.3.2 Knee	6
1.3.3 Ankle	7
1.4 Aim and Objectives of the research	7
1.5 Contributions	9
1.6 Thesis outline	10
Chapter 2: Exoskeleton systems	12
2.1 Exoskeletons and wearable robots	12
2.1.1 Lower extremity exoskeleton and human biomechanics	14
2.2 Exoskeleton design considerations.....	17
2.2.1 Exoskeleton frame and material.....	17
2.2.2 Actuators	18
2.2.3 Sensors	19
2.2.4 Power supply	21
2.2.5 Control strategy	22
2.3 Lower limb exoskeleton	26

2.4 Summary	31
Chapter 3: Modelling of humanoid and single leg exoskeleton	32
3.1 Introduction	32
3.2 SOLIDWORKS.....	33
3.3 MSC. visualNastran 4D (MSC.vN4D).....	33
3.4 Model Design	36
3.4.1 Humanoid	36
3.4.2 Exoskeleton	39
3.4.3 Models integration in MSC.vN4D and MATLAB Simulink.....	43
3.4.4 Humanoid and exoskeleton models validation.....	45
3.5 Summary	47
Chapter 4: Control strategy of the humanoid and single leg exoskeleton.....	48
4.1 Introduction	48
4.2 Control strategy	48
4.2.1 PID controller.....	50
4.2.2 Fuzzy logic control.....	53
4.2.3 Proportional-Derivative based Fuzzy control	60
4.2.4 Spiral dynamic optimisation algorithm	61
4.3 Summary	66
Chapter 5: Control of assistive single leg exoskeleton and humanoid for walking mobility.....	67
5.1 Introduction	67
5.2 Cycle of human gait	67
5.3 Implementation of closed-loop PID control.....	71
5.3.1 Humanoid model control.....	72
5.3.2 Control of humanoid and exoskeleton with SDA tuned PID parameters	78
5.4 Implementation of fuzzy-based PD controller	85
5.4.1 SDA optimisation of PD-fuzzy scaling parameters	88
5.4.2 Simulation with different gait speeds.....	94

5.4.3 Simulation with disturbance forces	97
5.5 Summary	100
Chapter 6: Control of single leg exoskeleton and humanoid for standing up and sitting down movements.....	102
6.1 Introduction	102
6.2 Standing up and sitting down motion cycles.....	103
6.3 Closed-loop PID control implementation	105
6.3.1 Assessment of humanoid behaviour and torque profiles	105
6.3.2 Control of humanoid and assistive exoskeleton.....	110
6.4 Fuzzy-based PD controller implementation.....	114
6.4.1 Tests with different standing up and sitting down cycle speeds	120
6.4.2 Tests with constant loads and disturbance forces.....	124
6.5 Summary	127
Chapter 7: Conclusion and future works.....	129
7.1 Summary and conclusion	129
7.2 Recommendations for future work.....	131
References	133

List of figures

Figure 1.1: types of paralysis (Pngkey, 2018).....	3
Figure 1.2: Ground reaction force during gait cycle (Mauritz, 2002).....	4
Figure 1.3: Lower limb anatomy (Pons, 2008)	5
Figure 2.1: Wearable robots: (a) upper limb orthotic exoskeleton; (b) upper limb prosthetic robot; (c) lower limb orthotic exoskeleton; (d) lower limb prosthetic robot (Pons, 2008) .	12
Figure 2.2: Body planes (Pons, 2008).....	15
Figure 2.3: Lower extremity soft exoskeleton: (a) soft exosuit for gait assistance (Wehner et al., 2013), (b) Wyss institute soft exosuit (Wyss Institute, 2017)	18
Figure 2.4: Generalised control framework for active lower limb prostheses and orthoses (Tucker et al., 2015)	22
Figure 3.1: constraints selection.....	34
Figure 3.2: Body customisation tools.....	35
Figure 3.3: Anthropometric dimensions of human model (Winter, 2009).....	37
Figure 3.4: Different views of the humanoid model	39
Figure 3.5: Exoskeletons structure: a) Anthropomorphic, b) quasi-anthropomorphic, c) non-anthropomorphic (Viteckova et al., 2018)	40
Figure 3.6: Humanoid and single leg exoskeleton in different positions.....	41
Figure 3.7: Different views of the single leg exoskeleton model.....	42
Figure 3.8: Humanoid and single leg exoskeleton in different positions.....	43
Figure 3.9: MSC.vN4D plant in Simulink	44
Figure 3.10: Simulink implememntation of vNPlant.....	45
Figure 3.11: Lower limb joints orientation during two gait cycles.....	46
Figure 3.12: Hip and knee joints orientation trajectories of standing up and sitting down	47
Figure 4.3: PID control system	51
Figure 4.4: Structure of fuzzy logic controller.....	55
Figure 4.5: Triangle fuzzy membership function.....	56
Figure 4.6: Simulink diagram of fuzzy-based PD controller	60
Figure 4.7: Trajectory of spiral search (Tamura and Yasuda, 2011)	62
Figure 4.8: Different cases of spiral model behaviour (Tamura and Yasuda, 2011)	63
Figure 4.9: Flow chart of SDA process.....	65
Figure 5.1: Cycle of human gait (Hsu et al., 2008).....	69

Figure 5.2: Joint kinematics of right-side hemiplegia gait cycle vs natural joint kinematics gait cycle (Kranzl and Kopf, 1997).....	70
Figure 5.3: Hip and knee torque profiles of hemiplegic and natural gait data.....	71
Figure 5.4: PID Control scheme of humanoid lower limbs joints in MATLAB Simulink.....	72
Figure 5.5: Orientation and torque for humanoid right hip and left hip joints during two gait cycles using two sets of PID parameters; (a,b,c,d) first trial; (e,f,g,h) second trial	75
Figure 5.6: Orientation and torque for humanoid right and left knee joints during two gait cycles using two sets of PID parameters; (a,b,c,d) first trial; (e,f,g,h) second trial	76
Figure 5.7: Orientation and torque for humanoid right and left ankle joints during two gait cycles using two sets of PID parameters; (a,b,c,d) first trial; (e,f,g,h) second trial	77
Figure 5.8: Single joint Simulink PID control diagram of humanoid and exoskeleton.....	79
Figure 5.9: SDA tuning PID parameters	79
Figure 5.10: Torque and orientation for humanoid and exoskeleton joints simulated with trial and error tuned parameters	82
Figure 5.11: Torque and orientation for humanoid and exoskeleton joints simulated with SDA tuned parameters	83
Figure 5.12: Orientation for humanoid left lower limb joints with SDA and trial and error tuned parameters	84
Figure 5.13: Gaussian input/output membership functions	86
Figure 5.14: Humanoid and exoskeleton PD-fuzzy control scheme.....	87
Figure 5.15: Optimising PD-fuzzy scaling parameters with SDA.....	89
Figure 5.16: Joints orientation of the humanoid and exoskeleton during two gait cycles ..	92
Figure 5.17: Output torque of the humanoid and exoskeleton joints during two gait cycles	93
Figure 5.18: Orientation and torque results of the humanoid and exoskeleton joints with medium speed gait trajectories.....	95
Figure 5.19: Orientation and torque results of the humanoid and exoskeleton joints with high speed gait trajectories	96
Figure 5.20: Positions of the disturbance forces applied on the humanoid and exoskeleton	97
Figure 5.21: Orientations and torques of the humanoid and exoskeleton joints under different disturbance forces.....	99
Figure 6.1: Cycle of standing up motion (Kralj and Bajd, 1989).....	103
Figure 6.2: Cycle of sitting down motion (Kralj and Bajd, 1989)	104

Figure 6.4: Humanoid model PID control scheme.....	106
Figure 6.5: Orientation and output torque of hip and knee joints with trial and error tuned parameters	108
Figure 6.6: Orientation and torque for humanoid joints with SDA tuned PID parameters	109
Figure 6.7: Unrestricted output torque of humanoid hip and knee joints	109
Figure 6.8: Simulink diagram of humanoid and exoskeleton joints PID control.....	111
Figure 6.9: Simulation results of humanoid and exoskeleton hip joints	113
Figure 6.10: Simulation results of humanoid and exoskeleton knee joints.....	114
Figure 6.11: Humanoid and exoskeleton PD-fuzzy control scheme.....	116
Figure 6.12: Orientation and output torque results for humanoid and exoskeleton hip joints	119
Figure 6.13: Orientation and output torque results for humanoid and exoskeleton knee joints	120
Figure 6.14: Orientation results of the humanoid and exoskeleton joints with slow speed cycle of standing up and sitting down.....	122
Figure 6.15: Torque results of the humanoid and exoskeleton joints with slow speed cycle of standing up and sitting down	122
Figure 6.16: Orientation results of the humanoid and exoskeleton joints with fast speed cycle of standing up and sitting down	123
Figure 6.17: Torque results of the humanoid and exoskeleton joints with fast speed cycle of standing up and sitting down.....	123
Figure 6.18: Constant load and disturbance force positions on the humanoid and exoskeleton models	124
Figure 6.19: Simulation results of the humanoid and exoskeleton right side joints orientation under different constant loads	125
Figure 6.20: Simulation results of the humanoid and exoskeleton right side joints orientation under different disturbance forces.....	126

List of tables

Table 2.1: Functions and applications of the exoskeleton technologies	13
Table 2.2: kinematics properties of human lower limb joints.....	16
Table 2.3: Comparison of commercial assistive exoskeletons (Choi et al., 2017; Esquenazi et al., 2012; Rewalk, 2016; RexBionics, 2011; Sankai, 2010; Sg robotics, 2017)	28
Table 3.1: Control measurement signals	36
Table 3.2: Humanoid model segments mass and length	37
Table 3.3: Humanoid model joints.....	38
Table 3.4: Exoskeleton structure components.....	42
Table 4.1: Fuzzy rules set.....	58
Table 4.2: Pseudo code of SDA n-dimension (Tamura and Yasuda, 2011)	64
Table 5.1: Gait cycle phases and sub-phases (Vaughan et al., 1999)	69
Table 5.2: Humanoid lower limb joints PID control parameters and RMSE values	74
Table 5.3: Trial and error and SDA tuned control parameters with RMSE values.....	80
Table 5.4: Membership functions linguistic terms.....	85
Table 5.5: Fuzzy rules set.....	86
Table 5.6: SDA tuned FLC parameters	90
Table 5.7: Comparison of torque RMS values generated with PID and PD-fuzzy controllers for the exoskeleton joints during walking simulations.....	101
Table 6.1: Trial and error and SDA tuned control parameters with RMSE values.....	107
Table 6.2: SDA tuned control parameters with RMSE values.....	112
Table 6.3: Fuzzy rules set.....	115
Table 6.4: SDA tuned FLC scaling parameters.....	118
Table 6.5: Comparison of torque RMS values generated with PID and PD-fuzzy controllers for the exoskeleton joints during standing up and sitting down simulations	128

Abbreviations

CAD	Computer aided design
CGA	Clinical gait analysis
CoG	Centre of gravity
CoM	Centre of mass
CoP	Centre of pressure
DE	Differential evolution
DoF	Degree of freedom
ECG	Electrocardiography
EEG	Electroencephalography
EMG	Electromyography
EOG	Electrooculography
FLC	Fuzzy logic control
KAFO	Knee-Ankle-Foot orthosis
MIMO	Multi input multi output
MISO	Multi input single output
MSC.vN4D	MSC. VisualNastran 4D
PD	Proportional Deravitive
PID	Proportional Integral Deravitive
PSO	Particle Swarm Optimisation
RMS	Root mean square
RMSE	Root mean square error
RoM	Range of motion
SCI	Spinal cord injury
SDA	Spiral dynamic algorithm
SISO	Single input single output

Chapter 1: Introduction

1.1 Background and motivation

Mobility is one of the most vital abilities for human being that enables her/him to preserve his independence while performing physical activities. It is described as the ability to use and control body position in order to carry out daily life activities (Webber et al., 2010). Human locomotion process depends on collaboration between the neuromuscular and musculoskeletal systems to achieve natural mobility, and any condition of injury, illness or disease will affect the nature of human locomotion (Woolley, 2001). Mobility disorder can result in reduced ability in performing daily life activities due to reduced functionality of muscles as in elderly people or due to medical or physical conditions in general.

According to the world health organization, worldwide 250,000 to 500,000 suffer from spinal cord injury (SCI) every year. SCI symptoms may include loss of full or partial body limb control and sensory functions. One of the essential measures to improve SCI medical care and rehabilitation services is to provide assistive devices to enable SCI patients to perform their daily life activities. However, only 5-15 % of people who live in low and middle income countries can afford assistive devices (World Health Organization, 2013). Globally around 185 million people rely on wheelchair for their mobility and almost 20% of the aged population are over 65 years, and this is expected to reach 35% by 2050, therefore the demand for assistive devices for injured and elderly people is growing so as to help them gain more independence with their daily life activities (Bogue, 2015).

In order to provide better quality of life for people who experience gait disorder to perform their usual daily tasks, attempts have been made to develop various solutions to

assist and support their locomotion. Assistive robotics such as exoskeletons could be an important key in addressing mobility issues. Exoskeleton can be described as a user-oriented robotic system worn to replace or support limb function (Pons, 2008). Currently, exoskeletons are considered as significant addition to assistive technology, in which interest has been intensified in the last decade. Lower limb exoskeletons used in rehabilitation and enhancing quality of life have been the most successful applications, but exoskeletons are used in different fields such as industry, military and medical care, and the growth of exoskeleton technology market is expected to reach \$1.8bn in value by 2025 (Bogue, 2018).

Recently several exoskeleton robotic devices have been launched to help paraplegic patients and wheelchair users to stand, walk and climb stairs. Among these Rewalk by Argo Medical Technologies (Rewalk, 2016), Ekso by Ekso Bionic (Chen et al., 2016) and HAL by Cyberdyne (Sankai, 2010) have proved efficiency in restoring gait disorder using sensing, actuation and control techniques. However, obstacles and challenges still exist in exoskeleton technology advancements such as energy efficiency, safe and lightweight mechanical design, actuation systems, control and sensing techniques and operation constraints (Viteckova et al., 2018).

1.2 Hemiplegia

The pathologies causing damage to neuromuscular and musculoskeletal system have significant consequences on mobility (Salzman, 2010). Stroke is the most common cause of neuromuscular injury such as paralysis, due to brain damage and disturbance of relationship with spinal cord (Spinalcord, 2017). Figure 1.1 shows examples of paralysis types based on affected portion of the body. Hemiplegia indicates the paralysis of one side of the body caused by damaged motor nerve cells or fibres within the brain and in some cases, paralysis maybe limited to some parts of the body. Paralysis is considered as one of the stages of

hemiplegia symptoms where the patient is unable to move face, arm or leg muscles and cerebral thrombosis is common cause of hemiplegia (Bierman, 1946). Reduced muscle strength and mobility impairment leads the patients with hemiplegia to suffer walking difficulties and tiredness. Therefore, more investigation is needed to explore the walking pattern and gait characteristics of hemiplegic patients.

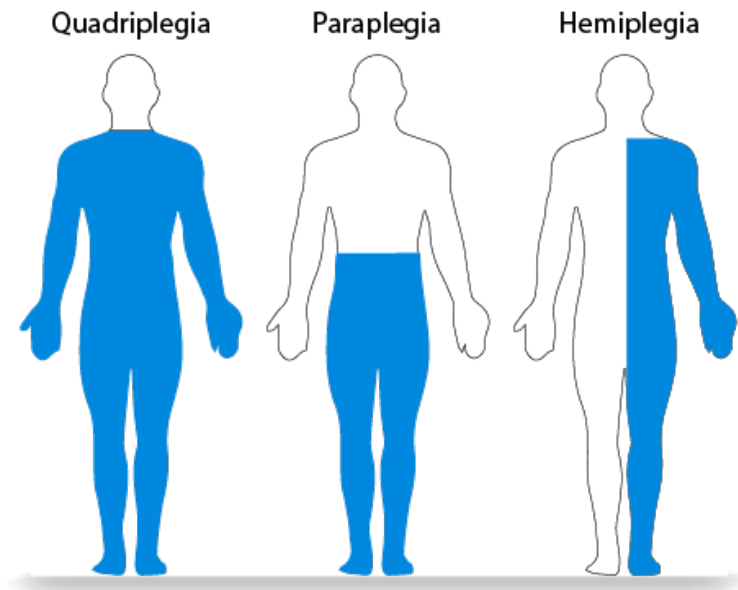


Figure 1.1: types of paralysis (Pngkey, 2018)

Pattern of extremity movement and body posture in ambulation of stroke patients are characterised by clinicians to describe hemiplegic gait as slow, difficult and uncoordinated (Kuan et al., 1999). Figure 1.2 demonstrates the ground reaction force between normal walking pattern and hemiplegic walking pattern. As noted, the curve of ground reaction force is represented with two peaks of heel strike and push off at the end of stance phase. Figure 1.2 shows the symmetrical difference between normal and hemiplegic gait cycles with right and left leg; the curve is symmetrical in case of normal gait but the curve of hemiplegic gait shows how the affected side is shorter than the unaffected side making the gait unsymmetrical (Mauritz, 2002).

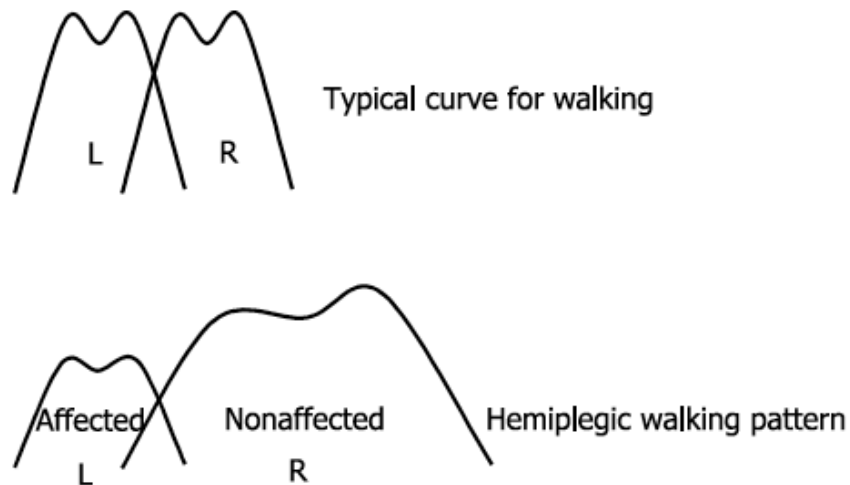


Figure 1.2: Ground reaction force during gait cycle (Mauritz, 2002)

Hemiplegia gait characteristics are different than normal gait in many aspects. Woolley (2001) reported that gait disorder within hemiplegia patients is related to their reduced walking velocity, and hemiplegic walking requires 50% to 67% more metabolic energy cost. Onley and Richards (1996) stated the difference in stance and swing phases during hemiplegic gait cycle, where the stance phase takes long time during the gait cycle both on affected and unaffected leg and the double support stage where both feet are attached to the floor takes the largest proportion of the gait cycle at normal speed.

Maeshima et al. (2011) have carried out a study on 16 stroke patients who were suffering from hemiplegia. The patients held gait training using Hybrid Assistive Limb (HAL) exoskeleton and knee-ankle-foot orthosis for comparison of their gait speed, stride length and physiological cost. The results of their study show that the stride length and walking speed increased with some patients, but the stride length and walking speed of other patients did not improve due to muscle weakness. Overall the experiment shows that, wearable robotics may improve gait disorder along with gait training and rehabilitation.

1.3 Lower limb joints

Human upper body is reinforced by the lower limbs carrying its weight while in locomotion. Lower limb consists of four main parts, they are foot, thigh, calf and pelvis linked to the trunk's lower part (see Figure 1.3). Hip, knee and ankle are the main joints linking the lower limb segments together (Moore and Dalley, 1999). Most of human body parts are engaged while in motion. However, it has been identified that lower limb joints are more relevant than other joints as they implement main motions and torques (Gálvez-Zúñiga and Aceves-López, 2016).

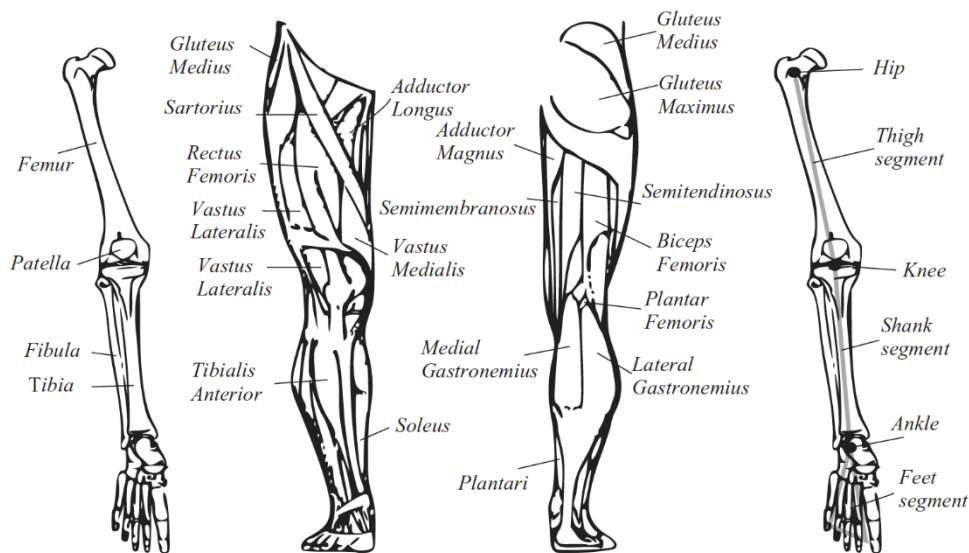


Figure 1.3: Lower limb anatomy (Pons, 2008)

1.3.1 Hip

The hip joint is the body's second most weight support joint after the knee because it is supported by many ligaments and surrounded by strong muscles that prevent dislocation and holding the joint together. It allows the body to carry out stable locomotion even in straight line due to its spherical shape allowing three degrees of freedom (DoF) (Pons, 2008). The hip joint is attached with the pelvis in a structure of ball and socket where the

pelvis acts as a socket surrounding the femur head. Hip joint can move in three different range of motions (Moore and Dalley, 1999):

- Flexion-extension: flexion is the motion that moves the thigh forward and upward with a range of motion up to 120 degrees. Extension is the opposite movement to flexion.
- Abduction-adduction: abduction is the movement of the lower limb away from the body centre with a range of motion up to 40 degrees. Adduction is the opposite movement with range of motion between 30 and 35 degrees.
- Medial-lateral rotation: medial and lateral rotation is the movement around femur bone axes with a range from 15 to 30 degrees for the medial and lateral rotation up to 60 degrees.

1.3.2 Knee

The knee joint is known as synovial hinge joint or condyloid joint, and it links the tibia and femur bones. The knee joint has the most restraints compared with other body joints, protected by strong muscles and ligaments to limit some movements that can damage the knee (Pons, 2008). It is deemed as the biggest and strongest joint in the human limbs as it plays vital part in walking and standing motions and supports body weight bearing. The knee joint's main movements are active in the sagittal plane, however, small rotations are achievable when knee in flex motion. These motions are (Pons, 2008):

- Flexion-extension: flexion is the motion when the leg is approaching the thigh while in the same plane; the range of motion is up to 160 degrees depending on the hip movement condition. Extension is the opposite movement with range of motion from 0-10 degrees.

- Medial-lateral rotation: medial is an internal rotation and happens at the end of extension stage which takes the knee to locked position to maintain stability with a range of motion of 10 to 15 degrees. Medial is external rotation and happens at the beginning of flexion stage with range of motion of 30 to 50 degrees based on knee flexion level.

1.3.3 Ankle

The ankle is a synovial joint located between lower end of the leg and upper part of the foot. The assembly of ankle and foot contains 26 bones linked by 30 joints and supported by 100 muscles (Pons, 2008). During walking the foot and ankle play crucial part in lower limb stability, where the foot works as shock-absorber transferring force between the lower limbs and the ground and acting as solid pedal to apply force while walking on uneven surface levels (Dawe and Davis, 2011). There are two movements for the ankle joint in the transverse plane (Pons, 2008):

- Dorsal-plantar flexion: dorsal flexion is the movement where the ankle rotates the foot towards the inner surface of the leg with a range of motion up to 20 degrees. Plantar flexion movement happens the when heel is off the ground and the toe is on the ground with range of motion from 40 to 50 degrees.

1.4 Aim and Objectives of the research

The aim of this research is primarily to design and develop a single leg exoskeleton to assist hemiplegic patients in their daily life activities for example walking, standing up and sitting down. The following objectives are defined in order to meet the main aim of this research:

- To design a computer aided design (CAD) model that imitates human characteristics in terms of dynamics and kinematics in a virtual software environment.

- To design a single leg exoskeleton frame with active hip, knee and ankle joints to be fitted to the humanoid waist and right lower limb.
- To develop a PID controller for the humanoid model to follow predefined trajectories of walking, standing up and sitting down cycles.
- To study the humanoid behaviour and examine the torque profiles generated from simulations of the humanoid model while simulating walking, standing up and sitting down in virtual environment.
- To investigate the implementation of PID controller for the humanoid and exoskeleton system in order to provide the necessary support to the humanoid to achieve walking, standing up and sitting down tasks.
- To investigate the implementation of an intelligent control method such as Proportional-Derivative based fuzzy logic controller, for the humanoid and exoskeleton system in order to provide the necessary support to the humanoid to achieve walking, standing up and sitting down tasks. The performance of the humanoid and exoskeleton system with intelligent control approach will be compared with PID control approach.
- To apply optimisation algorithm to tune and optimise the control parameters and achieve enhanced performance.
- To investigate the developed controller's efficiency and robustness while controlling the humanoid and exoskeleton system during the designated tasks, by applying different external disturbance forces, constant loads and different motion speed cycles.

1.5 Contributions

The contributions to knowledge of the research comprise the following:

- CAD model of a Single leg assistive exoskeleton system with active hip, knee and ankle joints that provides external assistance to the user to complete walking, standing up and sitting down movements simulated in virtual environment.
- A robust intelligent hybrid control approach that is capable to provide stable and symmetric locomotion with single limb orthosis device under different conditions and disturbance forces.
- Approach for acquiring optimised controller scaling factors based on spiral dynamic algorithm optimisation, achieving significant enhancement of the system performance by reducing torque consumption and smooth joints tracking.

Publications arising from the research include the following:

- **Alshatti, A.**, Tokhi, M. O., and Alrezage, G. (2016). Design and control of single leg exoskeleton for hemiplegia mobility. In *Advances in Cooperative Robotics: Proceedings of the 19th International Conference on CLAWAR 2016* (pp. 832–839). WORLD SCIENTIFIC.
- **Alshatti, A.**, and Tokhi, M. O. (2017). PD-fuzzy control of single lower limb exoskeleton for hemiplegia mobility. In *3rd International conference on artificial intelligence and soft computing (AIS 2017)* (pp. 53–62).
- **ALREZAGE, G.**, **ALSHATTI, A.**, and **TOKHI, M. O.** (2016). PD-fuzzy control of lower limb exoskeleton for elderly mobility. In *Advances in Cooperative Robotics: Proceedings of the 19th International Conference on CLAWAR 2016* (pp. 823–831). WORLD SCIENTIFIC.

- **Alshatti, Abdullah.**, Tokhi, M.O. (2016, November). Design and control of single leg exoskeleton for hemiplegia mobility. Poster session presented at ACSE PGR symposium 2016. ACSE, university of Sheffield, United Kingdom.

1.6 Thesis outline

Chapter 1: The study starts by a brief background of the topic with the incentive for the conducted research. Additionally, hemiplegia paralysis, human lower limb joints anatomy, objectives of the research, research contributions and publications arising from the research are also presented.

Chapter 2: This chapter includes a summary of orthotic exoskeleton systems developments and design considerations such as biomechanics, structure design, hardware components, power source and control strategies. Additionally, a description of lower extremity exoskeleton applications and their recent developments are included.

Chapter 3: This chapter presents the development of a single leg exoskeleton and humanoid CAD models in SOLIDWORKS software. Furthermore, the assembly and configurations of the CAD models in MSC. VisualNastran (MSC.vN4D) for simulation purposes are described, with the integration process in MATLAB Simulink for implementation of the control strategy.

Chapter 4: This chapter describes the control methods considered in this work to assist hemiplegic patient mobility. Two types of controllers are considered, namely Proportional Integral Derivative (PID) and PD type fuzzy logic control (FLC). Additionally, a description of the Spiral Dynamic optimisation algorithm for tuning and optimising the controller parameters is provided.

Chapter 5: In this chapter, control and simulation of the exoskeleton and humanoid models to support hemiplegic patient during walking are investigated. PID and fuzzy-based PD controllers are utilised to control the active joints of the humanoid and exoskeleton. Simulation of the humanoid and exoskeleton models is completed in MSC.vN4D virtual environment software. The system performance is evaluated by reference tracking minimum error and output torque presented in the simulation results. Control robustness is evaluated by applying disturbance impulse forces and different walking speed.

Chapter 6: in this chapter, control of single lower limb exoskeleton that assist hemiplegic patient to complete standing up from sitting position and sitting down from standing position are introduced. PID and fuzzy-based PD developed are employed to address the control of the humanoid and exoskeleton active joints, and simulation results are presented to demonstrate system performance. Finally, control efficiency and robustness are assessed by applying different disturbance forces and constant loads on the humanoid and exoskeleton models during simulation.

Chapter 7: This chapter concludes and evaluates the outcomes of the study in achieving the research objectives. Future work suggestions to extend and improve the system potentials are also included.

Chapter 2: Exoskeleton systems

2.1 Exoskeletons and wearable robots

Generally, robots are known as devices that perform human tasks in precise and repetitive way especially in industrial environment. However, the robotic technology has emerged widely in different environments and applications. Wearable robots are different from traditional robots because physical interaction is involved and are aimed to enhance human capability or replace human limb. Wearable robots can be classified based on their functionality in cooperation with the operator. Figure 2.1 shows different types of lower and upper limb wearable robots known as orthotic robots and prosthetic robots. An orthotic robot is a mechanical structure that is attached to human limb to restore human physical functions. A prosthetic robot is an electromechanical device used to substitute lost human limb to perform closer to natural human function (Pons, 2008).

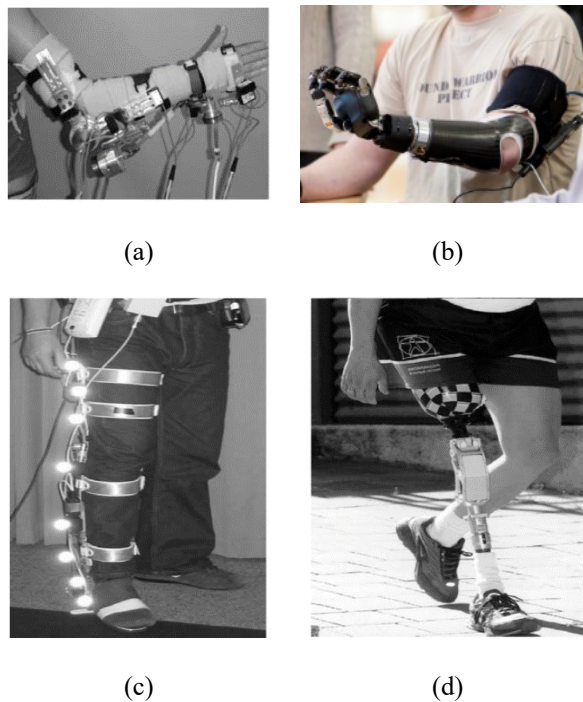


Figure 2.1: Wearable robots: (a) upper limb orthotic exoskeleton; (b) upper limb prosthetic robot; (c) lower limb orthotic exoskeleton; (d) lower limb prosthetic robot (Pons, 2008)

Another description to wearable robots has been given by Dollar and Herr (2008), to differentiate between exoskeleton and active orthosis. They have been defined exoskeleton as an active mechanical device, which fits to the user’s body and responds to the user’s movements accordingly. An active orthosis described as a device that enhances the gait of a person who is suffering from a leg pathology.

Research in exoskeleton systems has intensified in the late 20th century and researchers have reported various novel models of wearable robotics and exoskeleton has become a research focus in the field of robotics (Yang et al., 2008). The development in areas of sensing, actuation and power, transformed simple prosthetic and orthotic wearable devices into intelligent human wearable robots, which are able to think, sense and act to enhance human mobility functions. Table 2.1 highlights the functions and applications of the recent exoskeleton technologies. Recently, exoskeleton technologies are involved beyond medical rehabilitation and locomotion assistance, exoskeletons are employed by military and industrial organisations to protect and enhance users performance while lifting and handling heavy loads (Rovekamp et al., 2017).

Table 2.1: Functions and applications of the exoskeleton technologies

Exoskeleton technology	Function	Application
Rehabilitation	Regain mobility disorder	Medical rehabilitation
Assistive	Compensate physical disability and muscle weakness	Locomotion assistance for elderly and paralysed patient
Performance	Augment human strength, physical abilities and operator protection	Military, industry and load augmentation

Exoskeletons can be categorised based on their design mechanisms, such as full or partial body and lower or upper extremity. The current exoskeleton technology includes

three types, namely performance exoskeletons, rehabilitation exoskeletons and assistive exoskeletons. Performance and assistive exoskeletons are developed for supplementation of human physical ability to perform tasks such as lifting heavy weight, rehabilitation exoskeletons are developed to help people who suffer from neurological injury to retrieve their mobility and assistive exoskeletons are developed to benefit people with mobility disorders to perform daily tasks (Grosu et al., 2015).

2.1.1 Lower extremity exoskeleton and human biomechanics

Generally, lower extremity exoskeleton supports hip, knee and ankle joints. Therefore, the mechanical structure of lower limb exoskeleton should follow the characteristics of human lower limb biomechanics such as type of motion, range of motion (RoM), degree of freedoms (DoF) and torque. Lower extremity exoskeleton can be designed based on joint support, such as single joint, two joints or the entire leg. Exoskeleton design aspects are mainly based on the application target and biomechanics properties in respect with the biological limb (Cenciarini and Dollar, 2011; Pons, 2008). Furthermore, Cenciarini and Dollar (2011) investigates human biomechanical considerations associated to lower extremity exoskeletons development and analyse the main aspects in the exoskeleton design, such as kinematic considerations and joint torques as shown in Table 2.2, and other aspects related to the exoskeleton hardware design such as type of actuation, weight and device inertia. The latter aspects add more challenges in the exoskeleton design, because the performance of the system dynamics should integrate with the user biological characteristics.

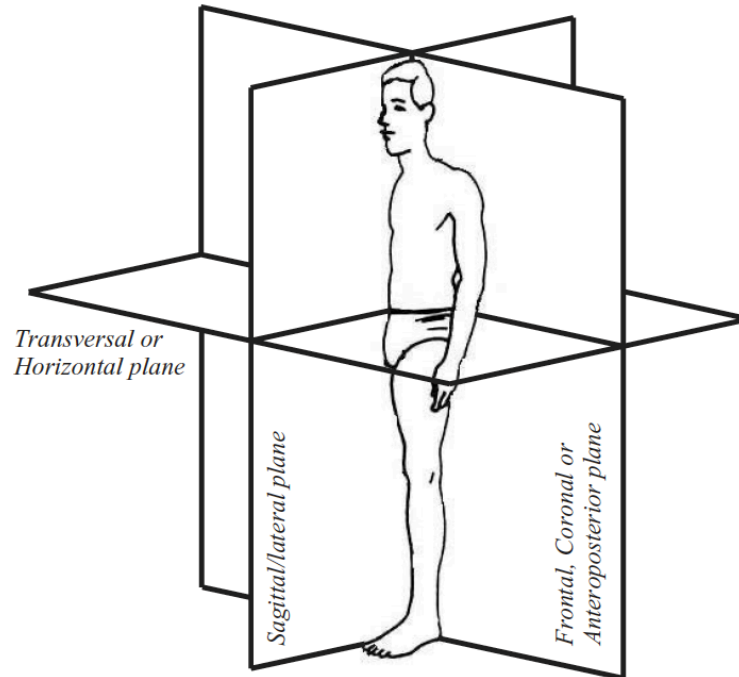


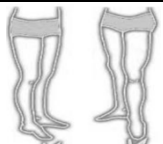
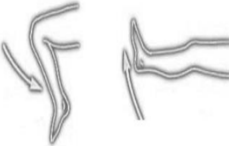




Figure 2.2: Body planes (Pons, 2008)

Table 2.2 adopted from (Crowell III et al., 2002; Low, 2011; Mackenzie, 2004; Shaari et al., 2015), shows the kinematics properties and the biological values of human lower limb joints. The data represents natural lower limb human RoM of each joint, i.e. during walking hip, knee and ankle motions are in the sagittal/lateral plane (Figure 2.2), while other lower limb joints maintain body balance. The torque values represent range of moment during walking and running. According to Crowell III et al. (2002), values of moment and range of motion varies during the gait phases based on foot position and muscle group.

Human joint kinematics is difficult to replicate because the nature of human joints is complex, consequently simple exoskeleton joint design will cause undesirable interaction force between human and exoskeleton, and complex exoskeleton joint design will add cost and reduce system reliability. Compatibility between exoskeleton design and human joints kinematics will provide suitable functionality (Low, 2011).

Table 2.2: kinematics properties of human lower limb joints

Joints	DoF	Motion	RoM (deg)	Torque (Nm)
Hip	3	 <p>Flexion/extension</p>	140/15	140/120 (walking) 40-80 (running)
		 <p>Adduction/Abduction</p>	40/30-35	N/A
		 <p>Internal/External</p>	15-30/60	N/A
Knee	2	 <p>Flexion/Extension</p>	120-140/0-10	5/140 (walking) 125-273 (running)
Ankle & Foot	4	 <p>Flexion/Extension</p>	40-50/20	165 (walking) 180-240 (running)
		 <p>Inversion/Eversion</p>	30-35/15-20	N/A

2.2 Exoskeleton design considerations

Exoskeleton system structure constitutes mechanical frame, actuators, sensing equipment and controller. Exoskeleton systems work in collaboration with human operators (user) by combining human intelligence and machine power to produce the required motion. Mechanic frame forms the exoskeleton interface with human body and support sensors, controller and actuators in place.

2.2.1 Exoskeleton frame and material

Frame design is essential property in exoskeleton design. In order to make exoskeleton user free from gravity, the exoskeleton mechanical design should transfer user's weight to the ground by producing a force path between the user and the ground. Some aspects are important in exoskeleton design such as light weight, comfortable design, robust structure, users compatibility and safety (Önen et al., 2014).

Exoskeleton frame design have important effect on the overall performance of the exoskeleton. The main target is to reduce the weight of the frame with respect to the dynamics of the device and interaction force with the user. According to Young and Ferris (2017), most of exoskeleton designs used rigid metal frames to support human limbs and link between joints. Furthermore, the use of thermoplastic and carbon composite has increased in exoskeleton frames to create light, strong and effective frame. Aluminium, titanium and carbon steel are further material commonly used in exoskeleton frames (Hsu et al., 2008). Another approach in exoskeleton design have been implemented by researchers is known as soft exoskeleton (Figure 2.3). Soft lower extremity exoskeletons form as wearable suit, made from fabric materials to augment muscle functions by using soft actuators. Exoskeletons made from soft materials provides ultra-lightweight exoskeleton suit to reduce control complexity and manufacture cost (Polygerinos et al., 2017). Wyss

institute has developed soft exosuit made of functional textile, the exosuit support specific leg joint to reduce metabolic cost during walking (Quinlivan et al., 2017). Another example of soft exoskeleton design developed by Wehner et al. (2013) to augment muscles of healthy people, the ultra-lightweight soft exoskeleton will help to reduce the mechanical impedance and the inertia between the device and the user.

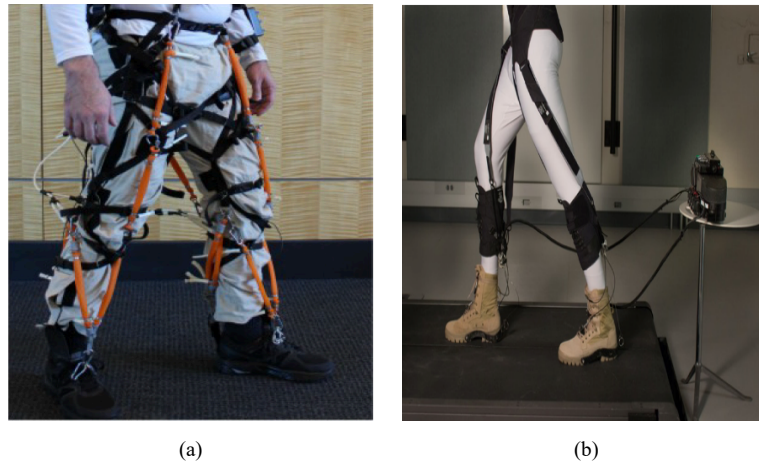


Figure 2.3: Lower extremity soft exoskeleton: (a) soft exosuit for gait assistance (Wehner et al., 2013), (b) Wyss institute soft exosuit (Wyss Institute, 2017)

2.2.2 Actuators

Exoskeleton systems should be coupled and synchronised with the user locomotion in natural way. Therefore, the peak joint torques, velocities and accelerations of the exoskeleton system should match those of the user (Crowell III, 1995). Actuators are used in exoskeletons to provide the required physical torque to support weight, inertia and size of the exoskeleton device and the user load during locomotion. Furthermore, actuators are necessary in an exoskeleton to achieve the desired motion set by the controller (Young and Ferris, 2017). Torque-mass ratio, range of motion, velocity and controllability are important measures in selecting exoskeleton actuators (Önen et al., 2014).

Variety of actuators are used in robotic applications such as hydraulic, pneumatic, electrical and electro active polymers. Actuators must generate enough torque to drive the

body motion while operating at high speed, therefore many types are not suitable for exoskeleton applications. Electric driving actuators are more common in lower exoskeleton robots, because they are easy to control with high precision compared to hydraulic and pneumatic actuators (Li et al., 2015). Investigations by Zoss and Kazerooni (2006) shows that electric motor actuation uses less power than hydraulic actuation during walking. A review of actuator technologies for wearable robotics by Veale and Xie (2016) shows that electrical actuators are highly used amongst orthoses robotics due to high specific power and easy to control. Furthermore, 72% of exoskeleton designs reviewed by Young and Ferris (2017) used electrical motors. Electric motor and harmonic drive are used in HAL-5 to obtain energy autonomous system, Lokomat exoskeleton incorporates DC motor and ball screw in their linear actuators design, Rewalk exoskeleton uses DC motors to drive hip and knee joints (Low, 2011). Brushless DC motors are popular in lower extremity exoskeletons due to their reliability, reduced noise and high torque to weight ratio. They have been used in several exoskeleton devices such as the Body Extender (Fontana et al., 2014), Mina (Neuhaus et al., 2011) and over-ground gait trainer exoskeleton NaTUre-gaits (Luu et al., 2014).

However, hydraulic actuators are common in performance exoskeletons such as military, industry and load augmentation applications due to high power to mass ratio. Several exoskeletons have used hydraulic actuators such as BLEEX (Zoss and Kazerooni, 2006), LEEX (Sahin et al., 2014) and XOS2 (Karlin, 2011) .

2.2.3 Sensors

Human biomechanical data correlated to motion can be categorised into three categories: kinematic, kinetic and bioelectric data. The kinematic data represents body posture and joint angles. The kinetic data represents the joints torques and interaction forces. The bioelectric

data forms biological signals during human motion, such as electromyography (EMG) signal, electrooculography (EOG) signal, electroencephalography (EEG) signal and electrocardiography (ECG) signal (Chen et al., 2016).

Sensors are used in robotics to update the controller system with certain online information regarding the condition of the system. Intelligent control system generally contains three layers: perception layer, decision layer and execution layer. Perception layer in exoskeleton controller relies on multi-sensor information; mainly angle sensors, pressure sensors and biological signal sensor to detect the condition of the system, wearer's posture and surrounding environment. Angle sensors include gyroscope, inclinometer, encoders, angular acceleration sensors and inertial measurement units. Pressure sensors are used for different reasons such as detecting walking phases, body mass transfer process and to detect interaction force between human body and exoskeleton. (Li et al., 2015).

Existing exoskeletons use various types of sensors based on exoskeleton application and control approach. HAL-5 developed by Cyberdyne employs different types of sensors. Joint angles are measured by using potentiometer, accelerometer and gyroscope is used to obtain trunk's absolute angle, floor reaction force sensor implemented in the shoes to detect motion information. Additionally, EMG electrodes are used to detect user motion intentions (Sankai, 2010; Tsukahara et al., 2010). ReWalk employs various sensors to measure knee and hip angles, ground force and wireless tilt sensor for the upper body (Esquenazi et al., 2012). Interaction force generated between the user and the exoskeleton is considered as one of the challenges in exoskeleton control. However, Lokomat exoskeleton uses force sensor to detect the force generated between the exoskeleton and user lower limb, joint angles are measured by position sensor (Jezernik et al., 2003).

A review of sensor fusion methods has been presented by Novak and Riener (2015), comparing the implementation of sensory systems in wearable robots, the review of sensor

fusion algorithm highlights the strength and weakness of different sensory systems such as unimodal and multimodal. The unimodal system processes multiple signals obtained from same type of sensors such as EMG signal, the multimodal system processes a combination of signals obtained from different type of sensors. The review concludes that multimodal sensor fusion is more suitable in wearable robotics.

2.2.4 Power supply

Portable power supply is an important enabling technology in developing portable exoskeleton systems, specifically batteries. However, power source considered as one of the main challenges in exoskeleton developments due to size, weight, running time and safety issues (Aliman et al., 2017).

The majority of current exoskeleton designs depend on batteries as power source. Lithium-ion battery is the most common technology used in exoskeletons due to their availability and safety. Currently, lithium ion batteries can supply exoskeleton systems up to 5 hours of continual movements. Alternatively, providing more power supply capacity in portable exoskeleton system will add more weight and reduce the overall functionality (Young and Ferris, 2017).

Fuel cell batteries are considered as an alternative source to power portable exoskeletons. The technology has been used in some exoskeleton applications, such as HULC developed by Lockheed Martin (Kopp, 2011) and Sarcos XoS2 developed by Raytheon (Army-Technology, 2010). The latter exoskeleton applications have been developed to augment human strength and capability in military operations. The actuation system used in both applications has high power demand. Therefore, fuel cell batteries selected to extend operating duration. A feasibility study to enhance exoskeleton systems by Jansen in (2000), found that fuel cell batteries are promising option for exoskeleton

system because of their relatively low temperature, noiseless operation and low emission. However, hydrogen source is mentioned as major concern in fuel cell batteries. Several researchers and exoskeleton technology reviewers have pointed out, that advancement in batteries technology such as running time, size and weight will have significant impact in exoskeleton development and success.

2.2.5 Control strategy

The main goal for exoskeleton controller is to synchronize exoskeleton motion with wearer's locomotion in natural and safe manner. Control strategies of lower extremity exoskeletons have been reviewed and discussed extensively in the literature. However, force based control and kinematic based control are the most common strategies implemented in exoskeleton designs (Young and Ferris, 2017). Yan et al. (2015) investigated assistive methods in active lower-limb orthoses and exoskeletons and Cao et al. (2014) reviewed control strategies for gait rehabilitation exoskeletons. Tucker et al. (2015) reviewed the state-of-the-art methods to control prosthetic and orthotic devices for locomotion and daily life activities. Their review paper provides general control framework (Figure 2.4) for active lower limb prostheses and orthoses.

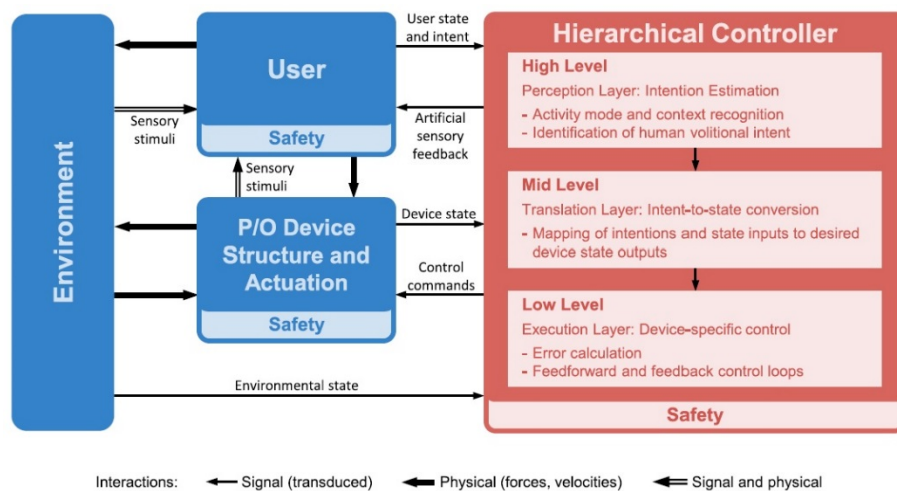


Figure 2.4: Generalised control framework for active lower limb prostheses and orthoses (Tucker et al., 2015)

Figure 2.4 shows the hierarchy of active lower limb prostheses and orthoses generalised control framework, where the high-level controller receives sensory information based on user, device and environment conditions to perceive user intent. Mid-level controller forms the decision of high-level controller into output state to control the system through low-level controller which acts as execution layer, low-level controller may build on a set of feedforward and feedback loops to calculate the error of the actual state and matching the system to the desired state (Tucker et al., 2015).

Yan et al. (2015) provide systematic overview for several existing exoskeletons based on their control approach. One of the strategies used in load augmentation exoskeletons is sensitivity amplification control strategy, where the exoskeleton models usually rely on inverse dynamic in the controller to use the exert force of the wearer on positive feedback loop to augment wearer support, but external disturbance force could be amplified by the controller which leads to unstable system. Therefore, high accuracy of the inverse dynamics is required. The Berkeley lower extremity exoskeleton (BLEEX) is one of the load carrying exoskeletons that uses sensitivity amplification controller in its assistive strategy.

Another control strategy widely used in exoskeleton applications such as HAL (Sankai, 2010), ATLAS (Sanz-Merodio et al., 2012), ReWalk (Esquenazi et al., 2012) and eLEGS (Strausser and Kazerooni, 2011) that support people with gait disorder is predefined gait trajectory control strategy. The strategy is based on recorded data analysis of healthy person desired joints trajectory. It is mainly implemented by exoskeleton applications to support patients with lost or partially lost mobility.

A modified version of HAL has been developed as a single leg version to support walking movement of hemiplegia (Kawamoto et al., 2009). The HAL controller called Cybernic control system is based on Bio-Cybernic control and Cybernic autonomous

control. Single leg version of HAL has avoided using the Bio-Cybernic control, which relies on bioelectrical signals of the muscles. Due to involuntary signal produced by paralysed wearer of the exoskeleton, the controller of the single leg HAL has adopted Cybernic autonomous control using predefined motion of healthy persons to provide autonomous motion such as walking, stand up and sitting.

Another assist controller applied on the modified version of HAL uses gait pattern data on the unaffected side to support hemiplegia patient on the affected side (Kawamoto et al., 2014). The control method stores the motion data from the unaffected leg during swing phase using potential meters to measure the joint angle, the controller uses the stored data to provide support motion on the affected leg in order to perform symmetric limb swing. The previous control methods implemented in HAL exoskeleton to support hemiplegia patients did improve the walking symmetry of the hemiplegia patients, but the control methods were not efficient to provide independence to the user and did not support different locomotion, for example stairs climbing and standing up.

Finite state controllers (FSCs) are widely used in exoskeleton devices. The main purpose of using FSCs is to decompose the human activity controlled by the exoskeleton into periodic activity that allows transition from phase to phase during the activity, for example, the phases of human cycle. Parametric control law is needed in the FSCs to trigger each phase of the activity. Position and impedance control are commonly used as parametric law in the FSCs, but the main issue with FSCs is that increasing the number of controlled joints and sensors will increase the number of parameters in the control law, and that will make the system more complex to control (Lawson et al., 2013).

Finite state controllers are used to detect motion intentions relying on movement of centre of gravity (CoG) and centre of Pressure (CoP) of the user body weight shifting, thus parameters are used as input to the mid-level FSC to perform the required motion. Farris et

al. (2012) adopted the previous method to develop lower limb exoskeleton to assist paraplegia patients to ascent and decent stairs. Furthermore, several lower limb orthoses that assist level walking of SCI patients demonstrated the same method (Farris et al., 2012; Kawamoto et al., 2014; Lawson et al., 2013).

Fuzzy control is one of the solutions to handle complicated and nonlinear systems when it is difficult to configure an accurate dynamic model (Passino and Yurkovich, 1998). The main advantage of fuzzy systems theory is to approximate system behaviour if the numerical relations of such a system do not exist. Generally, fuzzy controller contains four main blocks: the inputs of the system interpreted in the fuzzification block; the fuzzy-rules block holds the information of how to control the system; the appropriate rule selected and implemented by an interface mechanism block; the fuzzy results converted into required output signals by the defuzzification block (Ross, 2010). He and Kiguchi (2007) developed lower limb exoskeleton to assist human locomotion, where an EMG-based neuro-fuzzy controller provides the required assistance to support hip and knee joints to perform various movements such as standing up, sitting down and climbing stairs. Kong and Jeon (2006) developed EXPOS exoskeleton system to assist elderly people and patients with gait disorder. The fuzzy controller of the EXPOS provides the required support by configuring the fuzzy rules of the hip and knee joint angular velocity and torque signals.

One of the main issues related to wearable robotics is the interaction forces between the human body and exoskeleton suit. Such an interaction will cause instability due to changes in speed during walking and human reaction behaviour. Impedance control is one of the control methods used in exoskeletons to handle interaction with the operator, the previous method initially proposed by Hogan (1985). Tran et al. (2016) developed a method to control and regulate the mechanism of attached human-robot system. The control method adopted a fuzzy-based impedance control strategy to supply assistive torques during swing

and stance phase; the controller regulates the required impedance between the wearer's leg and the exoskeleton at certain motion speed. The main aim of the control method is to adapt the exoskeleton user to different walking speeds and reduce any physical interaction between the user and the exoskeleton.

2.3 Lower limb exoskeleton

Exoskeletons and active orthoses are currently considered as viable human physical assistance and support devices. In the last few years, several efforts have been made to integrate robotics technology to human body in order to improve human physical abilities for better performance and one of these efforts is the exoskeleton or in other term known as active orthosis. Late 1960s, "Hardiman" considered one of the earliest full body exoskeleton developed by General Electric in cooperation with Cornell University to augment wearer strength. "Hardiman" was hydraulically power-driven machine with 30 DOF (Dollar and Herr, 2008). Berkeley lower extremity exoskeleton (BLEEX) is one of the first autonomous load carrying exoskeleton with seven DOF in each leg with actuated joint supporting hip, knee and ankle while three DOF are unactuated on ankle and hip (Zoss et al., 2006).

Developments of exoskeleton systems have grown in the recent decades, several technology firms, research centres and universities are engaged in developing different applications of exoskeleton systems. The main objective in rehabilitation and assistive exoskeleton applications is to improve the quality of life for people with mobility disorder, for example disabled and elderly people. Furthermore, other exoskeleton applications used in military, industry and nursing care can improve the quality of work. In March 2018, Wearable Robotics Association Standards and Education Committee published a white paper on review of hip exoskeletons market (Sugar et al., 2018). The review focused on passive and active hip exoskeletons that assist workers to lift objects and moving around in

different work environments. The report highlights that, the exoskeleton devices do not help to lift more weight, but can improve lifting tasks and reduce fatigue, and it can possibly allow workers to report back to work after injury in shorter time. Interest in assistive exoskeleton for industry has increased in recent years. de Looze et al. (2016) provides an overview of industrial exoskeletons. The review includes 26 passive and active assistive exoskeletons developed for industrial purposes. The review is aimed to evaluate the potential effects on the users while carrying out physical activities such as dynamic lifting, static holding and load support. The review states that, using passive and active exoskeletons can reduce the muscle activities of the user and can potentially reduce the risk of work-related injury. However, safety issues, design drawbacks and technical challenges have been underlined and considered as barriers in large-scale implementation of industrial exoskeletons.

The research in this thesis is centred on assistive lower extremity exoskeleton to support people with paralysis to perform daily life activities. Several exoskeleton designs have recently been considered in medical field especially in rehabilitation as therapeutic exoskeletons and assistive exoskeletons to enhance gait disorder. Table 2.3 shows a comparison of four types of commercial assistive exoskeletons to support paraplegic patients and an overview of their configurations, capabilities, dimensions and requirements.

HAL by Cyberdyne (Cyberdyne Inc., 2011), ReWalk by Argo Medical Technologies (Rewalk, 2016), REX by Rex Bionics (RexBionics, 2011) and WalkON suit by SG Robotics (Sg robotics, 2017) are examples of state-of-art in assistive exoskeleton developments. These devices have proved efficiency in aiding paraplegics with activities of daily livings such as walking, climbing stairs, sitting down and standing up. WalkON suit and ReWalk exoskeletons participated in the Cybathlon powered exoskeleton race (ZurichETH, 2016). The race was designed to simulate the daily mobility tasks that faces disabled people such

as, sit and stand, climbing stairs, ascending and descending slopes, navigating through zig-zag course, stepping on stones and open doors. However, both exoskeleton pilots with lower body paralysis were able to complete the tasks independently. Generally, the outcome of the Cybathlon race shows how assistive exoskeletons can be resourceful in aiding people with gait disorder.

Table 2.3: Comparison of commercial assistive exoskeletons (Choi et al., 2017; Esquenazi et al., 2012; Rewalk, 2016; RexBionics, 2011; Sankai, 2010; Sg robotics, 2017)

Characteristics		HAL-5	Rewalk	Rex	WalkON suit
Design					
Control strategy		Predefined gait trajectory & Model based control	Predefined gait trajectory	Positioning control	Predefined gait trajectory
DOF	Hip	3	2	3	2
	Knee	1	1	1	2
	Ankle	1	1	2	2 Passive
Type of sensors		Force Kinematic EMG	Kinematic	Kinematic	Kinematic
Actuation type		Electric	Electric	Electric	Electric
Battery life		1 hour	2 hours 4 minutes	2 hours	Up to 5 hours
Motion performed		Standing and Sitting Walking Climbing stairs Load augmentation	Standing and Sitting Walking on different surfaces Climbing stairs	Standing up Walking Climbing stairs	Standing and Sitting Walking on different surfaces Climbing stairs
Additional support		none	crutches	none	crutches
Wight		12 kg	15 kg	39 kg	30 kg
Cost		£1,300 rent/month	£70,000	£118,000	N/A

WalkON suit (Choi et al., 2017) exoskeleton has been designed to support people with lower body paralysis. Since the paraplegic user is expected not to generate any voluntary muscle force, Knee-Ankle-Foot orthosis (KAFO) is used to connect the pilot leg with the robotic device. KAFO will allow exoskeleton actuation system to transfer actuation force to the human body and add stability and safety measures to the user during motion. However, such an extra fitting to the exoskeleton design will add more complexity and cost, because KAFO needs to be specifically designed for each user. WalkON suit actuation system has four electric (brush-less) dc motors to drive hip and knee joints. One motor is controlled in position mode and the others controlled in torque mode to achieve motors synchronisation. WalkON suit controller strategy is based on joint trajectory generation, where the pilot can execute each motion phase by using the switches on the crutches. Real-Time Risk Assessment and Management fault detection algorithm is added to the control system; the algorithm can monitor the risk factors during operation to improve the safety measures of the exoskeleton and provide management plan if any fault detected.

Cyberdyne launched a series of HAL (hybrid assistive leg) exoskeletons. HAL-5 has been designed to physically strengthen healthy people and assist people with gait disorder to perform their daily tasks, where the assistive strategy is determined by using controller based on activity of the hip and knee (flexion/extension) actuators and recording walking pattern of the user. EMG, GRF, potentiometers, gyroscopes and accelerometer sensors are used to feed the controller with the essential data (Sankai, 2010). Modified version of HAL developed as a single leg version to support walking movement of hemiplegia patient (Kawamoto et al., 2009). The model was tested only on walking motion and during the experiment the differential steps between right and left leg increased and the wearer complained about the fitting and weight of the exoskeleton, and these issues considered as drawback of the HAL single leg version.

Recently exoskeleton applications and related research outcome have shown more promise and have gained trust of governmental authorities. Japanese government recognised the HAL exoskeleton as medical device, and in 2015 US department of veteran affairs announced that the ReWalk exoskeleton cost is covered for qualified veterans (Marinov, 2016). In February 2015 USA government food and drug administration (FDA) has classified exoskeletons as class II device (Government Publishing Office, 2015), but the FDA identified some technical drawbacks and risks in current applications of exoskeleton such as:

- Instability, falls and related injuries.
- Battery failure.
- Electrical interference.
- Device failure and unintended movement.
- User error.
- Change in blood pressure.
- Skin effects and soft injuries.

Exoskeleton robotics developments are still considered by researchers as challenge with many technological issues. Lightweight, energy consumption and exoskeleton design aspects are essential to the user adaptability and functionality, but more sensors and actuation used in the exoskeleton device will lead to more operating complexity and high power consumption (Viteckova et al., 2013). Exoskeleton prices vary between \$100,000 to \$130,000 (Mertz, 2012). This range of cost is out of reach for many people. Therefore, one of the challenges and motivations in exoskeleton developments is to make them cheaper and affordable by considering the technology selection and exoskeleton design.

2.4 Summary

This chapter has presented an overview of exoskeletons and wearable robotics. The main focus was on orthotic lower limb exoskeleton key technologies and applications. Lower limb exoskeleton design considerations; hardware structure, control strategies and related human biomechanics are reviewed to highlight gaps and drawbacks in recent developments. Several lower limb exoskeletons have been designed to support people with mobility disorder, some are available commercially and others are published as prototypes. However, independent review and analysis in medical and engineering aspects are not widely available. Independent review will help to understand in details the efficiency of the exoskeleton technology, and will help developers and researchers to overcome the drawbacks in different aspects. Additionally, there is lack of details in published work specifically in mid-level and low-level control. Design of a control strategy to assist people with gait disorder is essential part of this project. Therefore, reviewing and understanding the implementations of intelligent control algorithm will help to overcome the complexity of exoskeleton system.

Chapter 3: Modelling of humanoid and single leg exoskeleton

3.1 Introduction

Modelling and simulation facilitate designers to test and evaluate their design performance by using virtual rather than physical prototype. The benefits of using virtual prototype are to reduce cost and time and provide immediate feedback on design assessment. Furthermore, simulation is important for designing a system with different components (electrical, mechanical, embedded control, etc.) to insure the system is coupled to achieve optimal performance (Sinha et al., 2000). Mathematical representations of nonlinear dynamic systems which include mechanical and electrical components is complex. Therefore, Computer aided design (CAD) is used in this study to model humanoid and exoskeleton coupled system. Modelling virtual prototype with aid of CAD tools to simulate the mechanical characteristics of real prototype, by selecting the correct features such as properties, heights and widths, materials, masses, frictions and gravity factor.

This chapter provides a description of modelling a single leg exoskeleton and humanoid system to perform mobility functions such as walking, standing from sit position and sitting down from standing position. CAD models of the humanoid and exoskeleton are developed in SOLIDWORKS software. MSC. visualNastran 4D (MSC.vN4D) virtual environment software is used to assemble and configure CAD models according to the required mechanical characteristics. Additionally, Simulink is used to connect MSC.vN4D with MATLAB to develop the control strategy and implement simulations.

3.2 SOLIDWORKS

SOLIDWORKS is 3D CAD software developed by Dassault Systems. The robust 3D design capabilities provided by SOLIDWORKS allows users to design detailed 3D parts, assemblies from 2D sketches and complex surfaces (Dassault Systèmes SolidWorks, 2016). SOLIDWORKS was selected in this research to design 3D segments and realistic limbs of the humanoid model according to human body parameters of height and weight given by Winter (2009). The exoskeleton was designed in SOLIDWORKS and incorporated to the humanoid to assist the right side of the lower body. Humanoid and exoskeleton segments were exported and assembled in MSC.vN4D.

3.3 MSC. visualNastran 4D (MSC.vN4D)

MSC. virtualNastran 4D (MSC.vN4D) is a virtual environment developed by MSC Software to design and assemble 3D parts using engineering tools. MSC.vN4D simulation properties and design tools allow realistic response to external disturbance forces, as well as interactions between bodies and gravity factor (MSC Software, 2003). The software is used in this research to avoid the complexity of using mathematical model of human musculoskeletal system. Therefore, humanoid and exoskeleton models are assembled in MSC.vN4D with applicable kinematic characteristics reflecting real human dynamics during the simulation and reacting to the external forces, for example gravity. Furthermore, MSC.vN4D has many capabilities to analyse and evaluate the design through simulation in virtual environment (MSC Software, 2004), such as:

- Torque, force, velocity and friction measurements.
- Vibration, stress, buckling, heat transfer and impact analysis.
- Interface with Simulink to implement control system.

MSC.vN4D tools have the capability to structure mechanical design by connecting rigid bodies using different type of constraints shown in Figure 3.1. Humanoid and exoskeleton segments are assembled by selecting the appropriate type of constraint assigned by the control system to achieve the required motion. Type of constraints selected represent the nature of body part movements, in terms of axes direction and joints dynamics. Active joints of the humanoid lower limbs and exoskeleton such as hip, knee and ankle are defined as revolute motors. Meanwhile, revolute joint constraint is used to represent other passive joints, and rigid joints are used to connect static body segments during simulation.

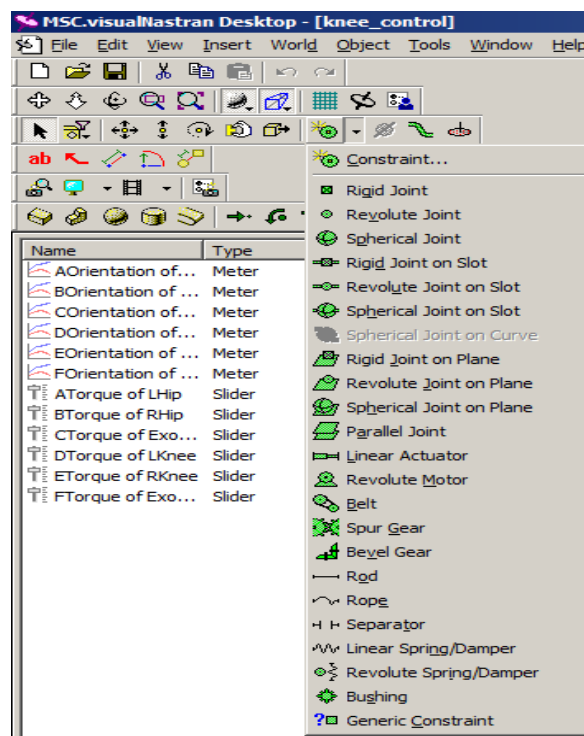


Figure 3.1: constraints selection

Testing and evaluating the design behaviour under realistic condition in virtual environment is important before implementing the physical prototype. MSC.vN4D tools allow to modify the properties of the humanoid and exoskeleton segments, such as material specifications, position, velocity and geometry properties to replicate the physical prototype. During simulation in virtual environment the humanoid and exoskeleton are subject to external force factors such as friction and gravity. Therefore, modifying CAD models

properties to replicate physical prototype is essential, to ensure the real environment is simulated properly. Figure 3.2 shows the body properties toolbox available in MSC.vN4D software. Further description of the humanoid and exoskeleton segments will be discussed in the next section.

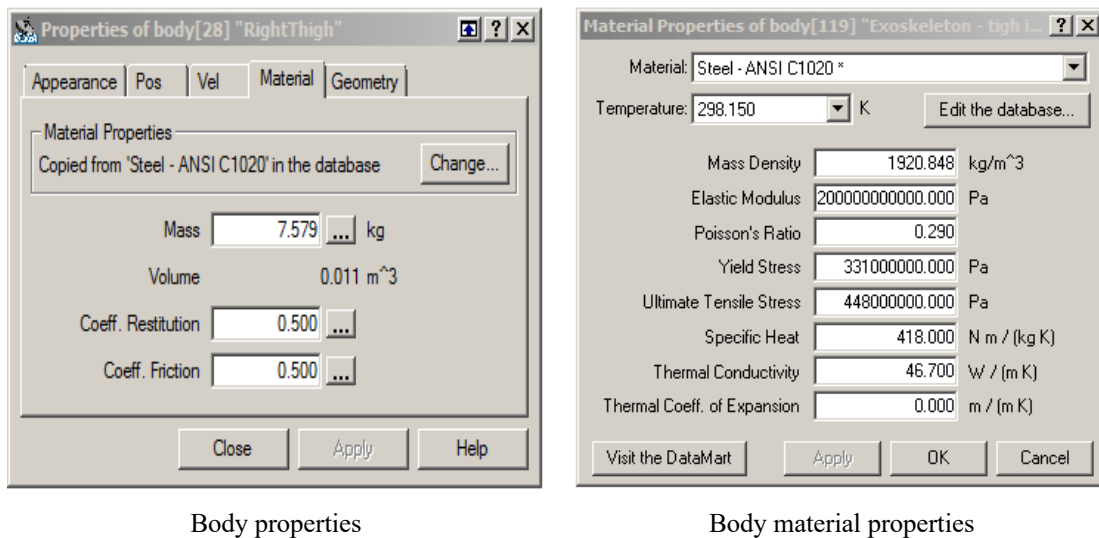


Figure 3.2: Body customisation tools

In this work, MSC.vN4D is chosen for three main reasons. Firstly, exoskeleton and humanoid segments designed in SOLIDWORKS can be exported and assembled in MSC.vN4D. Secondly, the software has measurement features for measuring position, torque, force, and orientation of the humanoid and exoskeleton joints during the simulation process. These features will allow to analyse the system behaviour and stability during the simulation process. Finally, the measurement parameters are used as inputs and outputs by linking MSC.vN4D and MATLAB Simulink to control the system, visualising and observing the motion of the system during the simulation process. Table 3.1 summarises the control measurement signals available in MSC.vN4D package. Each joint in the exoskeleton and humanoid is defined by control signal as an input and meter signal as an output. The control mechanism designed in MATLAB Simulink will determine control measurement signal selection during the integration process.

Table 3.1: Control measurement signals

Control (input)	Meter (output)
Force	Position
Length	Velocity
Velocity	Acceleration
Torque	Linear momentum
Rotation	Orientation
Rotation velocities	Angular velocity
Rotation acceleration	Angular acceleration

3.4 Model Design

3.4.1 Humanoid

Anthropometry measurement technique is used to develop and evaluate engineering design and application of human subject. Several researchers have studied human physical characteristics such as motion analysis. Motion analysis includes a description and analysis of human movements, visualisation of motion under external forces and computer simulation (Bjornstrup, 1995). Anthropometric data reported by Winter (2009) is the most prevalent and valid data for motion analysis. The anthropometric data defines each parameter of the body parts, such as volume, length, density and centre of mass.

In this work, a humanoid model of 74 kg in weight and 1.69 m in height was considered. The humanoid model is designed to simulate human body characteristics such as width, height and weight, and replicate human physical appearance and movements according to the anthropometric data shown in Figure 3.3 (Winter, 2009). The humanoid model design based on modified segments surfaces adopted from existent humanoid model (Cardero, 2012). The segments were adjusted in SOLIDWORKS to create solid parts and align each part origin according to the ‘world’ origin in MSC.vN4D environment.

Humanoid segments were exported to MSC.vN4D to join related segments through a set of joints, and amend their characteristics according to the anthropometric data given by Winter (2009). Humanoid design dimensions are shown in Table 3.2.

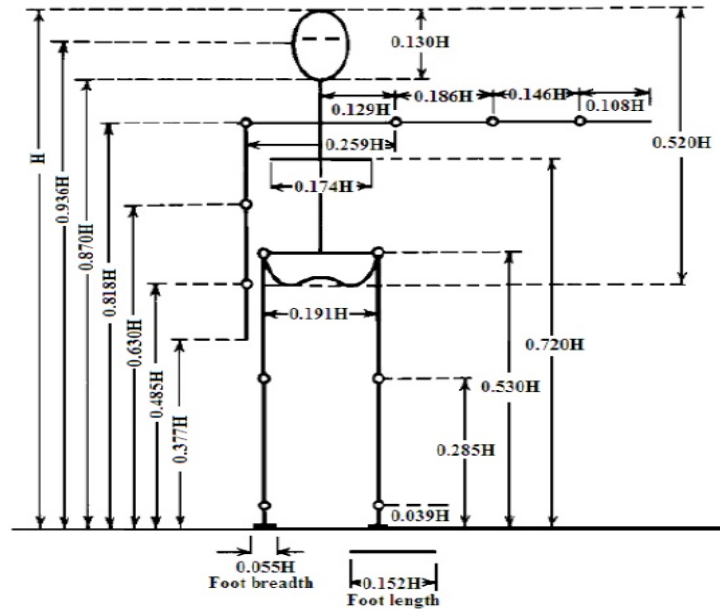


Figure 3.3: Anthropometric dimensions of human model (Winter, 2009)

Table 3.2: Humanoid model segments mass and length

Body segment	Length (m)	Mass (kg)	Mass percentage
Head and neck	0.35	6.64	8.10%
Upper arm	0.295	2.24	5.6%
Forearm	0.36	1.28	3.2%
Hand	0.202	0.48	1.2%
Trunk	0.575	37	49.70%
Upper leg	0.54	8	20%
Lower leg	0.48	3.72	9.3%
Feet	0.12	1.16	2.9%
Pelvis	0.25	11.6	-

Humanoid body segments assembly was implemented in MSC.vN4D by using different joint constraints such as revolute joint, revolute motor and rigid joints with respect to hip, knee and ankle anatomical position. Table 3.3 shows types of joint constraints used to connect humanoid body segments. Those were selected and modified to allow humanoid active joints to move in certain DoF. The humanoid model has 14 joints: active, passive and rigid, that allow the humanoid to move in sagittal plane, y axes and frontal plane, x axes, while transversal plane, z axes is barred. Lower body movement is the main focus in this project. Therefore, revolute motors are selected to control hip, knee and ankle joints in forms of orientation and Torque. Based on human kinematic properties restrictions shown in Table 2.2, lower limbs Joints limits were chosen according to those specified by Low (2011). Figure 3.4 shows different views of the developed humanoid model considered in this research. The humanoid model was tested in MSC.vN4D environment by implementing predefined trajectory control to validate humanoid performance.

Table 3.3: Humanoid model joints

Joint	Joint constraint	Control parameter	axes	Degree of freedom
Head	Rigid	-	-	0
Neck	Rigid	-	-	0
Shoulder	Revolute joint	-	Y	1
Elbow	Revolute joint	-	Y	1
Wrist	Revolute joint	-	Y	1
Waist	Revolute joint	-	Y	1
Hip	Revolute motor	Torque/orientation	Y	1
Knee	Revolute motor	Torque/orientation	Y	1
Ankle	Revolute motor	Torque/orientation	Y	1

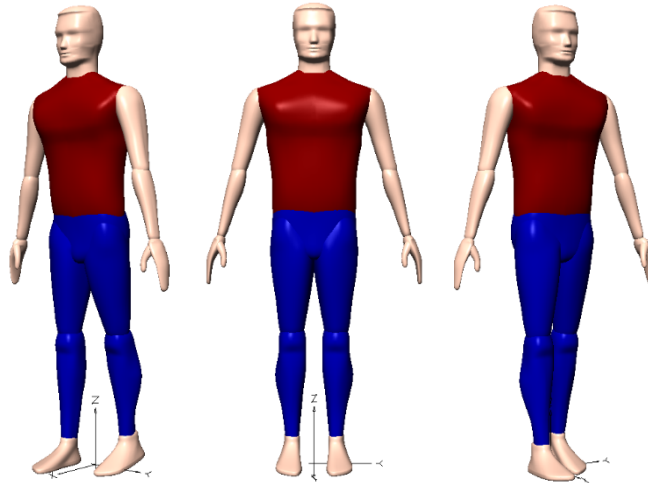


Figure 3.4: Different views of the humanoid model

3.4.2 Exoskeleton

Exoskeleton structural design is based on several aspects such as, application, lower or upper body support and alignment of the exoskeleton and human joints rotation axes. According to Kazerooni (2006), exoskeletons can structurally be classified as anthropomorphic, quasi-anthropomorphic or non-anthropomorphic based on design structure of the rotation axes alignment of the exoskeleton and human joints. Anthropomorphic exoskeleton structure (Figure 3.5a) is aligned with human lower limb joints; each exoskeleton joint rotation axes is aligned with human joints rotation axes to allow the exoskeleton to follow user movements in different degrees of freedom and range of movements at the same time. Soft exoskeleton suit is an example of anthropomorphic exoskeleton. Quasi-anthropomorphic exoskeleton structure design (Figure 3.5b) is aligned with human lower limb, but different joints alignments between human and the exoskeleton in terms rotation axes. Quasi-anthropomorphic exoskeleton structure allows the operator to move in designated degrees of freedom and range of movements in relation to the exoskeleton joints rotation axes. Non-anthropomorphic exoskeleton structure design (Figure 3.5c) does not correspond to human lower limb joints, and the structure design based on the dynamics of the exoskeleton device and distribution of masses. This structure design is used

in applications that focus on improve performance and user protection i.e. industrial and load augmentation exoskeletons.

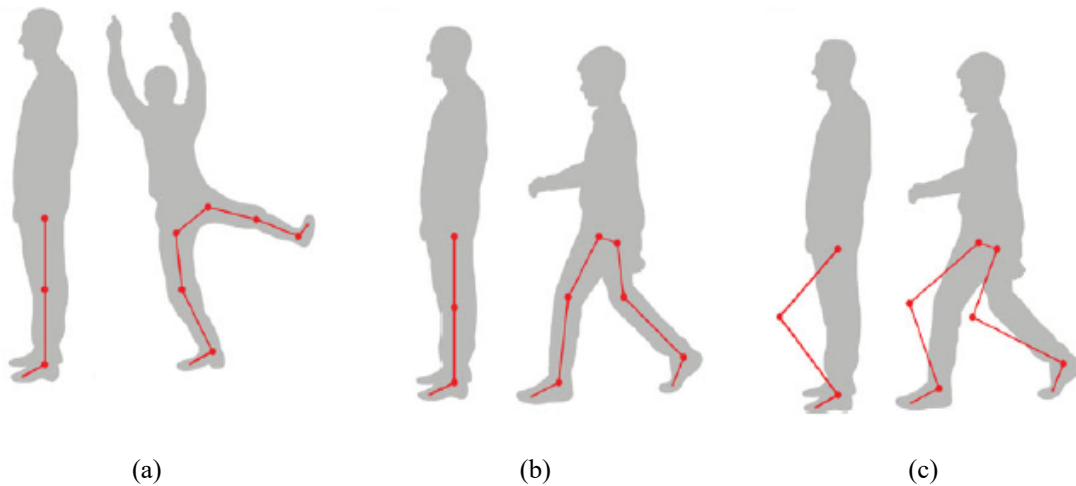


Figure 3.5: Exoskeletons structure: a) Anthropomorphic, b) quasi-anthropomorphic, c) non-anthropomorphic (Viteckova et al., 2018)

The concept of the exoskeleton design in this research is based on supporting people with hemiplegia paralysis to restore gait disorder. Hemiplegia patient suffers from paralysis on one side of the body, consequently quasi-anthropomorphic exoskeleton structure is designed to support one side of human lower extremity. Since weight, system complexity and power consumption aspects are considered as drawbacks in exoskeleton devices, the single leg exoskeleton design is aimed to reduce the weight of the wearable device and controlled joints. Furthermore, lightweight and less controlled joints lead to less power consumption and reduced system complexity.

At the first stage of this research and for the purpose of testing and evaluating humanoid model, simple exoskeleton structure was designed and assembled in MSC.vN4D by using different body shapes and constraint tools. The exoskeleton was designed to fit the right side of wearer and actuate hip and knee joints and support human back. Hip and knee joints of the exoskeleton were set to be parallel in position with human hip and knee joints and rotate in the sagittal plane (Y axes), while (X and Z axes) were locked to avoid any

excessive dynamics during simulation. Revolute motors are used to actuate exoskeleton hip and knee joints during the simulation process. Figure 3.6 shows different positions of the exoskeleton attached on the right side of the humanoid leg.

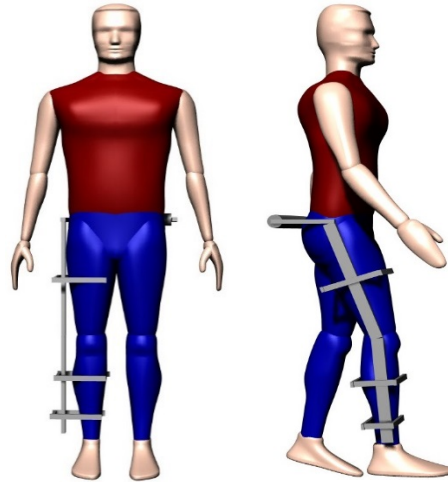


Figure 3.6: Humanoid and single leg exoskeleton in different positions

Due to limitation in MSC.vN4D body design tools, it was difficult to develop an exoskeleton model that imitate real time exoskeleton device in terms of active joints positions, physical support to other parts of the lower extremity and alignment with humanoid leg. Therefore, the exoskeleton model developed in the first stage of this work was upgraded to more realistic CAD model. The exoskeleton model was adopted from an open source library (Stratasys, 2016). The adopted exoskeleton model was dismantled and modified in SOLIDWORKS to create the required segments that suit the single leg exoskeleton structure design. The modified components were exported and assembled in MSC.vN4D, where segments dimensions selected according to the humanoid dimensions. Meanwhile, segments weight and material type were selected to ensure exoskeleton is as lightweight as possible. Table 3.4 presents the components of the single leg exoskeleton, constraints implemented in MSC.vN4D to represent active joints, links between exoskeleton segments and weight of each component. Figure 3.7 shows different views of the upgraded single leg exoskeleton model utilised in this research.

Table 3.4: Exoskeleton structure components

Exoskeleton component	Constraint	Link	Weight (kg)
Waist support	Rigid joint	Back-Stomach	3
Hip Joint	Revolute motor	Waist support-Thigh support	0.5
Thigh support	Rigid joint	Thigh belt-Thigh support bar	2
Knee joint	Revolute motor	Thigh support-Leg support	0.5
Leg support	Rigid joint	Leg belt-Leg support bar	2.5
Ankle joint	Revolute motor	Leg support-Shoe	0.4
Shoe	Rigid joint	Shoe-Humanoid foot	0.8

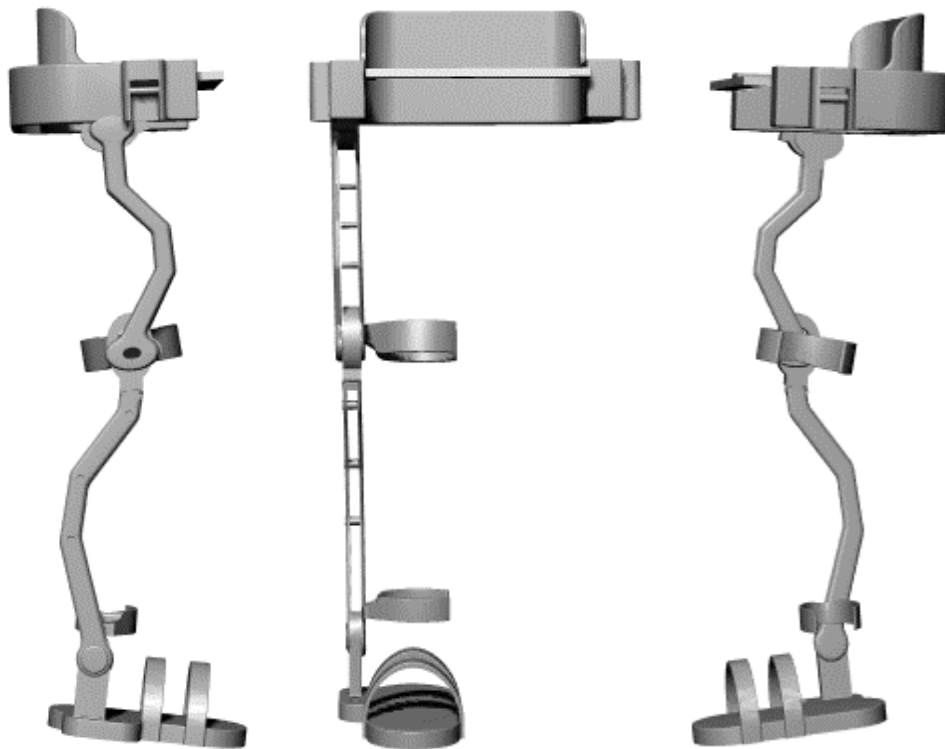


Figure 3.7: Different views of the single leg exoskeleton model

In MSC.vN4D software, the exoskeleton model was coupled to the humanoid right leg at waist by belt, at foot through shoe, and straps to hold and support leg and thigh while in motion. Waist belt, leg and thigh straps are configured to collide with the humanoid leg. These configurations allow physical interaction and provide force to support humanoid leg during motion tasks. Hip, knee and ankle joints of the exoskeleton are set to be parallel in

position with the humanoid joints, and revolute motors are selected to drive each joint by torque in the sagittal plan (Y axes). Figure 3.8 shows different positions of the single leg exoskeleton model attached to the humanoid right leg.

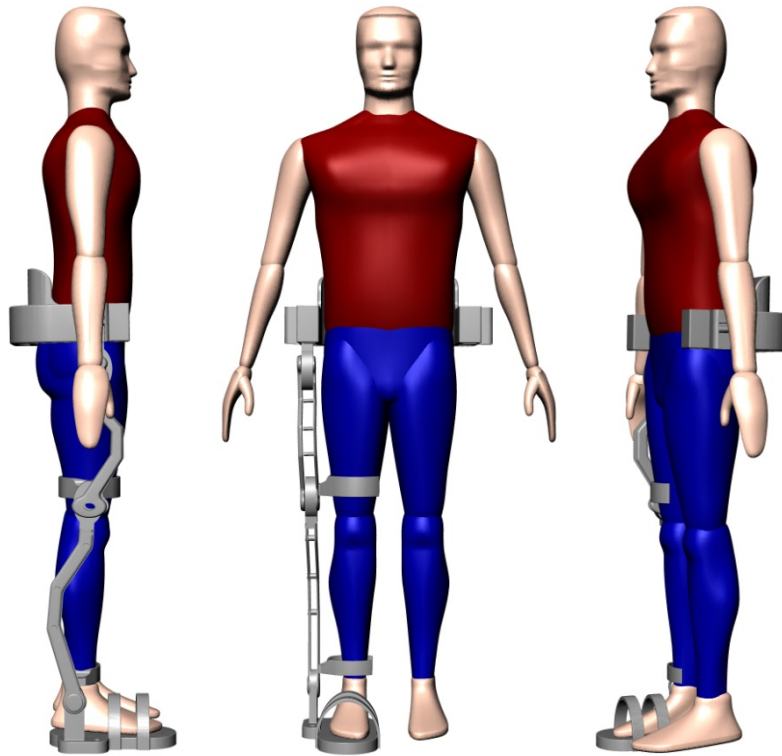


Figure 3.8: Humanoid and single leg exoskeleton in different positions

3.4.3 Models integration in MSC.vN4D and MATLAB Simulink

Controlling and simulating the exoskeleton and humanoid system in virtual environment is one of the objectives in this research. Therefore, integrating MSC.vN4D with MATLAB Simulink is important to allow the humanoid and the exoskeleton models to communicate in MSC.vN4D by applying closed-loop control. MATLAB can offer variety of tools to implement and investigate various control strategies and evaluate their implementation. Moreover, linking MSC.vN4D with MATLAB Simulink will provide instant measurement feedback and visual assessment of the system dynamics.

MSC.vN4D software was selected because it has the ability to interface with MATLAB Simulink, the interface allows data to be sent and received from MATLAB by

inserting vNPlant block from Simulink library. The vNPlant block allows to include the humanoid and exoskeleton models in Simulink environment by selecting MSC.vN4D file extension (WM3). Meanwhile, control measurement signals configured in MSC.vN4D as inputs and outputs (Table 3.1) can be selected to represent inputs and outputs of the control system created in MATLAB Simulink. In this study, torque is selected for most cases as a control parameter to actuate the revolute motors that represent active joints of the humanoid and exoskeleton, and orientation meter is selected to measure joint displacement in different axes. Figure 3.9 presents options of block parameters of input controls and output meters through vNPlant block in Simulink. Figure 3.10 shows a simple example of connecting MSC.vN4D with MATLAB Simulink by including vNplant block in the control diagram. The humanoid and exoskeleton system dynamics can be observed in MSC.vN4D when the simulation process is initiated in Simulink.

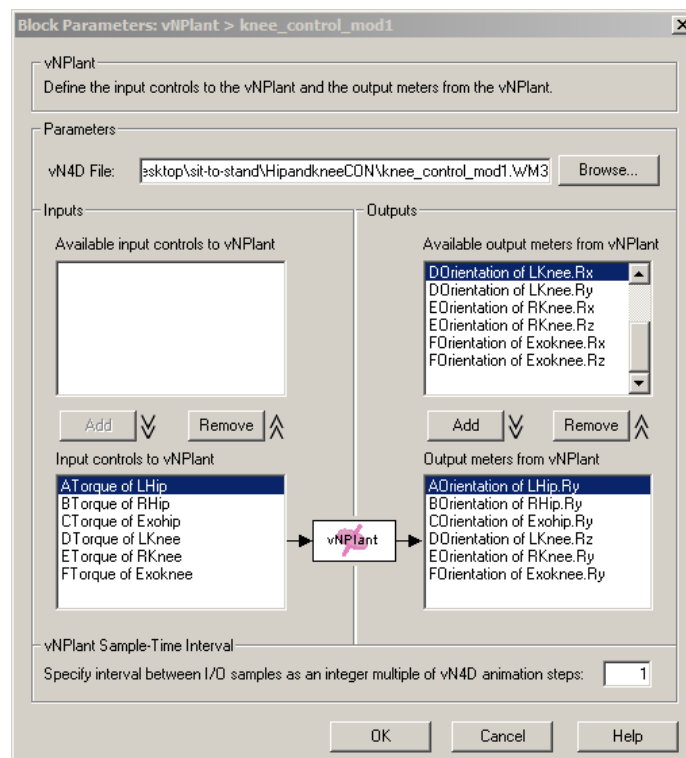


Figure 3.9: MSC.vN4D plant in Simulink

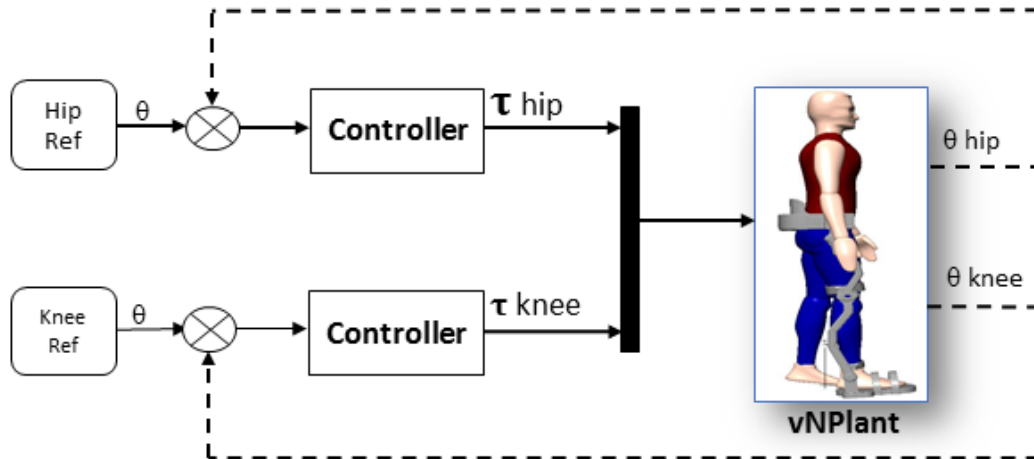


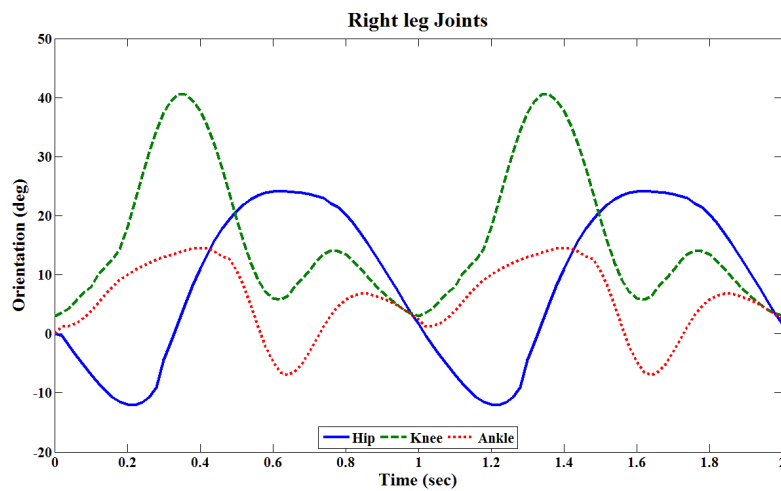
Figure 3.10: Simulink implementation of vNPlant

3.4.4 Humanoid and exoskeleton models validation

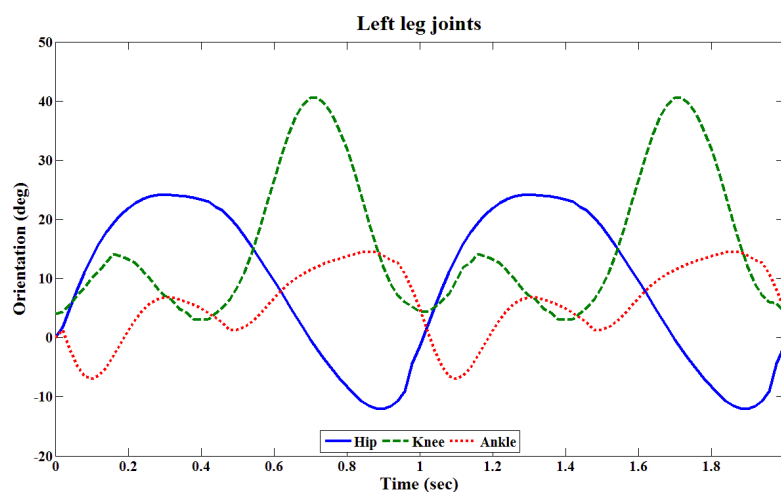
Following the assembly and integration process of the humanoid and exoskeleton models presented in the previous sections, simulations were implemented in MSC.vN4D to validate the kinematic structure of the humanoid and exoskeleton models. At this stage, simulations were carried out without utilising joints controllers, instead, orientation signals were used as a direct input to the system to actuate hip, knee and ankle revolute joints and orientation meters were assigned as an output to measure the actual joint position.

The orientation signals represent the kinematic data of the lower limb joints (flexion/extension) in the sagittal plane during walking, standing up and sitting down movements. The kinematic data of walking adopted from different gait analysis sources (Kirtley, 2005; Whittle, 1996) and the kinematic data of standing up and sitting down are based on analysis of sit-to-stand normative data adopted from (Kerr et al., 1997; Kralj et al., 1990). The kinematic data were examined and modified in terms of cycle duration, speed, initial angle position and joint displacement step size to achieve symmetric movements pattern between the humanoid model lower limbs and used as reference trajectories.

Humanoid and exoskeleton models were simulated in MSC.vN4D to perform walking, standing up and sitting down movements through MATLAB Simulink as described in section 3.4.3. Figure 3.11 and Figure 3.12 shows the lower limb joints orientation during two cycles of walking and complete cycle of standing up and sitting down movements. For the walking movement, simulation results demonstrate that symmetric motion have been achieved between the corresponding joints during the two cycles. However, for the standing up and sitting down movements, hip and knee joints of both sides of the leg are expected to follow the same trajectories while the ankle joints are considered as passive.



(a) Right leg



(b) Left leg

Figure 3.11: Lower limb joints orientation during two gait cycles

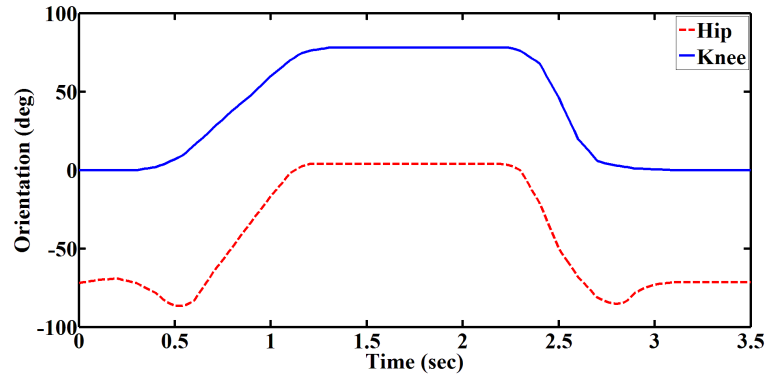


Figure 3.12: Hip and knee joints orientation trajectories of standing up and sitting down

3.5 Summary

This chapter has presented the approach utilised to design CAD models of a humanoid and single leg exoskeleton. Humanoid and exoskeleton design has been examined to ensure they replicate reality during simulation. Moreover, incorporation of humanoid and exoskeleton models has been implemented and simulated in virtual environment to evaluate their behaviour while being controlled, and to achieve the desired objective of providing mobility assistance for hemiplegic people.

A description of software capabilities used to design and assemble the CAD models has been included, along with a justification of model structure design such as, segments modification, components selection and actuation system.

Finally, the integration methodology to connect MSC.vN4D virtual environment with MATLAB Simulink has been explained. Integration mechanism is an important part of this work, since it forms a platform to implement and test control strategies planned in this research.

Chapter 4: Control strategy of the humanoid and single leg exoskeleton

4.1 Introduction

This chapter presents the development of humanoid and single leg exoskeleton system control strategies. Two types of controllers are considered, namely Proportional Integral Derivative (PID) and PD type fuzzy logic control (FLC). The development of the control strategy in this work is based on assisting exoskeleton user with one side hemiplegia in their mobility tasks, such as standing from sitting position, sitting from standing position and walking. The performances of the controllers are examined and assessed by comparing the output torque and trajectory tracking results.

Additionally, an optimisation algorithm, namely Spiral Dynamic Algorithm (SDA) is implemented to tune the controller parameters and achieve minimum root mean square output error.

4.2 Control strategy

Designing the controller for the humanoid and exoskeleton system is one of the main objectives of this research. In order to achieve the functionality and stability of the system, investigations are carried out to determine the system control method. The main goal of controlling the exoskeleton is to output and regulate the required torque to assist hemiplegic patient during walking and sit to stand movements.

Human intelligent control system is more advanced than recently developed control systems, therefore it is difficult to design a control system that can match human functions.

However, developing a control strategy for a coupled system is one of the challenges in this research. The key characteristics of the exoskeleton assistive strategy are, to deliver certain amount of assistive force to compensate for the lack of strength in order to restore mobility disorder, and to provide stability and safety measures for the user to avoid mobility complications.

Muscles and tendons are the main components in human biological actuation units. However, the level of force generated by human muscles depends on the condition and physical ability of each individual. In case of paralysis patients, muscles may include involuntary strong signals that influence the behaviour of controllers based on biological signals to provide motion support (Kawamoto et al., 2009). A review by Olney and Richards (1996) has discussed the characteristics of hemiparetic gait following stroke. The study has reported several experiments of muscle activity classifications measured by EMG. In many cases, the results show that EMG signals were inconsistent, out-of-phase, and with inter-individual variation. Based on the aforementioned facts about EMG, it is not possible to rely on the biological signals of muscles activity to estimate the support needed for the exoskeleton user.

Generally, the characteristics of exoskeleton systems shows that it is complex and non-linear system. The main reason is that, the orthosis device has to adapt to several factors such as human physical condition and complex manoeuvres. Humanoid and exoskeleton models are simultaneously driven by hip, knee and ankle joints, guided by the predefined gait trajectory to achieve the required tasks. However, due to coupling mechanism of the system, interaction forces between humanoid and exoskeleton parts will add complexity to the joints performance to follow predefined gait trajectory. Therefore, it is necessary to utilise a control algorithm to control the output trajectory and overcome complexity and non-linearity of the system.

A conventional PID controller was implemented to control the humanoid and exoskeleton system in a feedback loop, by regulating the joints torque and tracking the desired position of each joint. Nevertheless, it is difficult to obtain optimal results for most cases and maintain accuracy in position control. Additionally, dynamics of the exoskeleton and humanoid segments are interdependent, so it is complicated and time consuming to tune PID parameters through manual methods. Consequently, intelligent algorithm such as fuzzy logic control is used as supplementary control strategy to address such a complex and non-linear system. SDA optimisation algorithm is used to obtain optimum control parameters and achieve minimum root mean square error (RMSE).

4.2.1 PID controller

PID control is one of the common control algorithms employed by industrial systems. PID controllers are widely used because they are simple to implement, reliable and easy to tune. Additionally, it can provide robust performance to system uncertainties and it has proven to be advantageous when the controlled model is not represented mathematically. PID control algorithm measures the difference between the actual signal of the system output and the desired signal. The difference i.e. error ($e(t)$) is used as an input to the control system, where control action is generated to lower the error to almost zero (Ogata, 2010; Sung et al., 2009). The PID controller is comprised of three tuneable parameters, namely proportional K_p , integral K_i and derivative K_d as shown in Figure 4.1.

$$\text{Proportional term: } u(t) = K_p e(t) \quad (4.1)$$

$$\text{Integral term: } u(t) = K_i \int_0^t e(\tau) d\tau \quad (4.2)$$

$$\text{Derivative term: } u(t) = K_d \frac{de(t)}{dt} \quad (4.3)$$

where, $e(t)$ represents the variance of the set point input and the plant output, and $u(t)$ is the control output signal as a consequent to proportional, integral and derivative parameters.

The complete PID controller can be formed as:

$$U(t) = K_p e(t) + K_i \int_0^t e(\tau) d\tau + K_d \frac{de(t)}{dt} \quad (4.4)$$

Alternative representation to the integral and derivative gains can be formed as $K_i = K_p/T_i$ and $K_p = K_p T_d$, where T_i is the integral time and T_d is the derivative time (Ogata, 2010).

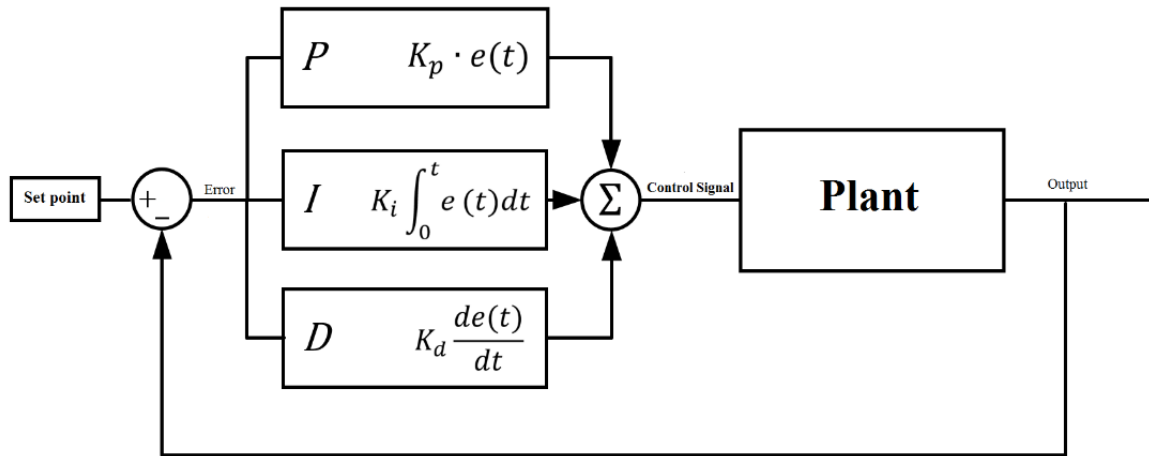


Figure 4.1: PID control system

As mentioned earlier, PID controller is comprised of three different variables: proportional, integral and derivative. Each variable could be implemented as independent controller. However, each variable has different outcome and advantages and disadvantages on the control action. Therefore, a mixture of P, I and D could poise the effect on the control action of each variable.

The proportional variable is basically an amplifier with tuneable gain known as K_p . It attempts to stabilise the system by regulating the control signal to reduce the system output

steady-state error and rise time. The steady-state error can be minimised by increasing K_p gain, but it could bring about oscillation to the system response (Ogata, 2010).

The integral variable used to remove or cutback the steady-state error by tuning the amplitude of the integral gain K_i . However, increasing or decreasing the integral gain could cause oscillatory response. Additionally, integral term increases system order which might lead to unstable system (Ogata, 2010).

The derivative variable is utilised to lower the overshoot of the response and increase system stability. It anticipates change of error and initialises corrective action to minimise the error. Combination of PID variables with measured gains could significantly minimise the error of the control signal (Ogata, 2010).

There are several methods used to obtain the optimal gains of the PID controller, such as Ziegler-Nicholas, Cohen-coon, trial-and-error and software tools. Trial-and-error tuning method helps to define suitable parameters of the controller, by examining the behaviour of the controller output signal. In order to achieve a successful trail-and-error parameter tuning, it is essential to inspect the effects of the parameters on the controller output behaviours. The following dynamic behaviours show the effect on the PID controller output in terms of the tuning parameters for step set-point changes (Sung et al., 2009):

- If the control output signal includes big oscillation, that means the proportional gain K_p is excessively large.
- If the control output signal includes overdamped response, that means the proportional gain K_p is excessively small.
- If the control output signal oscillates over the set-point more than below the set-point that means strong integral action.

- If the control output signal oscillates below the set-point more than over the set-point that means weak integral action.
- If the controller output signal includes several oscillation peaks from the beginning to the steady state phase, then derivative time T_d is too high. This is down to the amplification effect on the signal from a strong derivative part.

Additionally, to achieve an effective trial-and-error tuning while focusing to avoid the aforementioned dynamic behaviours, it is essential to keep the proportional gain K_p value as large as possible. Because the closed-loop dynamics tend to be slow if the proportional gain is not large enough.

4.2.2 Fuzzy logic control

Fuzzy set theory was proposed in 1965 by Lotfi Zadeh (1965). This theory is founded on the concept that any system, behaviour or decision making is not totally black or white, but a contrast of grey colour among them. The grey colour can be categorised as blacker or whiter, where categorisation of the grey colour builds on the previous condition of the white or black colour. Fuzzy logic has a feature that incorporates the system's uncertainty and nonlinearity. Moreover, non-statistical uncertainty is the type used to refer to the uncertainty in fuzzy systems, which is based on ambiguity, vagueness or imprecision. Non-statistical uncertainty or fuzziness is part of the system property and cannot be changed or determined by observations (Engelbrecht, 2007).

Fuzzy logic control (FLC) has shown great success in different applications in which conventional controllers have not been efficient or effective. Fuzzy logic has been applied successfully in several control systems, such as controlling lifts, traffic lights, home appliances, braking and gear transmission systems in vehicles and many others (Ross, 2010). In terms of computational intelligent method, fuzzy logic has the feature of being

close to human logic and decision-making. In addition, fuzzy logic implementation is effective in recognising the environment conduct and real system. In terms of theory and functionality, FLC proves its advantages over conventional control methods (Wang, 1993).

In this work, the humanoid and the exoskeleton models were developed using CAD tools as described in the previous chapter. The main reason to utilise CAD modelling, is to avoid the complex mathematical representation of the humanoid and exoskeleton dynamics. FLC is employed in this work, since mathematical model of the controlled plant is not needed. Furthermore, the following features of FLC strongly encourage the implementation of such a control method in this work:

- FLC is convenient for systems with complex mathematical representation, where the control system linguistic information can be determined by using human experts.
- FLC is a model free approach, where mathematical identification of the controlled system is not necessary.
- FLC can be appropriate for nonlinear systems due to fuzzy control nonlinearity components.
- FLC principles are easy to understand because it emulates human control strategy. Therefore, implementation of FLC in both software and hardware development is deemed as cost-effective and time saving.

Figure 4.2 shows the structure of typical FLC. The structure of the FLC is based on four important elements. The elements are fuzzification, fuzzy rule base, inference mechanism and defuzzification.

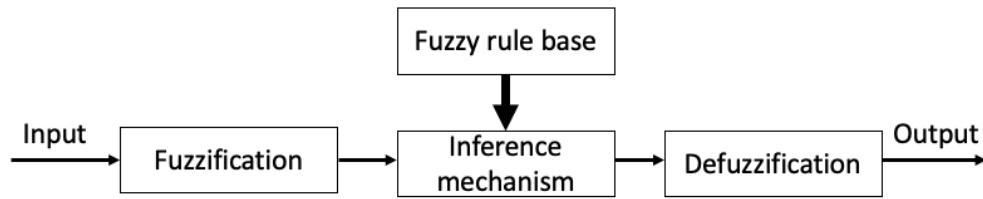


Figure 4.2: Structure of fuzzy logic controller

The first step in developing FLC is to distinguish the controlled system variables such as states, inputs and outputs. Then, it is important to split the universe of discourse for different fuzzy sets, and allocate each fuzzy set to a linguistic label, for example hot, warm and cold. The second step is fuzzification. This process contains converting crisp or numeric value into fuzzy set. The third step is inference mechanism, which involves mapping relationship between inputs and outputs by using logical approach, if-then rules. Defuzzification is the last step in the process, where linguistic variables are translated to crisp values to be as actual input to the plant.

Fuzzy set comprises of a membership function (MF) and universe of discourse U that locates all the elements in the universe of discourse to a membership value between 0 and 1 (Ying, 2000). If a fuzzy set is X , and u is a numeric data that is part of the universal set U , then $X: u \in U$ and the membership degree is $\mu_X(u)$, where μ_X defines if an element of U is part of X and to what degree. Membership functions can be represented by various shapes, such as Gaussian, Triangle and Trapezoidal. Figure 4.3 shows an example of triangle membership function with crossover point at $\mu_X(u) = 0.5$. Membership function scaling factor must be assigned to inputs and outputs in normalised interval $[0, 1]$ or $[-1, 1]$.

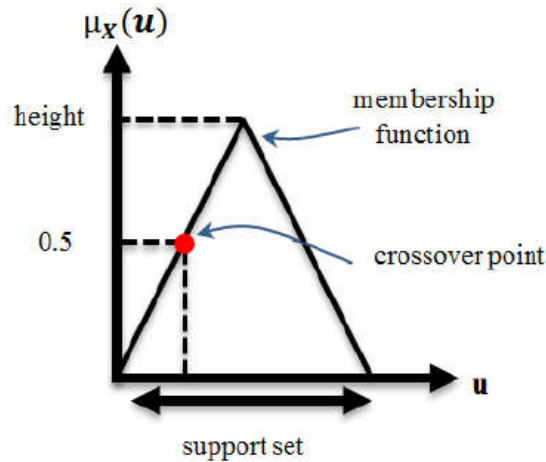


Figure 4.3: Triangle fuzzy membership function

Fuzzy rule base is considered as the core of fuzzy logic system. It is based on a collection of if-then rules. There are two important aspects in the fuzzy rule; the antecedent part (if-then) and the consequent part (outcome). Fuzzy rules are deduced from human knowledge and experience to form a set of linguistic statements that represent the dynamic behaviour of the system, by linking fuzzy input and output variables (Passino and Yurkovich, 1998). The number of total rules is specified by the number of inputs and linguistic variables allocated to each input. Therefore, FLC is suitable for different type of systems for example multi input multi output (MIMO), multi input single output (MISO) or single input single output (SISO) system.

The principle of fuzzy set demonstrates a logical method in formulating the linguistic variables imprecise and vague information (Wang, 1997). Fuzzy system linguistic variables are used to define the fuzzy variable that is associated with value of sentences or words in common language. Linguistic variables play important part in obtaining the fuzzy system rules (Passino and Yurkovich, 1998). The linguistic terms can be expressed in three different forms:

- Primary Term: this term is used to characterise the fuzzy sets, e.g. Short, Medium and Tall.

- Hedge term: is used as supplement term to the primary to describe more fuzzy sets, for example More, Most or Less.
- Connectives term: is used to determine the fuzzy set output based on the relation among the input variables and the operation. For example, And, Or and Not.

There are two main fuzzy inference methods widely implemented in fuzzy systems based on linguistic rules. These are Mamdani (Mamdani and Assilian, 1975) and Sugeno (Takagi and Sugeno, 1985) models. However, Mamdani is the most common method used in fuzzy system and fuzzy control (Wang, 1997). In the Mamdani method, the number of inputs and variables form the main factors used to define the number of rules. Additionally, the number of linguistic variables which can be included in the rules for condition and conclusion parts is not limited.

Based on fuzzy rules category, fuzzy systems can be classified into two groups: standard fuzzy system and functional fuzzy system (Passino and Yurkovich, 1998). Mamdani-type fuzzy rules are usually used in standard fuzzy system, because they are simple to develop from values and linguistic variables. Mamdani general form can be expressed as:

if x is A and y is B , then z is C

where x and y are the input, z is the output and A , B and C are the linguistic variables.

This type of fuzzy system is adopted in the development of fuzzy logic control strategy in this study. For example:

if $e(t)$ is NS and $\Delta e(t)$ is NS then $y(t)$ is Z

if $e(t)$ is PB and $\Delta e(t)$ is NB then $y(t)$ is PS

where $e(t)$ error and $\Delta e(t)$ change of error are the inputs, $y(t)$ is the output and NB (negative big), NS (negative small), Z (zero), PS (positive small) and PB (positive big) are the linguistic variables.

Functional fuzzy system is denoted as Sugeno or Takagi-Sugeno-Kang (TSK) fuzzy system. TSK adopt systematic approach to create fuzzy rules based on input-output data. Compared to Mamdani, the output of TSK fuzzy system is not considered as a linguistic variable but a crisp function of the input. TSK rules can be defined as:

$$\text{If } x_1 \text{ is } A_1^k \text{ and } x_2 \text{ is } A_2^k \text{ then } y^k \text{ is } B^k$$

The IF part of the rule in functional fuzzy system is similar to the IF-THEN in standard fuzzy system, however the THEN part is linear combination of the input variables $X = (x_1 \dots, x_n) \in U$ (Wang, 1997).

Mamdani standard fuzzy rules are commonly employed in control applications compared to functional fuzzy rules. This is because they are easy to deduce and implement by an expert, and the consequent parts are represented as fuzzy sets. Whereas, in TSK the consequent parts in functional fuzzy rules are a mathematical function. Therefore, it has more accuracy in terms of system and mathematical analysis.

Table 4.1: Fuzzy rules set

$e \backslash \Delta e$	NB	NS	Z	PS	PB
NB	PB	PB	PB	PS	Z
NS	PB	PB	PS	Z	NS
Z	PB	PS	Z	NS	NB
PS	PS	Z	NS	NB	NB
PB	Z	NS	NB	NB	NB

■ Group 1
 ■ Group 2
 ■ Group 3
 ■ Group 4
 ■ Group 5

Fuzzy rules set can be developed in a specific way according to the system desired performance and behaviour. Table 4.1 shows an example of fuzzy rules set which is presented based on the most extreme condition. In general, the controller must produce an opposite action to reverse the direction of the output closer to the set point for instance, if e and Δe are PB, then the control action is NB as located in group 5 region. In contrary, if both e and Δe are NB then control action is PB as allocated in group 2 region. The other two extreme system conditions, if e is PB and Δe is NB or vice versa, then the control action is Z, as the system is in a steady-state condition. Similar level of control action is applicable within group 3. In case smaller action is required for the reparation, then control action is applicable within group 1 and 4 regions. The arrangements of fuzzy rules set depends on the system performance which is problem dependent. Therefore, some systems may require wider range of fuzzy rules set. However, many controllers adopt the standard rule and similar arrangements shown in Table 4.1. In this work, the pattern of fuzzy rules shown in Table 4.1 is initially used and modified according to the system behaviour.

In order to formalise the output obtained in the inference mechanism, it needs to be defuzzified, that means to transform the linguistic variables into crisp values. Defuzzification plays essential role in the FLC process, by interpreting the controller output into a real signal that can be proceed by the plant, where the rule base and the physical system are linked (Chen and Pham, 2000). There are different defuzzification methods that can be used depending on the requirements of the application such as, Centre of Gravity (CoG), Max Membership, Mean Max Membership and Middle of Maxima. CoG method is used in this study for all the attempts of implementing the fuzzy logic controllers. CoG method is more convenient for feedback control systems due to smooth output transformation.

4.2.3 Proportional-Derivative based Fuzzy control

The efficiency and robustness of the controller plays essential role in obtaining fine and fast tracking. A fuzzy-based PD controller is employed in this work to reinforce the performance of the system, by combining the advantages of FLC and conventional PD controllers. A hybrid of PD parameters is integrated with FLC to form fuzzy-based PD controller. PD parameters are used to provide sensitivity and add more stability to the control system. Moreover, PD controller is capable to reduces the overshoot and allow the use of large gains by adding damping to the system. The derivative (D) action is utilised to reduce disturbances and maintain the output to desired one (Akkizidis et al., 2003). Figure 4.4 shows the application of fuzzy-based PD controller used to control a selected joint of the humanoid and exoskeleton system in order to achieve the desired joint position.

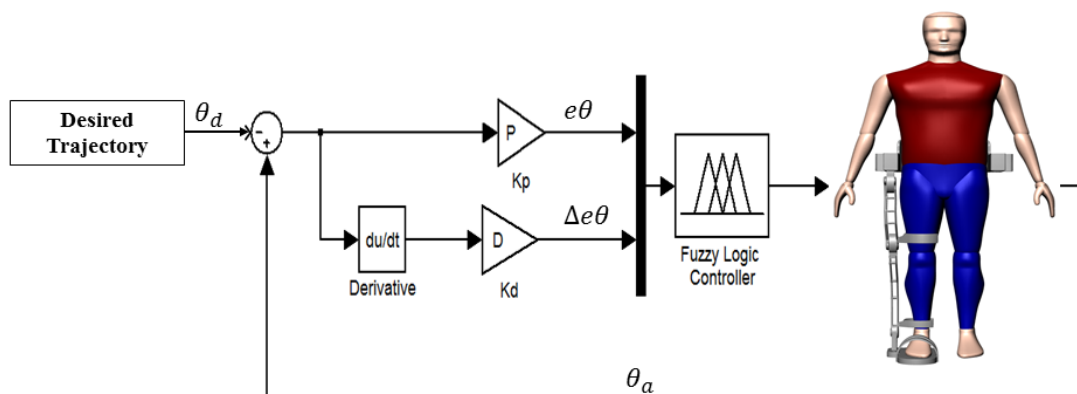


Figure 4.4: Simulink diagram of fuzzy-based PD controller

There are vital components in implementing fuzzy-based PD controller such as determining input/output variables, format of fuzzy rules, number of rules and optimal parameters for the controller. In order to utilise the PD parameters successfully, it is important to select the optimum scaling factors (SF) such as inputs and outputs, which can scale the universe of discourse. Input and output SFs are essential part of the fuzzy-based PD controller due to their influence on the control performance and robustness, which means tuning and optimisation of SFs is an important aspect in the control development (Mudi and

Pal, 1999). Therefore, an optimisation algorithm is used in this work to obtain optimal PD parameters optimal values.

4.2.4 Spiral dynamic optimisation algorithm

Research in optimisation algorithms is one of the most emerging interdisciplinary research fields. It can provide significant solutions to address various real problems in several areas (Zang et al., 2010). Defining the optimum control parameters is significantly important in control design criteria, which can enhance the system performance and the controller efficiency.

Spiral dynamic algorithm (SDA) has been presented by Tamura and Yasuda (2011a). The algorithm is inspired by the spiral pattern of natural phenomena such as hurricanes, DNA molecule, galaxies and nautilus shell, and its search strategy is based on the feature of logarithmic spirals. The initial development of SDA starts with two-dimensional problem model then it was improved into n-dimension general model (Tamura and Yasuda, 2011c). A comparison of SDA algorithm was carried with other verified search algorithms, such as Particle Swarm Optimisation (PSO) to prove it has efficient resolutions for two-dimensional problems with different types of benchmark functions. Tamura and Yasuda (2011b) developed spiral optimisation method for n-dimensional optimisation problems and compared with to PSO and differential evolution algorithm (DE). Simulation results of 100 runs for several benchmark problems shows that spiral optimisation was more effective than PSO and DE algorithms.

The SDA algorithm is simple and straightforward to execute with a small number of control variables, has fast convergence and good local search capacity (Benasla et al., 2014). SDA has several features which make it simple to implement, such as simple structure, fast computational speed and easy to programme. The searching mechanism of SDA includes

two features, diversification and intensification. Diversification occurs at the initial stage of the search procedure, where the search is based on exploration approach to locate a good possible solution in the global area. Intensification is the following stage, where the search points shift and converge around the good solution located at the global area to find better possible solution. This combination is effective technique on the search strategy to determine accurate solution. Figure 4.5 shows the adaptation of the logarithmic spiral as a model in the search strategy, where the diversification and intensification approach can be accomplished naturally by the spiral movements which are exponentially converged toward the spiral centre.

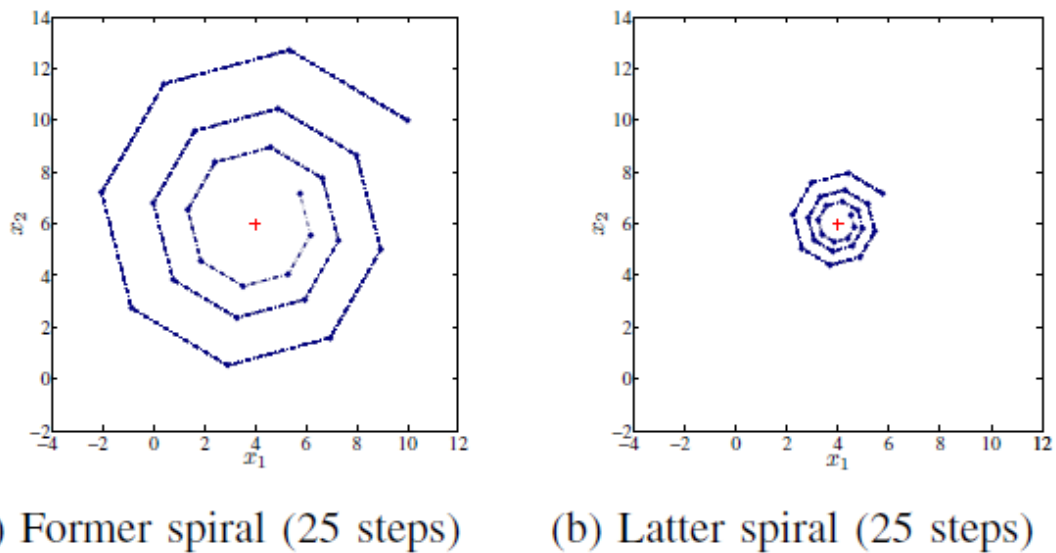


Figure 4.5: Trajectory of spiral search (Tamura and Yasuda, 2011)

In SDA, the searching agents move in anti-clockwise direction starting from the initial point to the next one towards the centre of the spiral. Meanwhile, the step size of the spiral motion will reduce gradually while approaching the centre of the spiral. This type of approach enables SDA to reach the global optimal solution for multi modal and uni-modal problems. In each iteration, the best fitness will be highlighted and used as a guidance in the spiral search. This approach will lead to faster convergence toward the optimal point in each iteration. Figure 4.6 shows different spiral search cases in respect to spiral radius (r) and

rotation angle (θ). Spiral radius and angular displacement parameters have a considerable impact on the performance of SDA in terms convergence speed and accuracy.

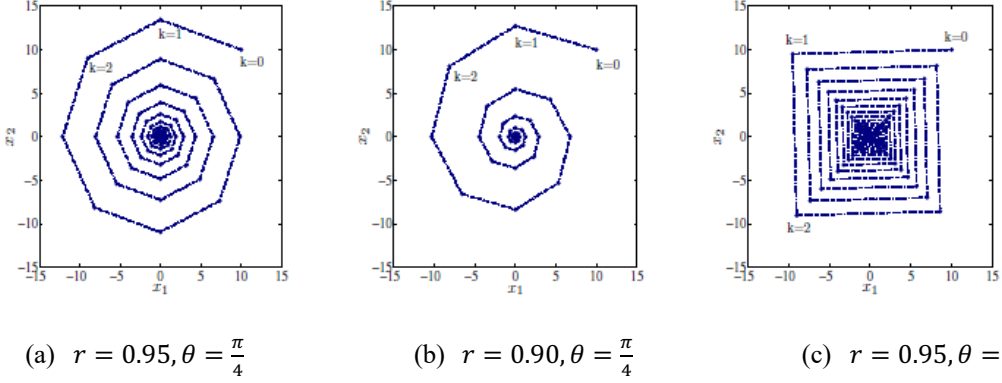


Figure 4.6: Different cases of spiral model behaviour (Tamura and Yasuda, 2011)

SDA mathematical model for n-dimensional problem can be expressed as:

$$x_i(k+1) = s_n(r, \theta)x_i(k) - (s_n(r, \theta) - I_n)x^*, i = 1, 2, \dots, m \quad (4.5)$$

where, the rotation angle θ is in the range $0 < \theta < 2\pi$, identity matrix is I_n , x^* is spiral centre, number of iterations is k , r is spiral radius $0 < r < 1$. Using $R^{(n)}(\theta_{1,2}, \theta_{1,3}, \dots, \theta_{n,n-1})$ the n-dimensional spiral model can be expressed mathematically as:

$$R^{(n)}(\theta_{1,2}, \theta_{1,3}, \dots, \theta_{n,n-1}) = \prod_{i=1}^{n-1} (\prod_{j=1}^i R_{n-1, n+1-j}^{(n)}(\theta_{n-i, n+1-j})) \quad (4.6)$$

Generally, r and θ parameters are the main factors in SDA performance where the searching points will conclude a result of one point. However, adding a number of iterations may affect the searching points to remain in the region of local optimum instead of the global optimum, and this will limit the searching points to converge toward the best global solution. This drawback in SDA is referred to as trapped at local optimum. Moreover, the computational time will be increased when high number of dimensions and variables are included in the algorithm, because the matrix size will be bigger in the spiral model. In this work, SDA is used as part of the control strategy to determine the best possible optimal

control parameters. However, the algorithm was implemented with consideration of the aforementioned drawbacks to reduce computational time and obtain the optimal solutions to enhance control performance. Table 4.2 presents a general description of the n-dimensional SDA pseudo code, which is used to generate and execute SDA code in MATLAB environment. The SDA process flow chart to calculate the objective function is presented in Figure 4.7.

Table 4.2: Pseudo code of SDA n-dimension (Tamura and Yasuda, 2011)

Step	Action
Step 0: Preparation	Select the number of search points $m \geq 2$, the parameters $0 < \theta < 2\pi$, $0 < r < 1$ of $S_n(r, \theta)$, and the maximum iteration number k_{max} . Set $k = 0$.
Step 1: Initialization	Set the initial points $\mathbf{x}_i(0) \in \mathbb{R}^n, i = 1, 2, \dots, m$ in the feasibility region at random and the centre \mathbf{x}^* as $\mathbf{x}^* = \mathbf{x}_{i_g}(0)$, $i_g = \arg \min f(\mathbf{x}_i(0)), i = 1, 2, \dots, m$.
Step 2: Updating \mathbf{x}_i	$\mathbf{x}_i(k+1) = S_n(r, \theta)\mathbf{x}_i(k) - (S_n(r, \theta) - I_n)\mathbf{x}^*$, $i = 1, 2, \dots, m$.
Step 3: Updating \mathbf{x}^*	$\mathbf{x}^* = \mathbf{x}_{i_g(k+1)}$, $i_g = \arg \min f(\mathbf{x}_i(k+1)), i = 1, 2, \dots, m$.
Step 4: Checking Termination Criterion	If $k = k_{max}$ then terminate. Otherwise, set $k = k + 1$, and return to Step 2.

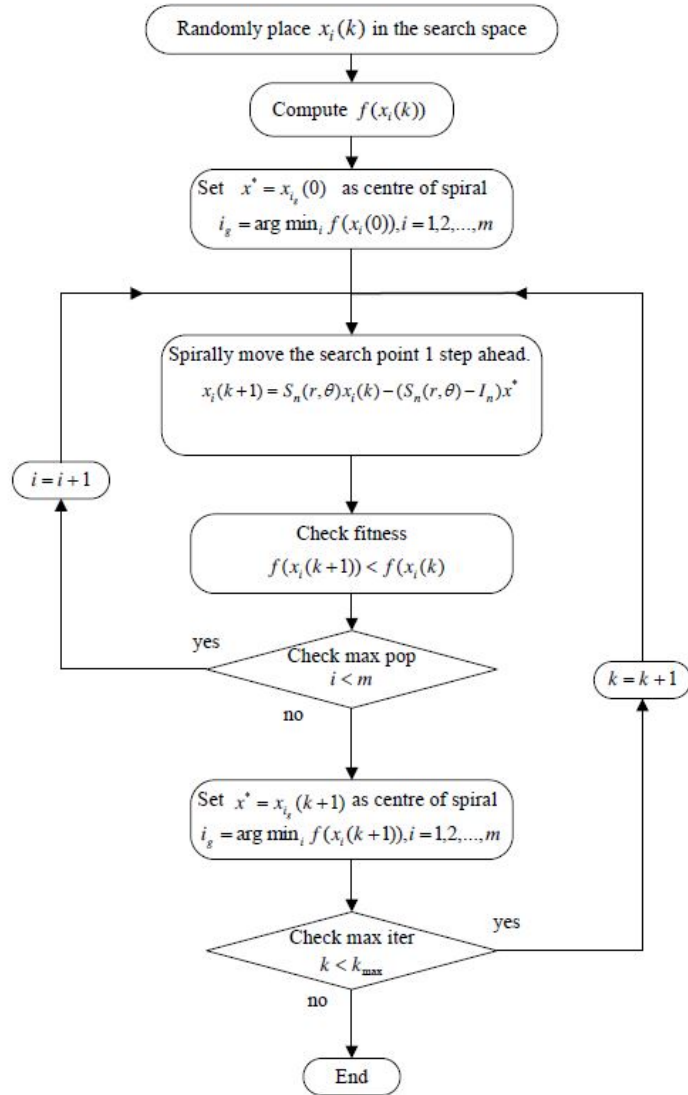


Figure 4.7: Flow chart of SDA process

4.3 Summary

In this chapter, a description of the control strategy employed to control the humanoid and single leg exoskeleton models has been presented. The description includes an overview of the control algorithms theory that involves the implementation process of the control strategy. Two different control algorithms are utilised to control the humanoid and exoskeleton system, namely PID and fuzzy-based PD controllers. The implementation process and results of the control strategies are reported in subsequent chapters.

A general description of spiral dynamics optimisation algorithm has been presented. The benefits of adopting optimisation algorithm within the control strategy has been highlighted, where control performance can be enhanced by obtaining the best possible optimal control parameters.

Chapter 5: Control of assistive single leg exoskeleton and humanoid for walking mobility

5.1 Introduction

Control and simulation of the single leg exoskeleton used to support hemiplegic patient during walking are investigated in this chapter. The investigation is carried out using actuated exoskeleton model incorporated with the right lower limb of the humanoid model. Two kinds of controllers are utilised to control the active joints of the humanoid and exoskeleton such as hip, knee and ankle. These are PID controller and fuzzy-based PD controller, developed in MATLAB Simulink to regulate the output torque that actuates the joints to the desired position. Control parameters are tuned by implementing SDA optimisation algorithm to achieve optimal values. Simulation of the humanoid and exoskeleton models is carried out in MSC.vN4D virtual environment software, where motions are visualised in graphic animation form. Predefine joints orientation is used as a reference, where system performance is evaluated by reference tracking with minimum error. Finally, control robustness is evaluated by applying disturbance impulse forces and different walking speeds.

5.2 Cycle of human gait

In order to control a system that is capable of recovering hemiplegic patient walking, it is important to study the mechanism of walking in healthy humans in terms of gait cycle, phases and duration. Walking is three dimensional movement, where the upper and lower

limb can move in three different axes (Vaughan et al., 1999) as shown in Figure 2.2 and Table 2.2. However, this study focuses on motions in the sagittal plane where most of the walking dynamic aspects take place.

Gait analysis is the study of human locomotion that includes description, measurement and human locomotion characteristics (Ghoussayni et al., 2004). The aim of gait analysis is to identify the phases of the gait cycle and determine the kinematic and kinetic parameters of the gait cycle. Gait analysis has been an essential method and assistive tool for describing human locomotion in many fields such as sport, rehabilitation and biomedical engineering (Tao et al., 2012).

Human gait cycle comprises of two phases, stance phase which refers to the actual stepping and swing phase where foot contacts the ground to support the other leg during swinging. Sequence of gait cycle phases and sub-phases are shown in Figure 5.1 adopted from (Hsu et al., 2008). Stance phase is composed of four sub-phases: loading response, mid-stance, terminal stance and pre-swing where the swing phase comprises of initial swing, mid-swing and terminal swing. Table 5.1 describes feet posture and the interval of each sub-phase during a complete gait cycle. A complete walking cycle with a single step for each leg takes approximately 1.1 second on average, taking into account the speed of the gait as 5 km/h and the length of the stride as 76 cm. However, the stance phase takes 60% of the gait cycle, whereas swing phase is 40% of the gait cycle (Physiopedia, 2016).

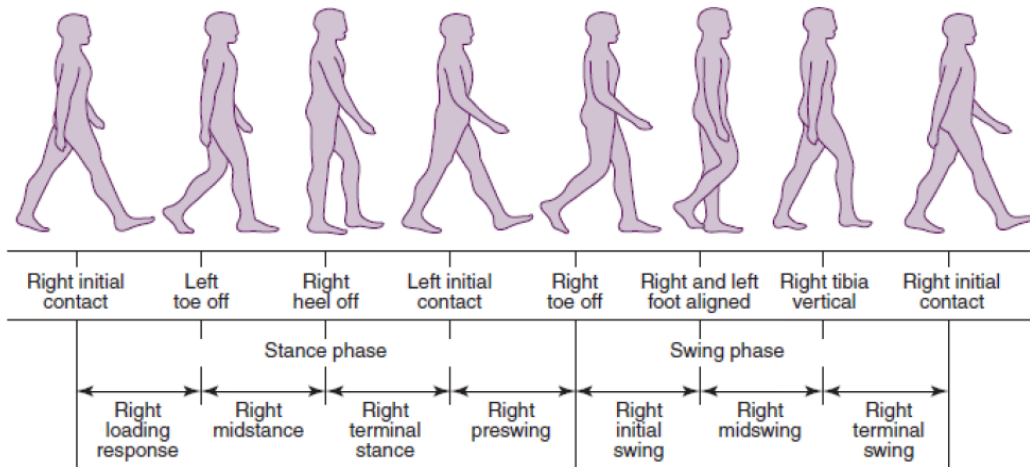


Figure 5.1: Cycle of human gait (Hsu et al., 2008)

Table 5.1: Gait cycle phases and sub-phases (Vaughan et al., 1999)

Phase	Sub-phase	Gait cycle percentage	Feet posture
Stance	Initial contact	0%	Right heel and left toe touch the ground.
	Loading response	0-10%	Body weight shifts to the right when right foot in complete contact with the ground and left toe leaving the ground.
	Mid-stance	10-30%	Right foot in complete contact with the ground and left foot off the ground.
	Terminal stance	30-50%	Right heel rises off the ground and left foot starts landing. At this stage, body centre of gravity is on the right foot.
	Pre-swing	50-60%	This phase is initiated when right foot departs the ground and body weight shifts to the left foot on the ground.
Swing	Initial swing	60-70%	Right toe leaves the ground while right knee in maximum flexion.
	Mid-swing	70-85%	Right foot completely off the ground and leg is vertical.
	Terminal swing	85-100%	Right heel makes initial contact with the ground while left toe on the ground.

Lower limb joints complete six major movements in the sagittal plane during walking cycle; hip joint extension and flexion, knee joint extension and flexion and ankle joint plantar flexion and dorsiflexion (Okamoto and Okamoto, 2007). The motion signals of lower limb joints (flexion/extension) in the sagittal plane during two gait cycles used in this work are shown in Figure 3.11.

Initial simulation of the humanoid model was implemented using two set of data provided from clinical gait analysis (CGA) (Kranzl and Kopf, 1997) to analyse the torque required to support hip and knee joints in different conditions. The data includes two cases; natural human gait analysis and a case of 65 years old man with hemiplegia gait analysis shown in Figure 5.2. The controller of the exoskeleton and humanoid use predefined gait trajectory to achieve motion support during walking. Therefore, both hemiplegic and natural gait data are used to evaluate the support needed for hemiplegic mobility. Figure 5.3 shows the torque profiles of knee and hip joints generated by simulating the humanoid model using the hemiplegic and natural gait cycle data. Based on a comparative analysis, the torque profiles are used to determine the desired torque needed to restore hemiplegic patient mobility while using the exoskeleton. In the case of natural gait data, maximum output torque for hip and knee joints is 120 Nm and 60 Nm respectively. However, in the case of hemiplegic gait data the maximum output torque for hip and knee joints is 90 Nm and 38 Nm respectively. Therefore, the assumption, that external support is needed to restore mobility of the exoskeleton user is based on the difference of the torque generated in the two cases.

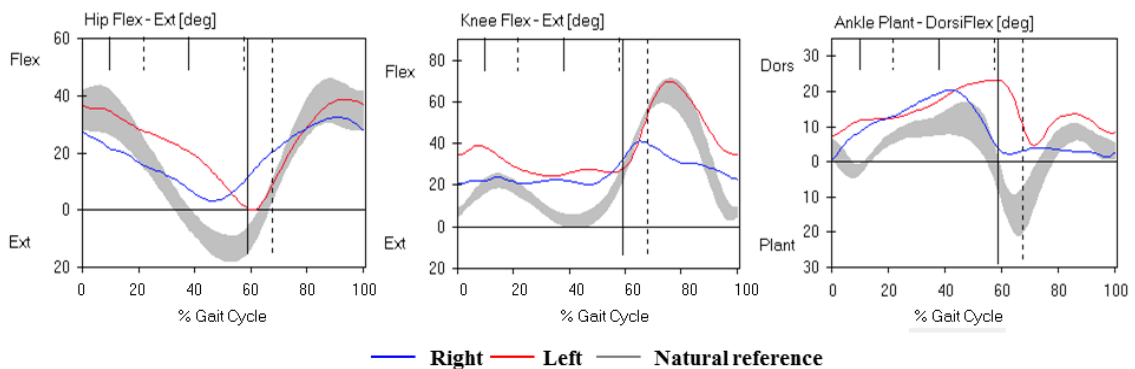


Figure 5.2: Joint kinematics of right-side hemiplegia gait cycle vs natural joint kinematics gait cycle (Kranzl and Kopf, 1997)

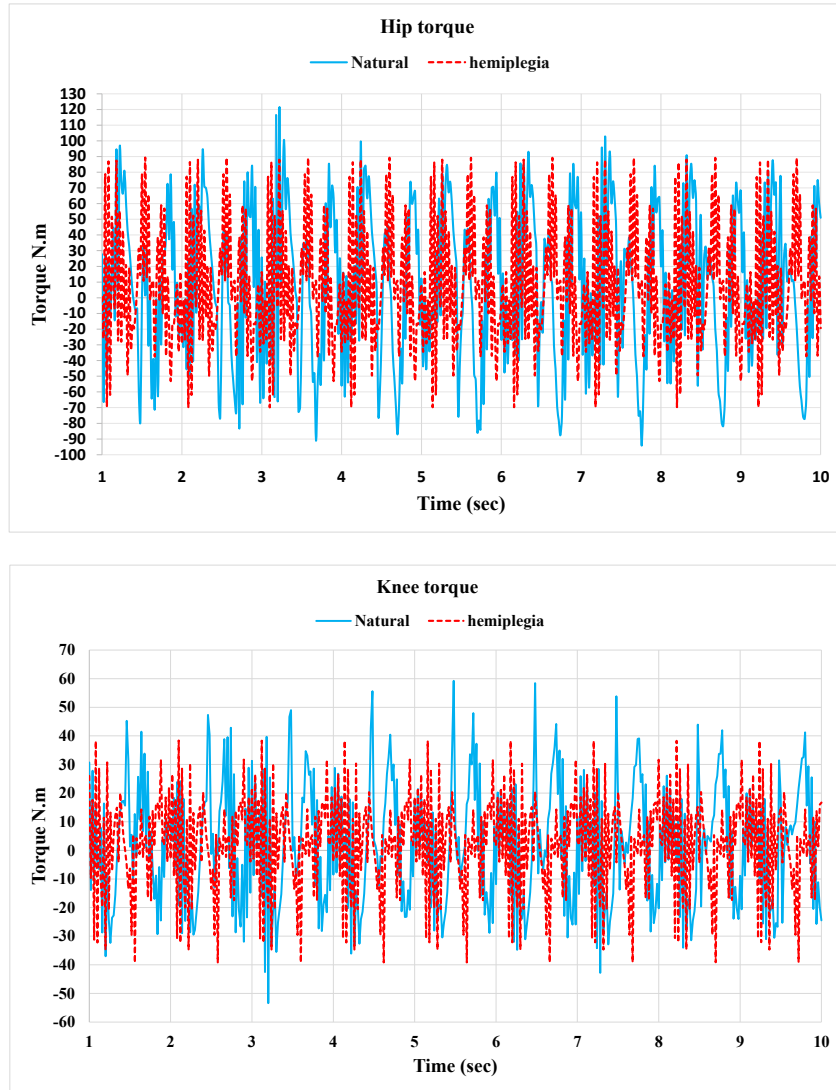


Figure 5.3: Hip and knee torque profiles of hemiplegic and natural gait data

5.3 Implementation of closed-loop PID control

In this section, reference tracking closed-loop PID controller was designed to control the exoskeleton and the humanoid lower limb joints. The control method is based on regulating the output torque which actuates the selected joints to achieve the desired position. Initially, the humanoid model was controlled without the exoskeleton model to gain deep understanding of the system and the total torque needed, through the analysis of the control output while simulating walking motion. Thereafter, investigations were conducted by

coupling the humanoid and exoskeleton models, in which the exoskeleton is used to compensate the humanoid with the necessary torque needed.

5.3.1 Humanoid model control

Humanoid lower limb joints such as hip, knee and ankle were configured as revolute motors type of constraint in MSC.vN4D, actuated by torque (Nm) as control signal and measured as orientation (degree). The control scheme shown in Figure 5.4 present the six closed-loop PID controllers created in MATLAB Simulink to control the left and right lower limb joints of the humanoid model. The difference between the desired joint angle position and the corresponding angle position measured during simulation, i.e. error is used as the PID controller input to output the desirable torque to drive the revolute motor to the desired position. PID control parameters were tuned using trial and error method to find the best possible tracking to the predefined trajectory reference.

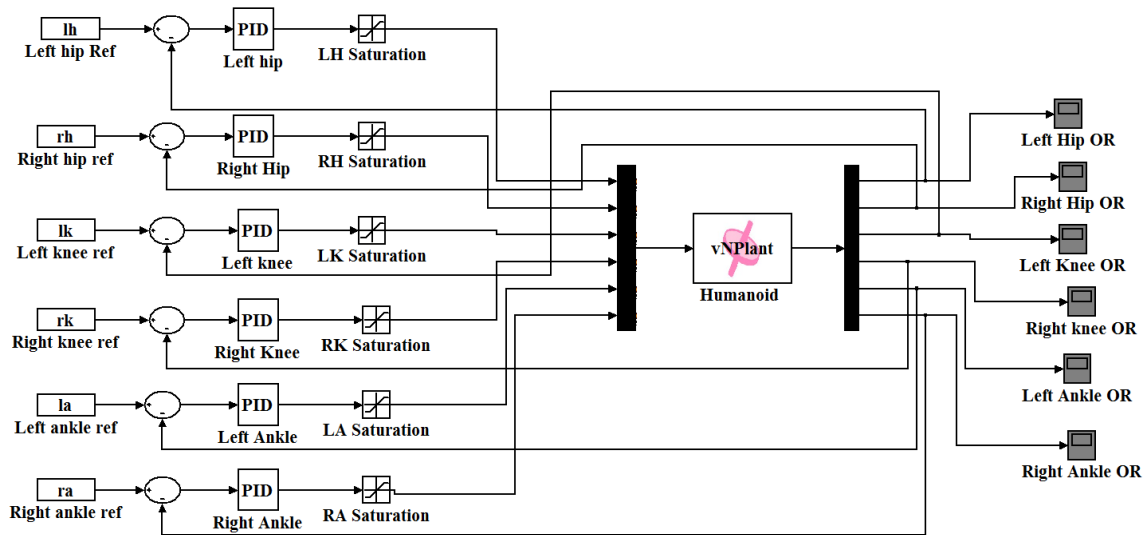


Figure 5.4: PID Control scheme of humanoid lower limbs joints in MATLAB Simulink

The objective in this section is to evaluate the torque generated to actuate the revolute motor of each joint and the tracking of the predefined gait trajectory. Therefore, several simulations were carried out using different combinations of gains for the PID

controller to obtain trajectory tracking and acceptable torques. However, the output torque generated from the PID controllers was constantly greater than 350 Nm. Consequently, saturation blocks were inserted to each joint controller to limit the output torque and avert control signal peaks. The saturation blocks added to controllers were ± 200 Nm for the hip joints, ± 150 Nm for the knee joints and ± 50 Nm for the ankle joints.

PID control parameters were tuned based on predefined set of distributed gains: 5 to 50 for K_p , 0.1 to 10 for K_i and 0 to 5 for K_d . The set of gain were deduced from initial simulation tests carried out to obtain reasonable system behaviour. Thereafter, a script of MATLAB code was developed to launch several simulations and assign each PID parameter with different gain value at each run from the predefined set.

Root mean square error (RMSE) and output torque are used to evaluate the control performance. RMSE between the actual output signal and the reference signal is calculated using

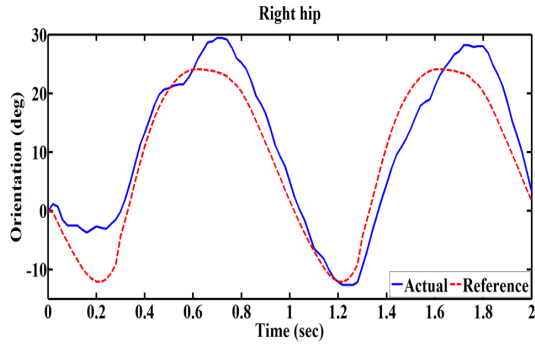
$$RMSE = \sqrt{\frac{\sum_{i=0}^n (\theta_{reference} - \theta_{actual})^2}{n}} \quad (5.1)$$

Table 5.2 shows the PID parameters obtained from heuristic tuning from two simulation trials and their RMSE values. Gains implemented in the second trial are based on optimised version of the gains used in the first trial. Lower limb joints orientation and torque results of the two simulation trails are presented in Figure 5.5, Figure 5.6 and Figure 5.7. These figures demonstrate the effects of optimised parameters on the control performance in terms of torque behaviour and trajectory tracking. For example, RMSEs of the right hip joint for the first and second trials are 6.35 and 2.29 respectively. In this case trajectory tracking of the second trial shows significant improvement compared to the first trial as shown in Figure 5.5a and Figure 5.5e. Moreover, Figure 5.5c and Figure 5.5g shows that the output torque becomes smoother with lower RMSE, which leads to saving in energy

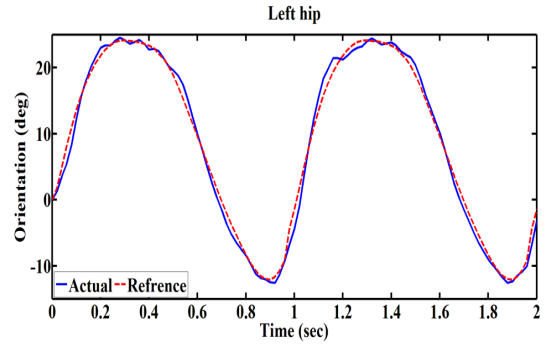
consumption and less damage to actuation system. RMSEs values with less than 10% of the reference amplitude are considered as acceptable, because in most cases tracking has less than 10 degrees deviation from the reference signal. However, it was noticed that RMSEs with more than 10% lead to unstable behaviour as illustrated in Figure 5.7b.

Table 5.2: Humanoid lower limb joints PID control parameters and RMSE values

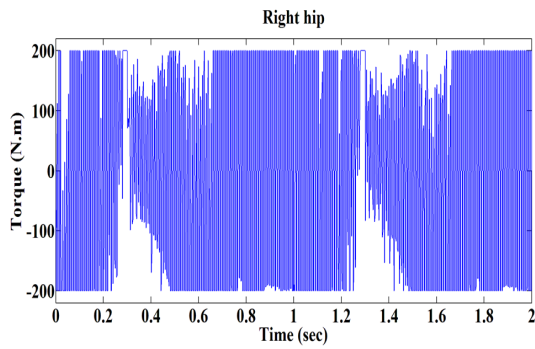
Joint controllers	PID parameters	First trial	RMSE	Second trial	RMSE
Left hip	Kp	35	1.95	41	1.09
	Ki	2.6		1.8	
	Kd	0.9		1.2	
Right hip	Kp	14	6.35	48	2.29
	Ki	4.8		0.6	
	Kd	0.8		0.3	
Left knee	Kp	19	2.78	24.3	1.35
	Ki	4.7		4.4	
	Kd	0.5		0.02	
Right knee	Kp	24	7.4	32.5	2.13
	Ki	2.8		4	
	Kd	1.3		2.2	
Left ankle	Kp	12.3	12.23	8.3	0.85
	Ki	4.5		2.7	
	Kd	0.3		0.07	
Right ankle	Kp	11.9	3.24	8.6	2.27
	Ki	2.7		3.8	
	Kd	0.12		0.08	



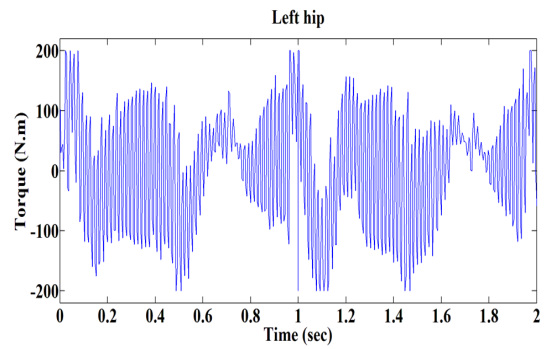
(a) Orientation



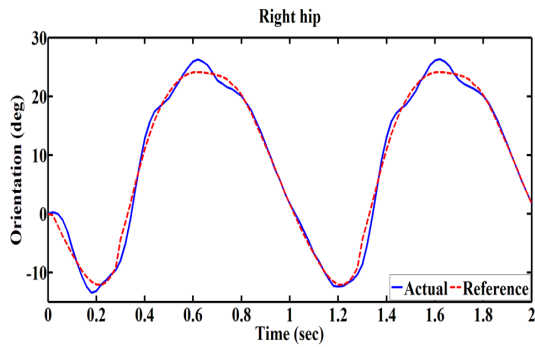
(b) Orientation



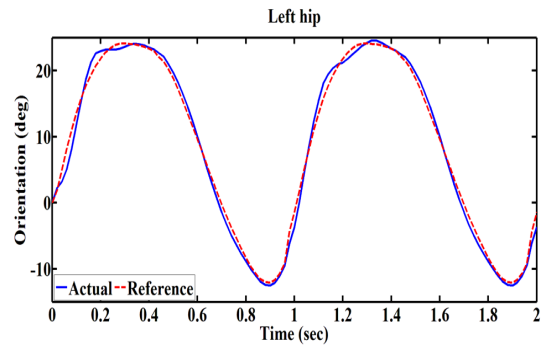
(c) Torque



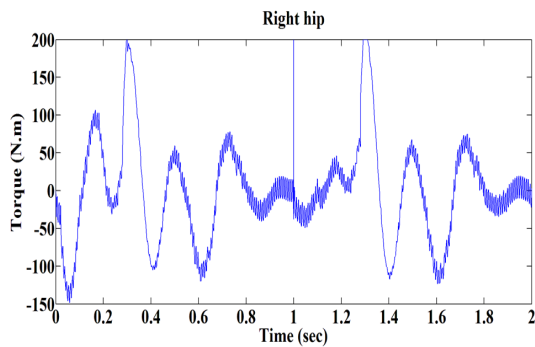
(d) Torque



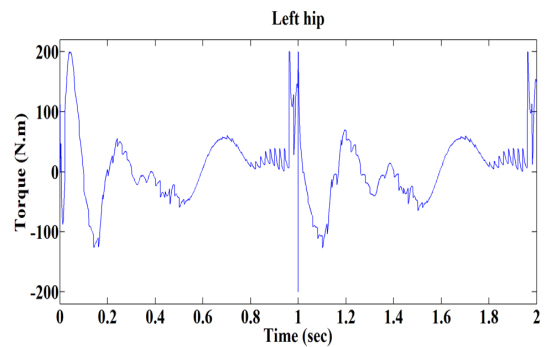
(e) Orientation



(f) Orientation

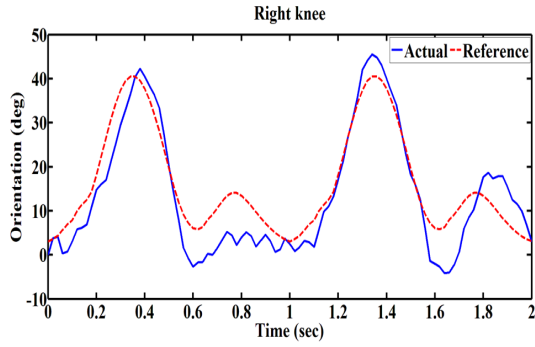


(g) Torque

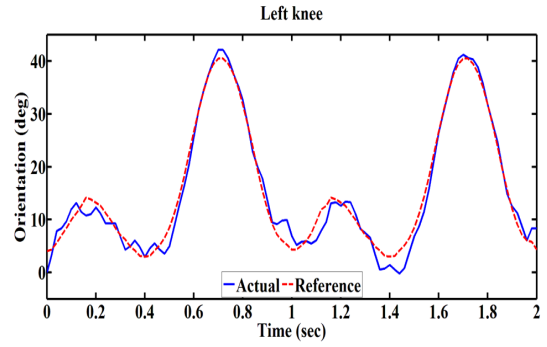


(h) Torque

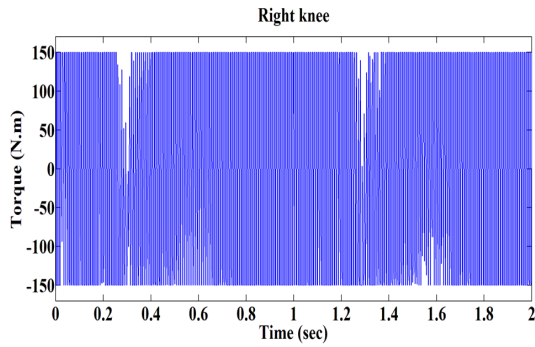
Figure 5.5: Orientation and torque for humanoid right hip and left hip joints during two gait cycles using two sets of PID parameters; (a,b,c,d) first trial; (e,f,g,h) second trial



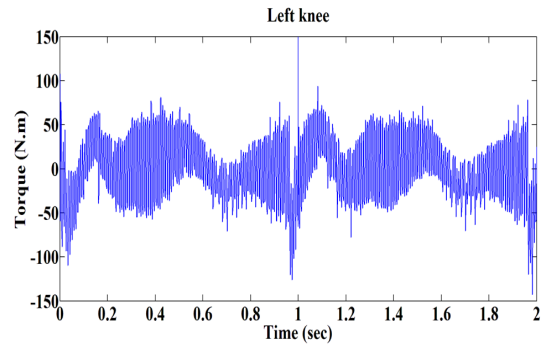
(a) Orientation



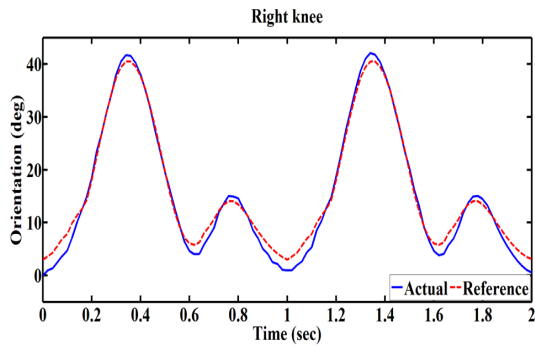
(b) Orientation



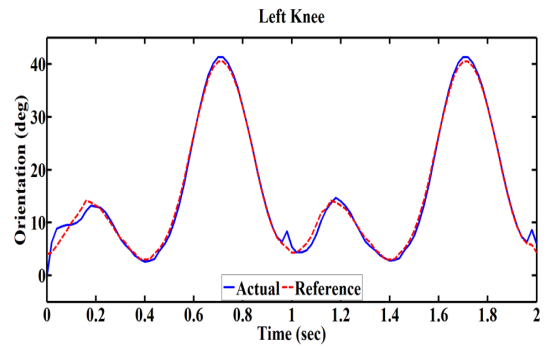
(c) Torque



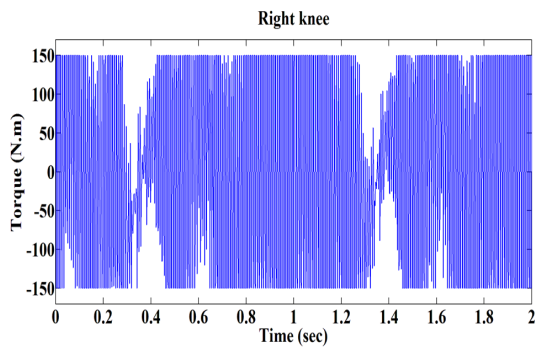
(d) Torque



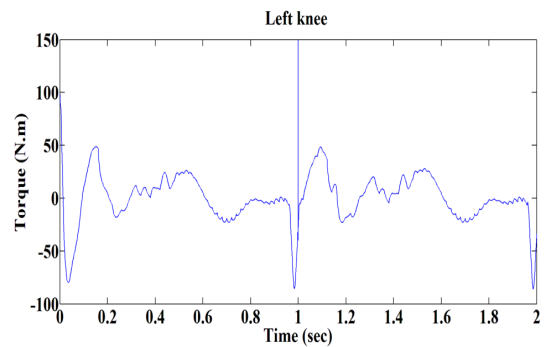
(e) Orientation



(f) Orientation



(g) Torque



(h) Torque

Figure 5.6: Orientation and torque for humanoid right and left knee joints during two gait cycles using two sets of PID parameters; (a,b,c,d) first trial; (e,f,g,h) second trial

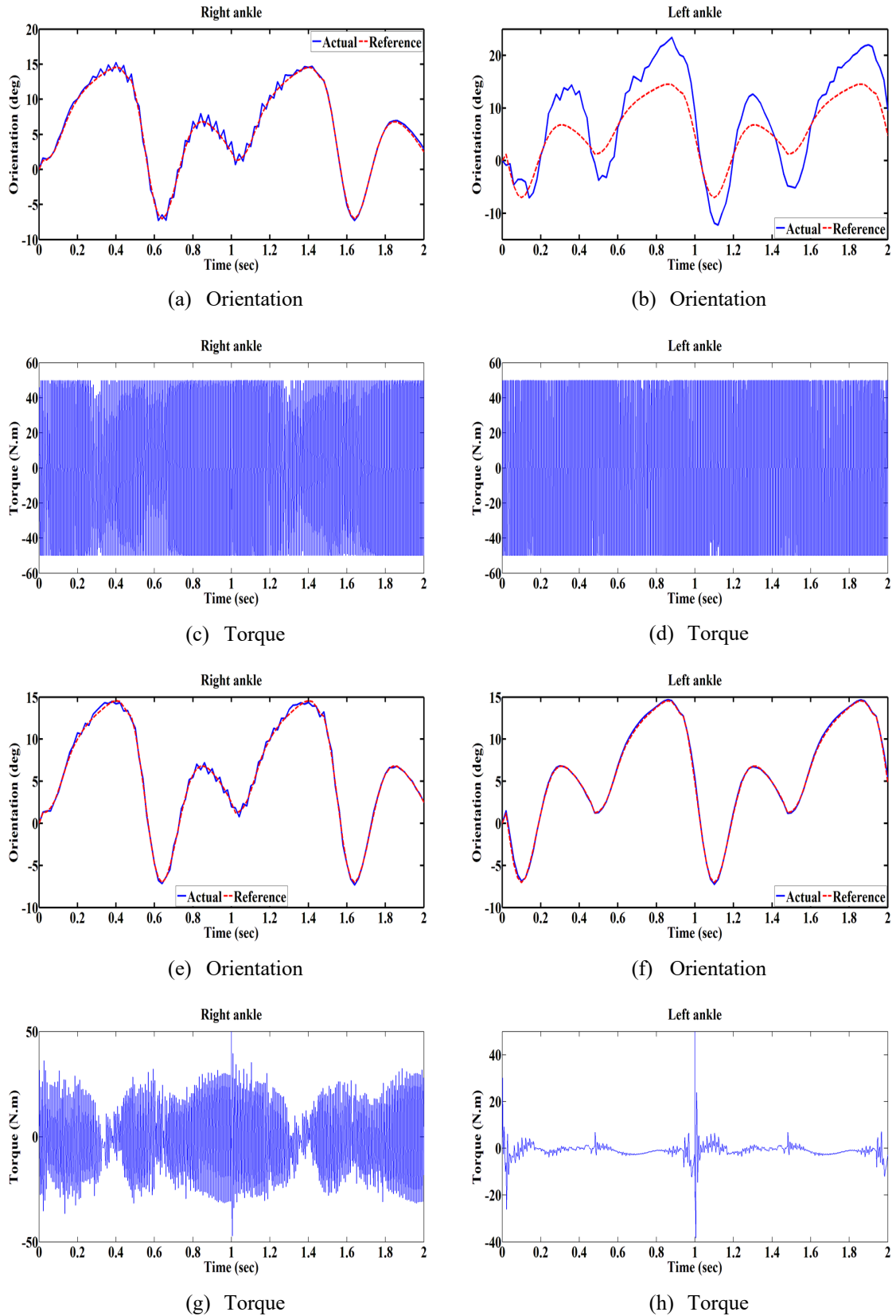


Figure 5.7: Orientation and torque for humanoid right and left ankle joints during two gait cycles using two sets of PID parameters; (a,b,c,d) first trial; (e,f,g,h) second trial

5.3.2 Control of humanoid and exoskeleton with SDA tuned PID parameters

Analysis of the humanoid model carried out in the previous section helped to gain deep understanding of the system behaviour during walking motion. In this section, humanoid and exoskeleton models are incorporated to carry out investigation of the external assistance mechanism provided from the exoskeleton. Humanoid and exoskeleton joints are configured in MSC.vN4D with revolute motors to actuate in the sagittal plane, where each exoskeleton joint is set to be parallel in position to the humanoid joints. The exoskeleton is coupled to the humanoid lower limb and collision is allowed between exoskeleton support parts and humanoid thigh, leg and foot. Collision settings allow the exoskeleton and the humanoid to follow the same predefined trajectory.

The PID controller developed in the previous section to control humanoid active joints was modified to include the exoskeleton active joints in the control loop. The modification involves the ratio of external torque needed from the exoskeleton to support humanoid lower limb. Therefore, each controller output was divided to provide 70% to the humanoid joint and 30% to the exoskeleton joint of the overall torque. That signifies a user with 30% deficiency of the required torque to complete one gait cycle and therefore, compensation is needed to restore gait disorder. The configuration of a single joint PID controller is shown in Figure 5.8. Whereas, the overall control system includes the controllers of all humanoid and exoskeleton active joints.

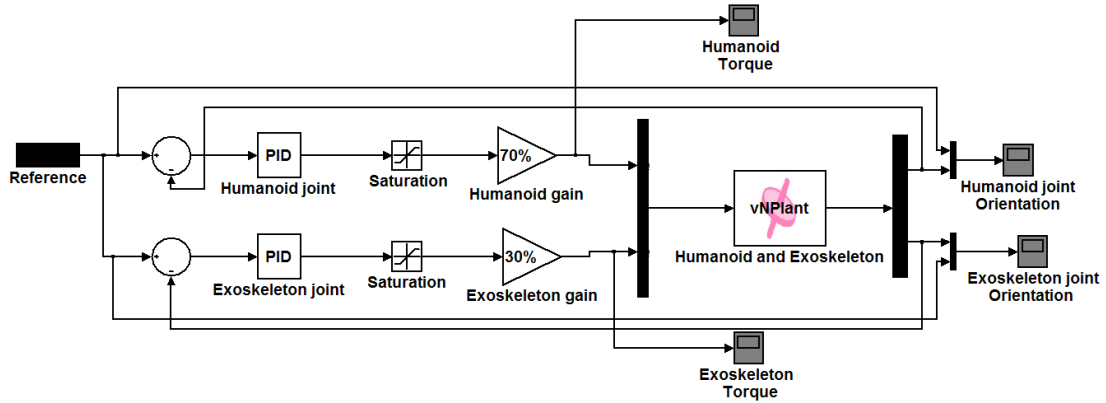


Figure 5.8: Single joint Simulink PID control diagram of humanoid and exoskeleton

PID parameters of the humanoid and exoskeleton joints controllers were tuned by two different methods. Initially, PID parameters were tuned by trial and error using the optimal PID gains obtained in the previous section as a starting point for the tuning process. However, the dynamics of the humanoid and exoskeleton add more complexity to the system behaviour, due to interaction between the collided bodies during simulation. Therefore, SDA optimisation is implemented in the control loop to tune the PID parameters as shown in Figure 5.9. SDA optimisation can improve the tuning process by implementing systematic search for the optimal solutions and covers wider range of gain with less computational time compared with trial and error tuning.

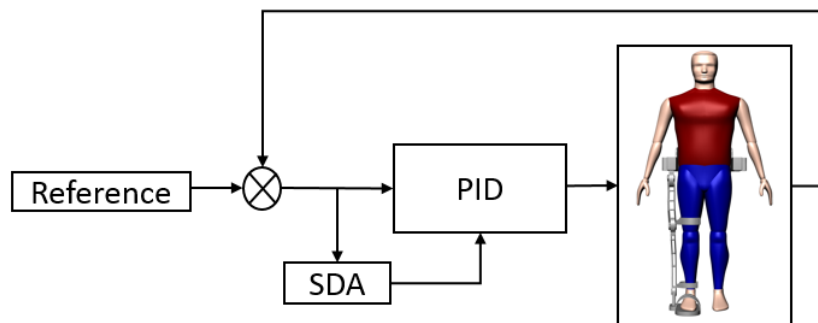


Figure 5.9: SDA tuning PID parameters

In the SDA process, 50 searching points with 10 iterations, $\theta = \pi/2$ and $r = 0.9$ were considered to obtain the optimal solution. The best solution is evaluated by the smallest cost function, which is the sum of the six PID controllers RMSE's calculated using

$$Cost\ function = RMSE1 + RMSE2 + \dots + RMSEn \quad (5.2)$$

A total of 18 parameters (K1-K18) were assigned in the optimisation algorithm to represents the parameters of the exoskeleton and humanoid lower limb joints PID controllers. At each iteration, the optimisation algorithm highlights the potential optimal solutions, and at the end of the process the most optimal parameters are presented based on the smallest value of cost function. Several SDA optimisation processes were executed with different range of gains and the smallest cost function value obtained was 7.08 with the optimal solutions of PID parameters and their RMSE's values shown in Table 5.3.

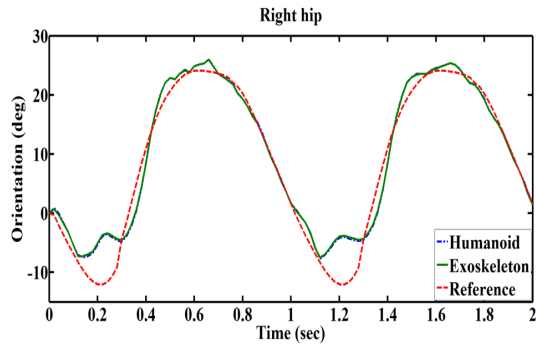
Table 5.3: Trial and error and SDA tuned control parameters with RMSE values

Joint	PID parameters	Trial and error	RMSE	SDA	RMSE
Right hip	Kp	49.7	3.89	66.9	3.12
	Ki	0.61		9.46	
	Kd	0.24		4.07	
Right knee	Kp	31.5	4.23	56	0.98
	Ki	4.05		1.63	
	Kd	2.22		1.05	
Right ankle	Kp	8.65	6.28	26.78	3.76
	Ki	3.83		6.67	
	Kd	0.07		1.55	

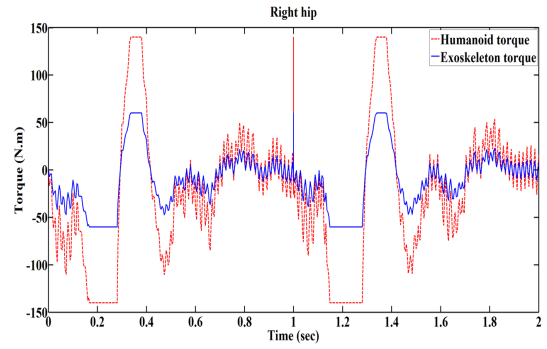
Simulation of the humanoid with support of the exoskeleton to perform two gait cycles were carried out using the two set of tuned PID parameters shown in Table 5.3, and their results are presented in Figure 5.10 and Figure 5.11. As noted, the simulation results with SDA tuned parameters showed improvements in terms of reference tracking and output torque compared to trial and error tuned parameters. The most notable improvement involved in knee and ankle right joints were their RMSE's reduced significantly, but in the case of right hip joint RMSE was reduced by 19% which did not reflect improvement in

terms of reference tracking as shown in Figure 5.10a and Figure 5.11a. Joint torque consumption was reduced at some phases of the gait cycle with the optimised parameters compared to the trial and error parameters as shown in Figure 5.10(b,d,f) and Figure 5.11(b,d,f), as the red line signifies the humanoid joint torque and the blue line signifies the exoskeleton joint torque.

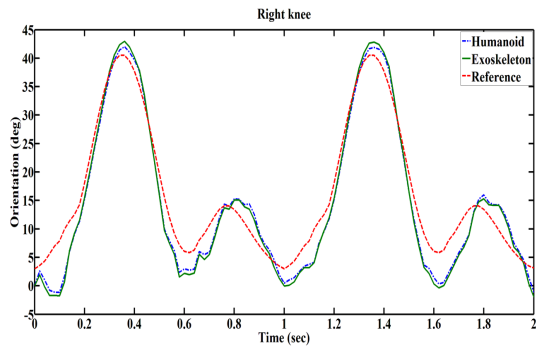
The simulation results show that the humanoid torque was augmented with the necessary torque from the exoskeleton to complete two gait cycles, based on the predefined torque proportion between humanoid and exoskeleton joints. The exoskeleton has provided the humanoid with a compensation torque of almost 50 Nm for the right hip joint, 38 Nm for the right knee joint and 15 Nm for the right ankle joint. In this section, the main focus is on the assistance provided from the exoskeleton fitted on the right leg of the humanoid to support its hip, knee and ankle joints. However, simulation results show that the controller provided the required torque to the right and left joints to perform balanced and symmetric walking cycle. Simulation results of the humanoid left leg joints are shown in Figure 5.12.



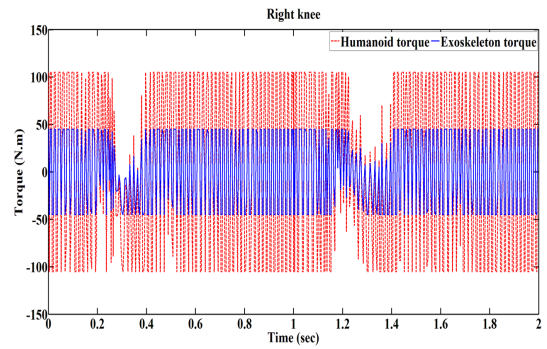
(a) Orientation



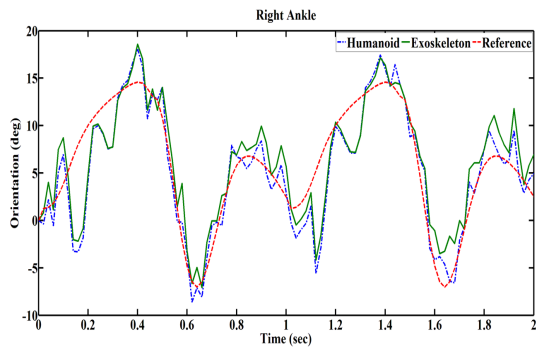
(b) Torque



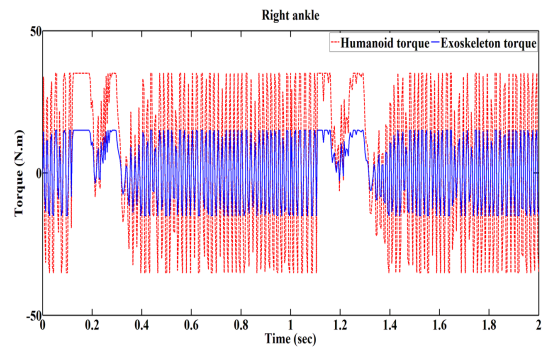
(c) Orientation



(d) Torque



(e) Orientation



(f) Torque

Figure 5.10: Torque and orientation for humanoid and exoskeleton joints simulated with trial and error tuned parameters

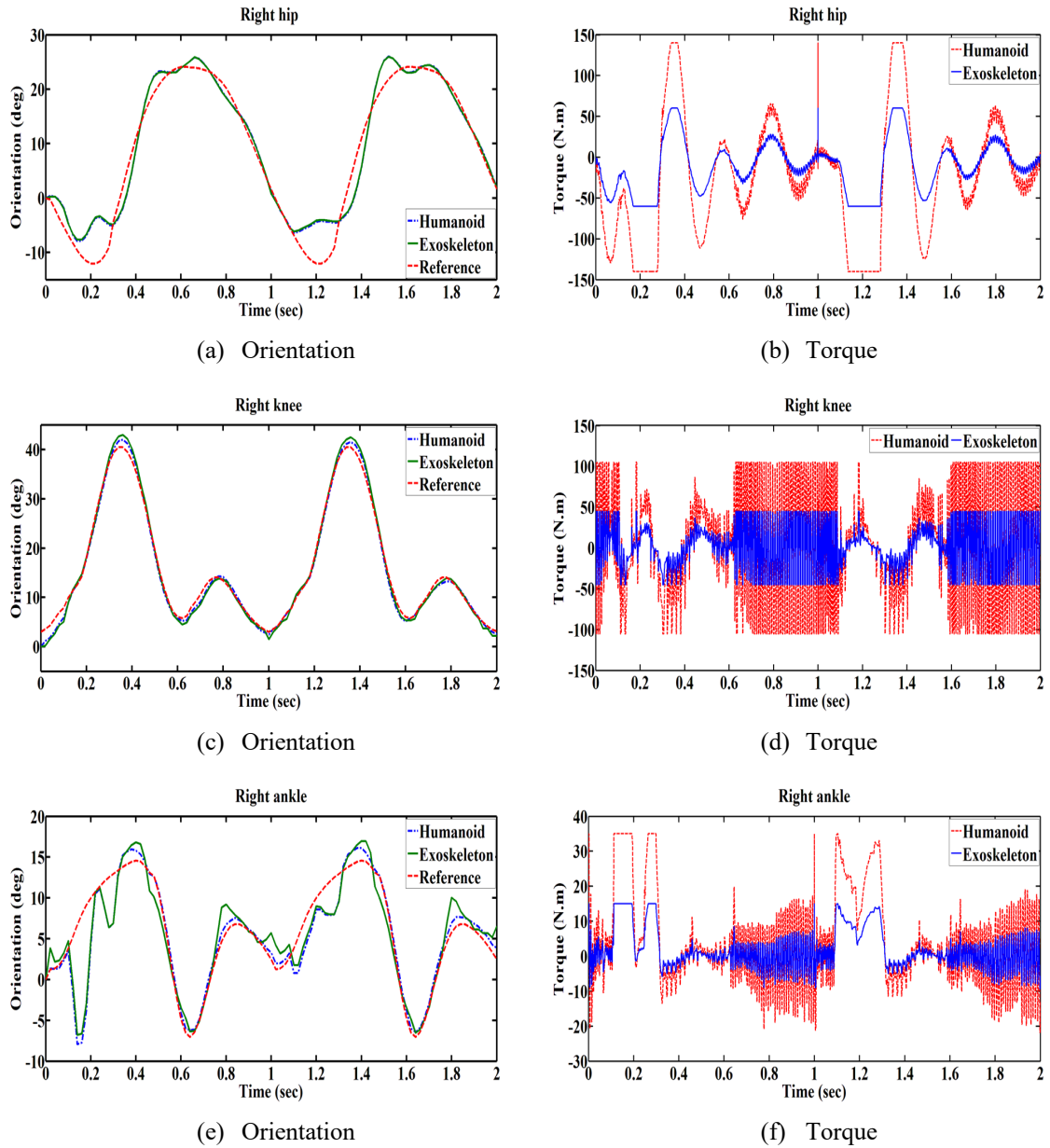


Figure 5.11: Torque and orientation for humanoid and exoskeleton joints simulated with SDA tuned parameters

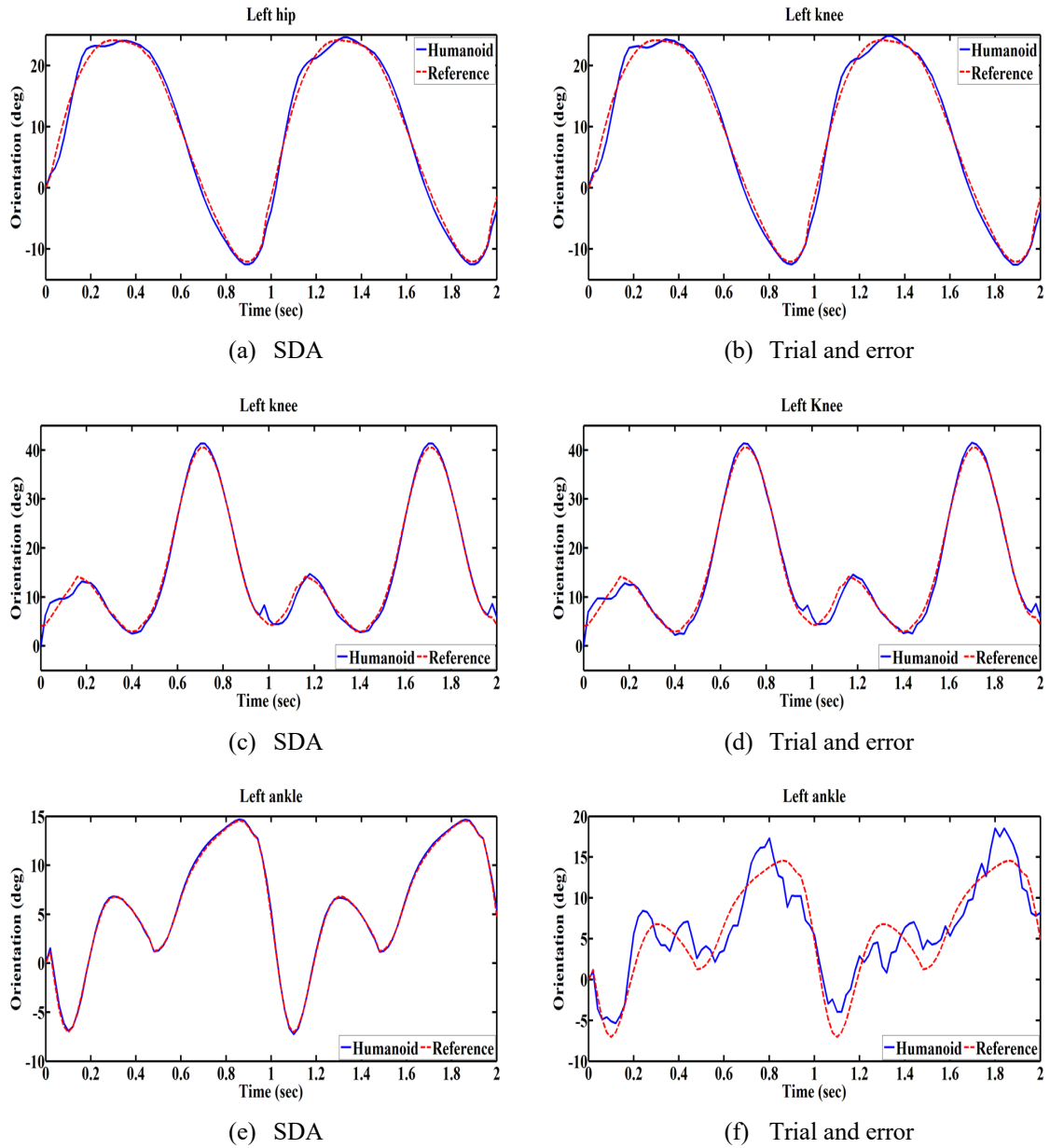


Figure 5.12: Orientation for humanoid left lower limb joints with SDA and trial and error tuned parameters

5.4 Implementation of fuzzy-based PD controller

Fuzzy-based PD controller is an FLC formed with proportional and derivative gains. It is widely employed because of its capability in eliminating the rise time and steady-state-error. Due to the benefits discussed in section 4.2.2, fuzzy-based PD controller with MISO Mamdani type is selected to control the active joints of the humanoid and exoskeleton. The Mamdani type inference was chosen in this work because its rules are simple and easy to form. The Mamdani type can be used with less information needed to be known about the system, however, the Sugeno type is suitable when comprehensive information is known about the system (Engelbrecht, 2007).

Several linguistic levels can be used as input and output variables of the FLC such as 3,5,7,9 of membership functions. In this work, five linguistic terms of membership functions are used to develop the fuzzy rules set as shown in Table 5.4. As the system performance depends on the problem, it is difficult to adopt a standard fuzzy rule set such as the one shown in Table 4.1. However, fuzzy rules can be developed in a specific way that is suitable to the system's desired performance. Therefore, the standard fuzzy rules were modified by evaluating the system performance through simulation trials with different fuzzy rules. Table 5.5 shows the set of fuzzy rules developed for this work.

Table 5.4: Membership functions linguistic terms

Label	Term
NB	Negative big
NS	Negative small
Z	Zero
PS	Positive small
PB	Positive big

Table 5.5: Fuzzy rules set

$e \setminus \Delta e$	NB	NS	Z	PS	PB
NB	PB	PB	PS	PS	Z
NS	PB	PS	PS	Z	NS
Z	PS	PS	Z	NS	NS
PS	PS	Z	NS	NS	NS
PB	Z	NS	NS	NS	NB

Humanoid and exoskeleton control system consist of nine independent subsystem controllers to control the position of each active lower limb joint. While in operation, there is no connection or interaction between the subsystem controllers. Therefore, each joint is controlled with separate PD-fuzzy controller. As shown in Figure 4.4, the fuzzy-based PD controller involves two inputs: error (e) and change of error (Δe). Error is the measured variance between actual and required joint position, while change of error is the derivation of the error. FLC output is the torque generated to actuate joints revolute motors to the desired position.

Gaussian membership functions with five levels and 50% crossing are shown in Figure 5.13. FLC input and output used normalised membership function values with the range of $[-1, 1]$. The five levels of membership functions result in $5 \times 5 = 25$ fuzzy rules for each FLC.

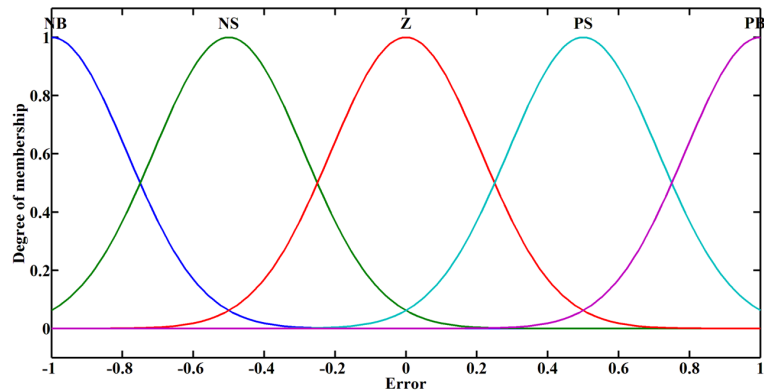


Figure 5.13: Gaussian input/output membership functions

FLC's of the humanoid and exoskeleton joints were developed in MATLAB Simulink, using fuzzy logic toolbox facility. Scaling factors gains were added to the FLC inputs and output in order to adapt the normalised inputs and output membership functions to the system. P and D gains were added to the FLC inputs, and fuzzy gain was also added to the FLC output. Figure 4.4 shows the structure of one fuzzy-based PD controller used in this work. However, the overall implementation of the humanoid and exoskeleton PD-fuzzy control scheme is shown in Figure 5.14. The overall control system involves nine feedback loops of FLC controllers to the control hip, knee and ankle joints of the humanoid and exoskeleton models. Joints orientation reference for two gait cycles is used as a set point for each controller. Humanoid right leg joint and exoskeleton joint share the same orientation reference in order to follow the same gait trajectories.

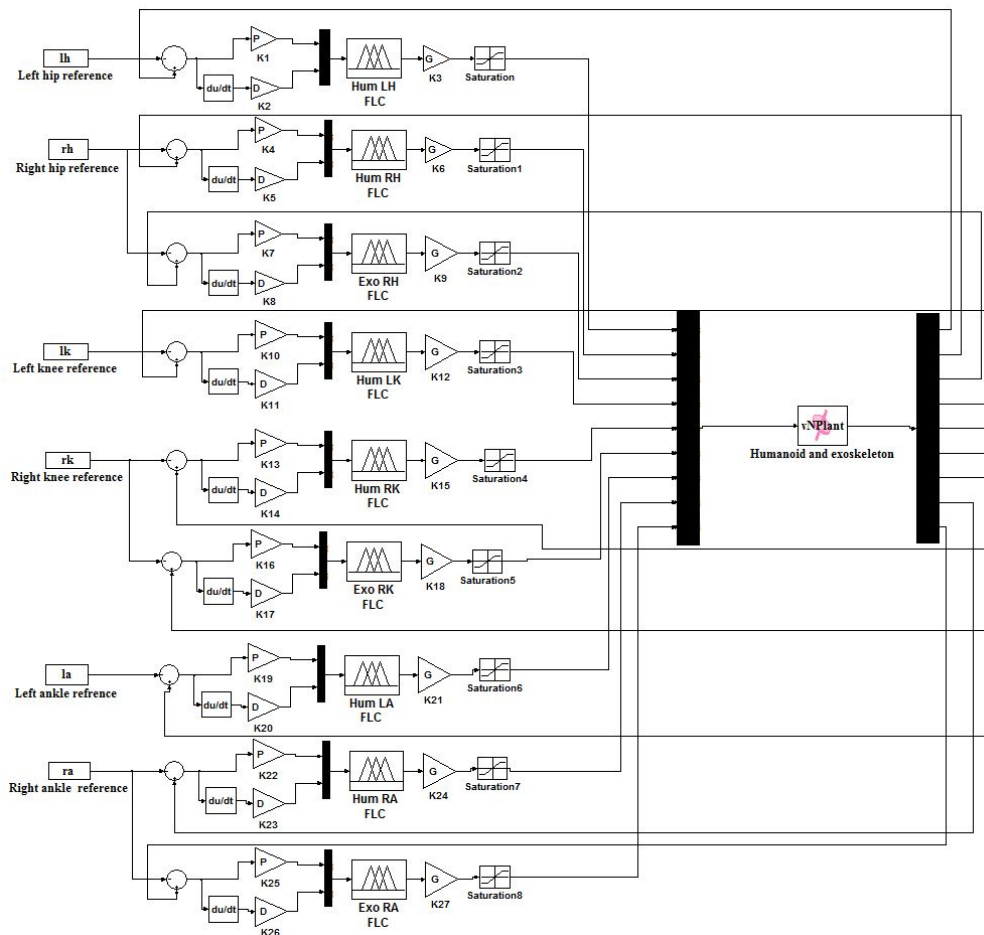


Figure 5.14: Humanoid and exoskeleton PD-fuzzy control scheme

Saturation blocks were inserted after the FLC output to restrict the output torque sent to the actuators within acceptable range. The saturation blocks were configured as ± 200 Nm for the hip controllers, ± 150 Nm for the knee controllers and ± 50 Nm for the ankle controllers. Humanoid and exoskeletons models were integrated with the control scheme in MATLAB Simulink through MSC.vN4D plant block. During the simulation, joint positions are measured in real-time by position sensor in MSC.vN4D environment and fed back to the joint controllers, to generate the necessary control action based on the corresponding reference. A total of 27 gains (K1-K27) were used to tune scaling parameters of the FLC controllers

5.4.1 SDA optimisation of PD-fuzzy scaling parameters

Several optimisation algorithms have been implemented to optimise fuzzy controller elements such as membership functions, rule base and scaling factors. Various studies were found in which the authors have concluded improved results by implementing different optimisation algorithms to optimise fuzzy scaling factors (Almeshal et al., 2013; Cheong and Lai, 2007; Hoffmann, 2001). In order to achieve appropriate and feasible performance for the nonlinear system, it is important to select fuzzy parameters carefully (Wang, 1993). In this work, SDA optimisation is used to minimise the performance error by tuning the FLC scaling factors to their optimum values. Input scaling factors were tuned in such a way to activate the fuzzy rules effectively by adapting the inputs with the universe of discourse, whereas, the FLC output was tuned in order to generate the required torque magnitude as shown in Figure 5.15 based minimum cost function calculated using equation 5.2.

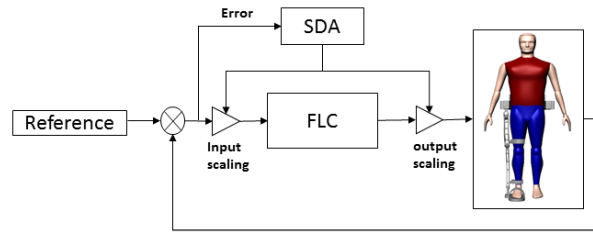


Figure 5.15: Optimising PD-fuzzy scaling parameters with SDA

Using trial and error tuning method for the control parameters to obtain convenient system performance was inefficient and time consuming due to the large number of gains used in the overall system control. Moreover, in the previous section, SDA tuned control parameters improved the behaviour of the output torque and reference tracking compared to trial and error tuned parameters. Therefore, SDA is employed to acquire the best possible optimal scaling factors for the FLC's inputs and output.

In the SDA process, 100 searching points with 20 iterations were considered to obtain the optimal solution. A total of 27 parameters (K1-K27) of the control system were assigned in the optimisation algorithm to be optimised. The objective is to reduce joints orientation error of the humanoid and exoskeleton models while performing walking task. Each PD-fuzzy controller is evaluated by RMSE calculated as in equation (5.1). The overall control system performance is evaluated by cost function calculated as in equation (5.2).

Humanoid and exoskeleton models were simulated for two gait cycles, orientation and output torque results of the controlled joints were obtained and presented in Figure 5.16 and Figure 5.17. The minimum cost function obtained through the SDA optimisation process was 5.54. SDA tuned scaling parameters for the FLC joint controllers are shown in Table 5.6 along with the RMSE values. Fuzzy-based PD controller shows significant improvement in regards to trajectory tracking and output torque compared with the PID controller implemented in the previous section. Joints orientation results demonstrates smooth tracking towards the trajectory reference with small margin of error. Consequently,

humanoid and exoskeleton dynamics became more stable and balanced during simulation in virtual environment. Moreover, simulation results show that the output torque frequency of the controlled joints were reduced significantly and did not reach the maximum torque level set by the saturation blocks.

Table 5.6: SDA tuned FLC parameters

Joint controllers	FLC parameters			RMSE
Left hip	K1	K2	K3	0.85
	0.28	0.51	200	
Right hip	K4	K5	K6	0.52
	0.13	0.01	140	
Exoskeleton hip	K7	K8	K9	0.57
	0.28	0.12	60	
Left knee	K10	K11	K12	0.93
	0.24	0.06	150	
Right knee	K13	K14	K15	0.76
	0.96	0.82	105	
Exoskeleton knee	K16	K17	K18	0.81
	0.58	0.04	45	
Left ankle	K19	K20	K21	0.32
	0.98	0.15	50	
Right ankle	K22	K23	K24	2.04
	0.85	0.02	35	
Exoskeleton ankle	K25	K26	K27	2.96
	0.82	0.23	15	

For the Humanoid right leg joints with mobility disorder, FLC output scaling factors were defined according to the level of external torque required from the exoskeleton as shown in Table 5.6. Whereas, the healthy left leg joints were set to actuate without external support. Figure 5.17(a,c,e) demonstrates the augmentation torques provided from the exoskeleton during two gait cycles to achieve balanced and symmetric walking pattern. The exoskeleton has compensated the humanoid right leg joints with nearly: 45 Nm for the hip, 30 Nm for the knee and 10 Nm for the ankle which represent almost 30% of the overall torque needed. Meanwhile, the humanoid right leg joints were actuated by nearly 100 Nm for hip, 80 Nm for the knee and 30 Nm for the ankle which represent 70% of the overall torque needed. Figure 5.17(b,d,f) shows the torque provided to the humanoid left leg joints without external support. Orientation results shown in Figure 5.16, demonstrate that the overall system can achieve balanced and symmetric gait cycle while receiving external support from the exoskeleton on one side of the humanoid lower limb.

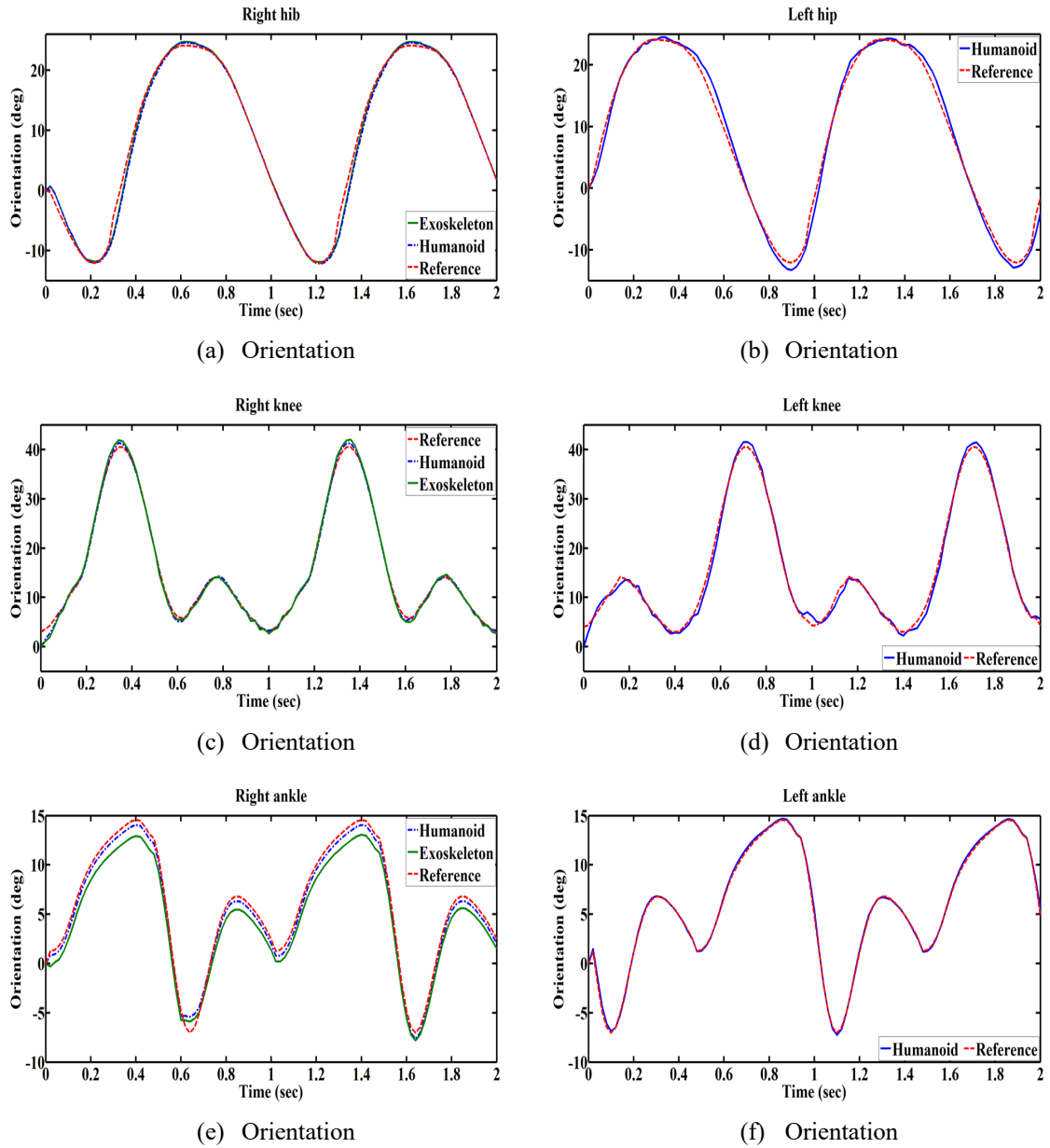
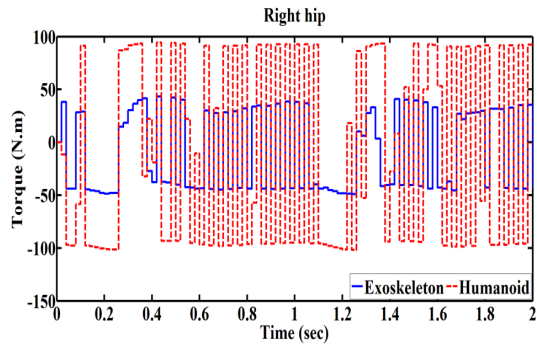
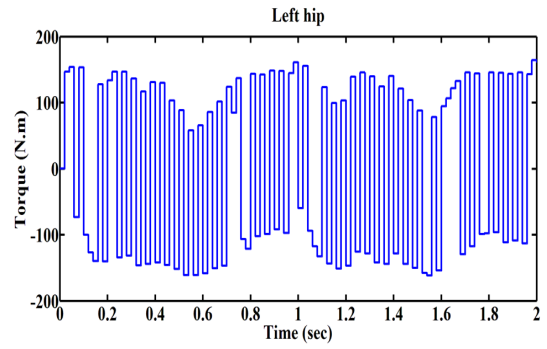


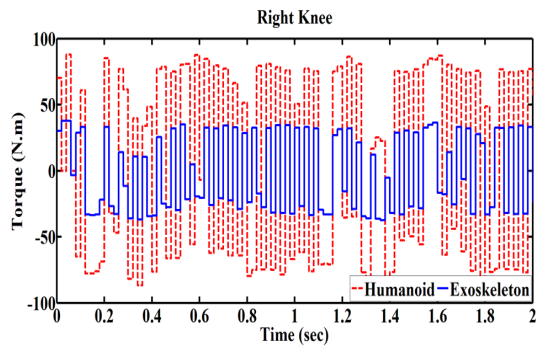
Figure 5.16: Joints orientation of the humanoid and exoskeleton during two gait cycles



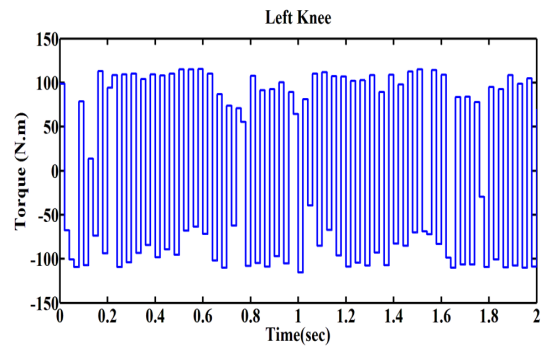
(a) Torque



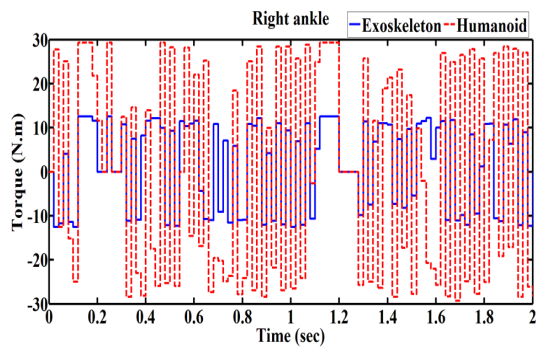
(b) Torque



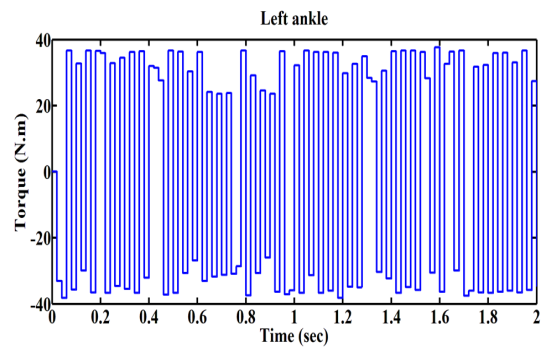
(c) Torque



(d) Torque



(e) Torque



(f) Torque

Figure 5.17: Output torque of the humanoid and exoskeleton joints during two gait cycles

5.4.2 Simulation with different gait speeds

In order to validate the efficiency of the humanoid and exoskeleton control system while performing walking task, several simulation tests were carried out using different gait speeds. Gait trajectories used in the previous sections were modified with average speed gait of 1 second for the complete gait cycle. Therefore, the orientation reference of hip, knee and ankle joints shown in Figure 3.11 were modified to develop two sets of gait trajectories with different time scale of a complete gait cycle. Two different gait speeds were selected for this test:

- Medium-speed, where the complete gait cycle duration is 0.8 second.
- High-speed, where the complete gait cycle duration is 0.6 second.

Humanoid and exoskeleton models were simulated for two gait cycles, with a total of 1.6 seconds for the medium-speed gait and 1.2 seconds for the high-speed gait. The configurations of fuzzy-based PD controller implemented in the previous section are used for the gait speed test. Additionally, the optimised fuzzy scaling factors obtained with SDA optimisation are also used as the control parameters. This investigation is focused on the unhealthy side of the humanoid lower limb, to examine the control action in terms of maintaining the external support in different conditions.

For the medium-speed gait, the RMSE values obtained for the hip, knee and ankle joints were 1.84, 1.35 and 2.96 respectively. The RMSE values were higher compared with the values obtained with average speed gait cycle shown in Table 5.6. However, the tracking trajectories of the controlled joints shown in Figure 5.18(a,c,e) demonstrate that the system dynamics was still smooth and stable during simulation with medium-speed gait. Meanwhile, Figure 5.18(b,d,f) shows that the torques generated from the humanoid and

exoskeleton joints during the two gait cycles were within acceptable levels and did not reach the maximum levels set by the saturation blocks.

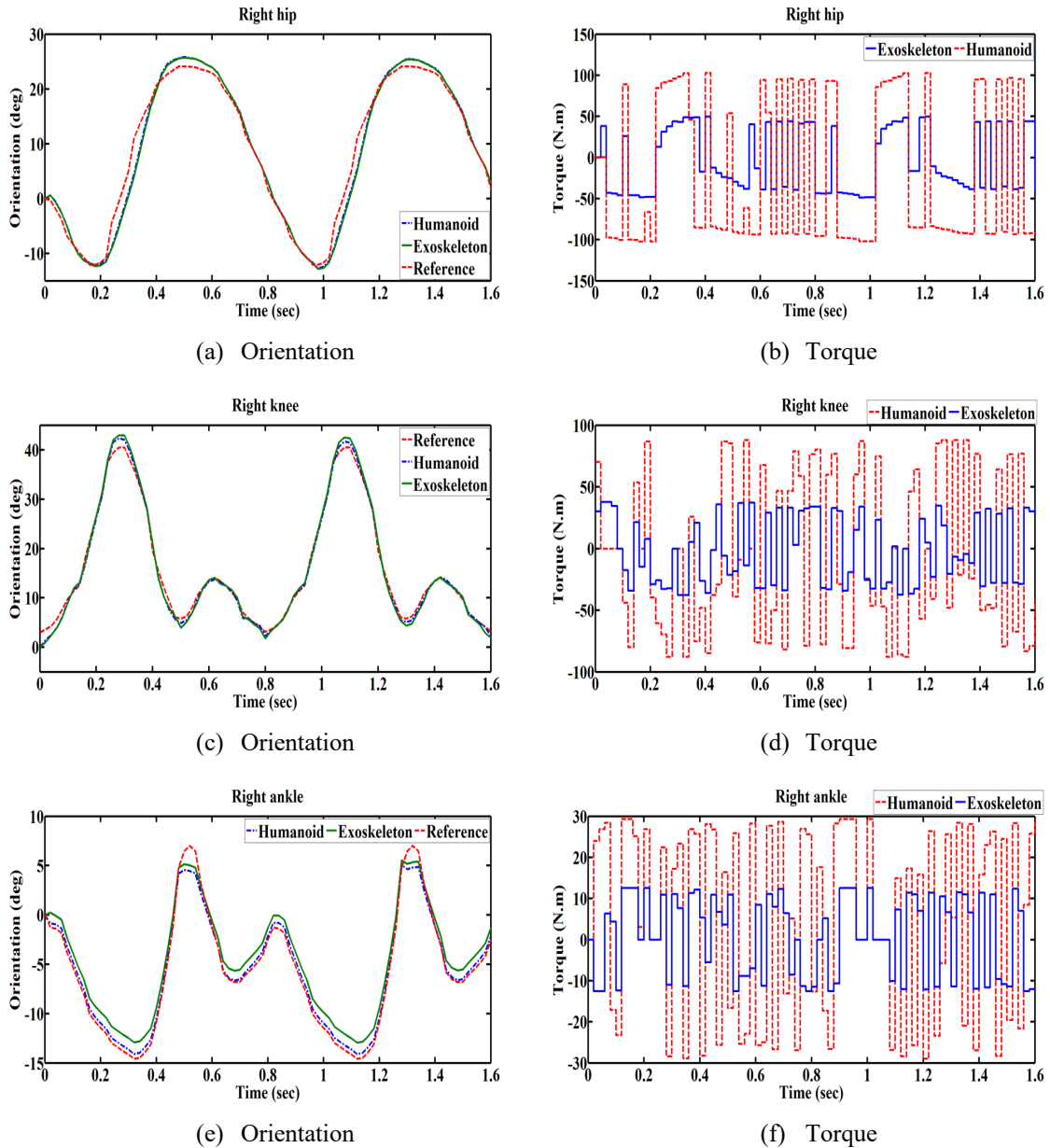


Figure 5.18: Orientation and torque results of the humanoid and exoskeleton joints with medium speed gait trajectories

For the high-speed gait, the RMSE values obtained for the hip, knee and ankle joints were 8.75, 6.86 and 4.34 respectively. It is noted that the reference tracking error of the controlled joints were higher during the swing phase and the highest error occurred at hip joint, although the error margin was still within the acceptable level which is less than 10 degree of the reference. Nevertheless, Figure 5.19(a,c,e) shows that the humanoid and

exoskeleton performance was smooth and stable during most of the two gait cycles. Figure 5.19(b,d,f) shows that the torques generated from the humanoid and exoskeleton joints during the two gait cycles were within acceptable levels and did not reach the maximum levels set by the saturation blocks.

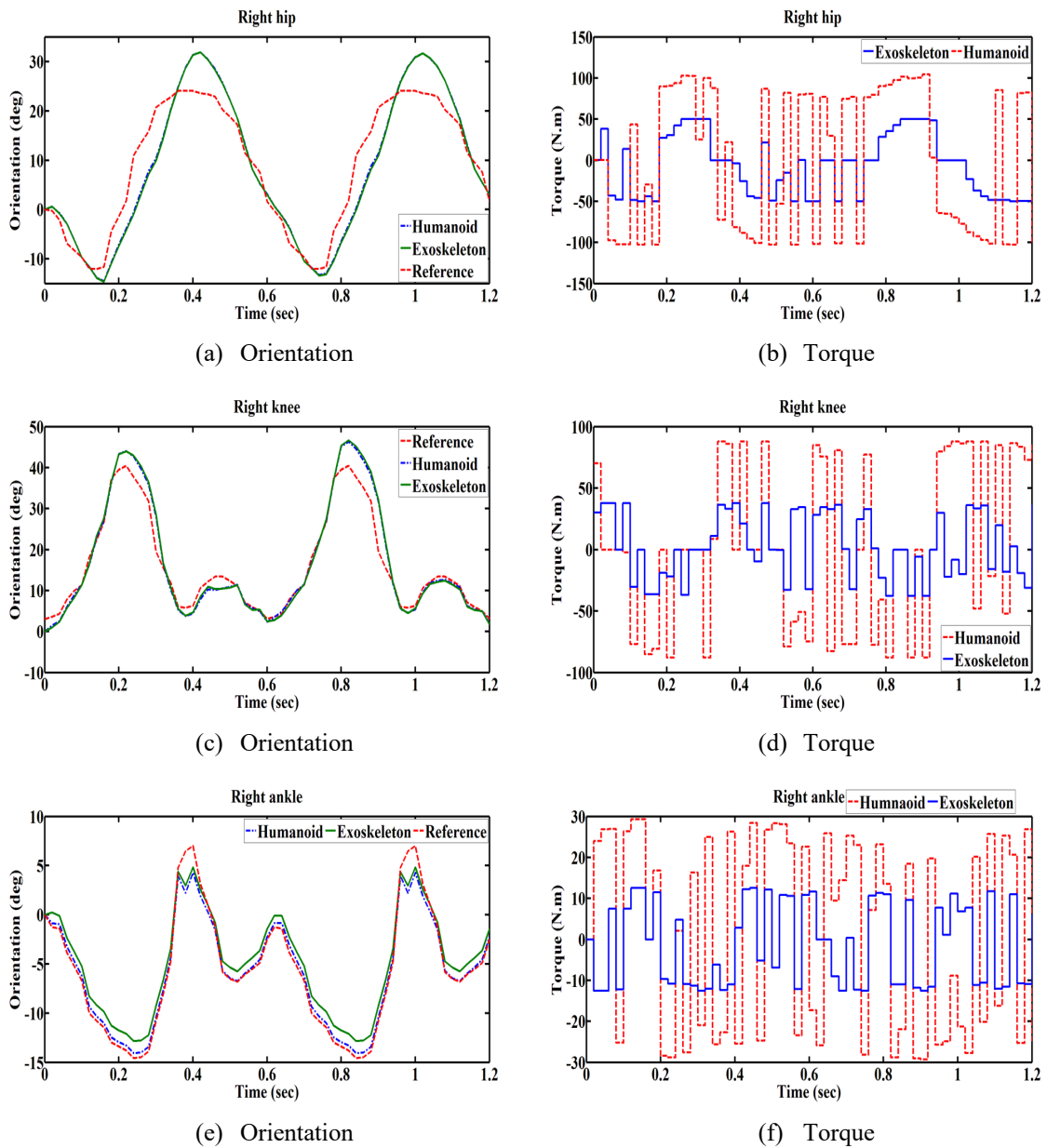


Figure 5.19: Orientation and torque results of the humanoid and exoskeleton joints with high speed gait trajectories

5.4.3 Simulation with disturbance forces

The system was subjected to a series of external impulse forces to examine the system behaviour and evaluate the robustness of the controller. The disturbance forces were applied during two gait cycles at different phases of the gait. Figure 5.20 shows the positions of the disturbance forces applied on the humanoid right thigh and leg in the sagittal plane direction (Y axes), while forces applied on the exoskeleton foot were in the transversal plane (Z axes). The positions were selected to examine the response of the controlled joints attached to the humanoid lower limb part. Three levels of disturbance forces were applied; 500N, 1500N and 3000N for a duration of 0.1s. The impulse forces were applied on the opposite direction of lower limb movements. For the thigh part, impulse forces were applied at 0.4s during flexion and at 1.4s during extension. For the leg part, impulse forces were applied at 0.5s during flexion and at 1.5s during extension. For the exoskeleton foot, impulse force was applied at 0.4s during flexion. The disturbance forces were repeated to examine the control action recovery during two gait cycles. Fuzzy-based PD controller with SDA tuned scaling parameters were used to implement this test.

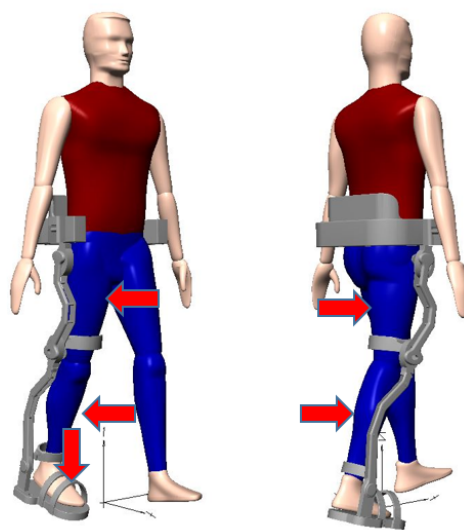
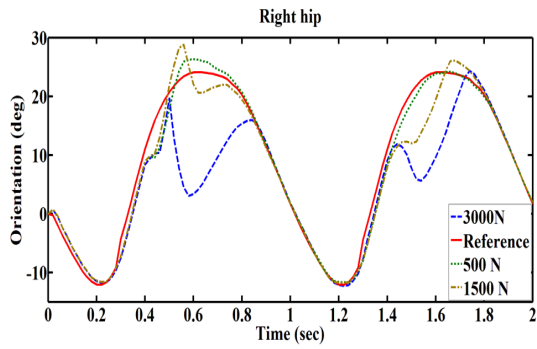
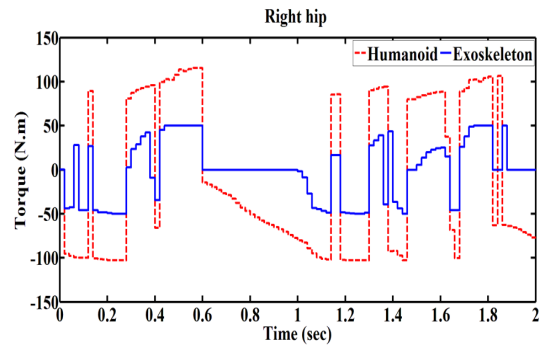


Figure 5.20: Positions of the disturbance forces applied on the humanoid and exoskeleton

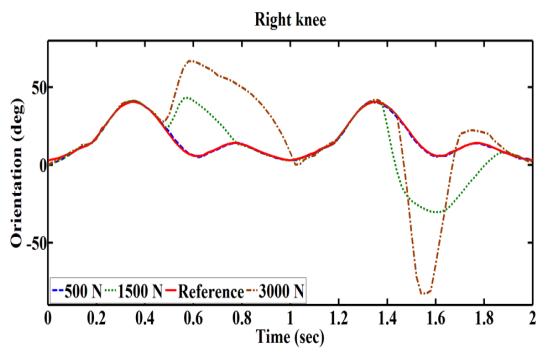
Simulations of the humanoid and exoskeleton were carried out with different levels of disturbance force at each time. Figure 5.21(a,c,e) shows the combined tracking trajectories results of the humanoid and exoskeleton controlled joints with three levels of disturbance forces. With a disturbance force of 500N, the system behaviour was not affected and was stable for most of the two gait cycles. While, with disturbance forces of 1500N and 3000N, joints trajectories tracking was deviated from the reference for part of the gait cycle due to the disturbance force. Nevertheless, the controller managed to regain system stability with an average of 0.25s for the 1500N and an average of 0.4s for the 3000N. It is noted that the system become unstable with disturbance forces beyond 3500N. Figure 5.21(b,d,f) shows the control effort in terms of output torque under the effect of 3000N disturbance impulse force. The results show that the controller maintained the output torque within acceptable levels under extreme conditions.



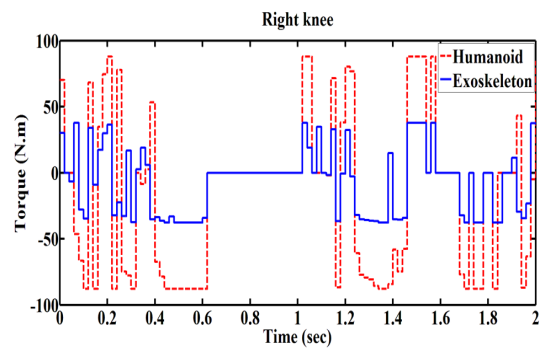
(a) Orientation



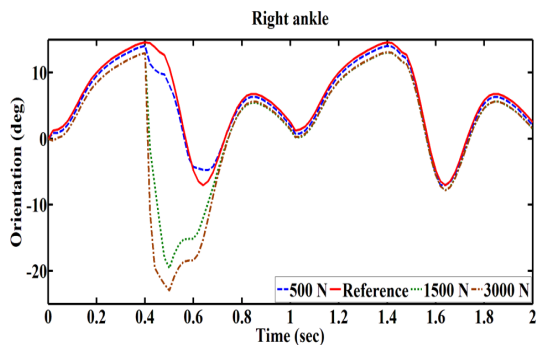
(b) Torque With 3000 N



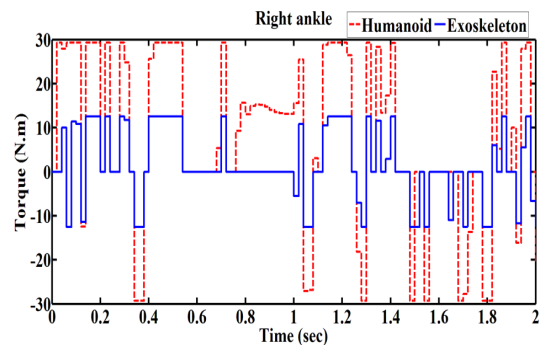
(c) Orientation



(d) Torque With 3000 N



(e) Orientation



(f) Torque With 3000 N

Figure 5.21: Orientations and torques of the humanoid and exoskeleton joints under different disturbance forces

5.5 Summary

The humanoid and exoskeleton models have been simulated in MSC.vN4D virtual environment, for examinations of walking mobility to provide assistance to hemiplegic patient with gait disorder, using two different controllers developed in MATLAB Simulink. Torque profile assessments have been carried out to achieve safe and stable actuation for the active joints revolute motors, with the application of PID and fuzzy-based PD controllers. Control performance has been evaluated using recorded trajectories and output torque results, through simulations of the humanoid and exoskeleton in MSC.vN4D virtual environment.

The simulation results obtained from the different implemented controllers have shown that fuzzy-based PD controller has improved the system performance compared to PID controller, in terms of reference tracking by minimising RMSE value and output torque. Additionally, SDA optimisation has shown great advantage in reducing RMSE by tuning the control parameters as compared to heuristic tuning. The simulation results demonstrate that the controller can provide suitable control action to perform walking movements, by generating the required torque to the active joints within admissible limits. The output torque results demonstrate that the exoskeleton is capable to compensate the humanoid deficiency with the required torque to perform natural walking cycle. A comparison of the torque root mean square (RMS) values of the exoskeleton joints generated with PID and PD-fuzzy controllers is shown in Table 5.7. The RMS values shows that PD-fuzzy controller reduced the torque consumption of the controlled joints which lead to less energy consumption.

Table 5.7: Comparison of torque RMS values generated with PID and PD-fuzzy controllers for the exoskeleton joints during walking simulations

Joint / torque RMS	Torque RMS with PID controller (Nm)	Torque RMS with PD-fuzzy controller (Nm)	Torque reduction (%)
Hip	33	27	18.18
Knee	40	29	27.5
Ankle	12	10	16.67

Finally, two types of tests have been carried out to evaluate the control efficiency and robustness under different conditions. The tests were carried out using different gait speeds and disturbance impulse forces. For both tests, the controller has demonstrated capabilities to maintain the system stable and recover from external disturbances.

Chapter 6: Control of single leg exoskeleton and humanoid for standing up and sitting down movements

6.1 Introduction

This chapter investigates the control of single lower limb exoskeleton in assisting hemiplegic patient to complete standing up from sitting position and sitting down from standing position. The investigated system includes CAD models of humanoid and lower limb exoskeleton, where the exoskeleton model is attached to the right side of the humanoid model. MATLAB Simulink facilities are used to develop humanoid and exoskeleton control system integrated with MSC.vN4D for dynamic visualisation in virtual environment.

The assistance strategy is based on following the lower limb joints trajectories and providing the necessary torque to compensate humanoid right hip and right knee joints through the exoskeleton system to perform the movement. Two types of controllers are employed to address the control of the humanoid and exoskeleton active joints. The controllers are PID and fuzzy-based PD developed and executed in MATLAB Simulink. Performance of the controllers is evaluated by minimum RMSE and output torque.

SDA optimisation is used to enhance the control performance by optimising the control gains. Finally, control efficiency and robustness are assessed by applying different disturbance forces and constant loads on the humanoid and exoskeleton models.

6.2 Standing up and sitting down motion cycles

Standing from sitting position and sitting from standing position are one of the most important movements for daily life activities. Healthy adults need 1.5 to 2 seconds to perform complete sit-to-stand motion (Nuzik et al., 1986; Schenkman et al., 1990). During this motion, human body posture changes as a reaction of the corresponding body part movement, following forward trunk lean and upward extension, transforming the body from stable base while sitting to less stable base while standing (Aissaoui and Dansereau, 1999).

Standing up and sitting down have been involved in various studies. Kralj and Bajd (1989) have investigated standing up motion cycle, and proposed a definition to formalise the detection and separation of the phases. Figure 6.1 shows the cycle of standing up motion phases.

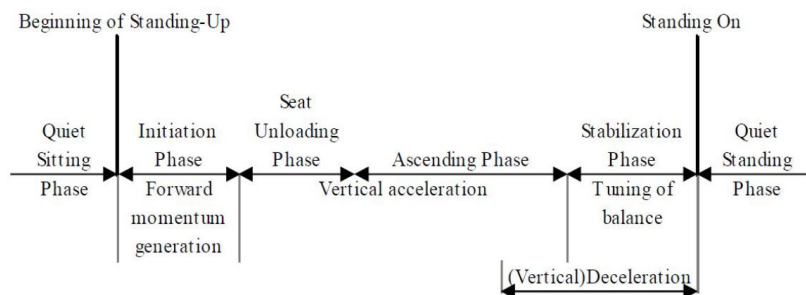


Figure 6.1: Cycle of standing up motion (Kralj and Bajd, 1989)

The quiet sitting phase is the initial body posture for the standing up followed by the initiation phase. In this phase, the flexion-momentum to bring the upper body forward is generated to transfer support of body weight from the seat to the leg. Meanwhile, lower body part remains static during this phase. In the following phase, seat unloading is detected by rapid positive change in vertical acceleration, to push the centre of mass (CoM) upwards and overcome momentum demands through decreasing the upper body forward momentum and increasing lower limb joints extension velocity. This phase is considered as the shortest and least stable. In the ascending phase, vertical acceleration continues until the CoM

achieve its maximum forward position and the knee joint is fully extended to end the vertical upward movement. At this point stabilisation phase begins, where standing position is reached after the hip and knee joints are completely extended. During quiet standing phase, movements involve the hip and ankle joints in different planes so to achieve body balance while standing (Aissaoui and Dansereau, 1999; Kralj and Bajd, 1989; Laporte et al., 1999).

Studies on sitting down motion are fewer compared to standing up motion. However, Figure 6.2 shows the cycle of sitting down motion phases reported (Kralj and Bajd, 1989). Sitting down motion cycle is similar to standing up motion but in reversed order. The first phase of the motion is called initiation, where the upper body is in transition from upright posture to stooping posture through flexion of hip joints. The following phase is called descending and involves vertical acceleration when the trunk is in descending motion by hip and knee joints flexion, thereafter, vertical deceleration of upper body is involved until seat loading phase. In this phase, support of the body weight is shifted from the leg to the seat when the lower body is in contact with the seat. Stabilisation phase is the last phase of the motion, where the hip joints extend to move the trunk backward and achieve balanced sitting posture (Kerr et al., 1994).

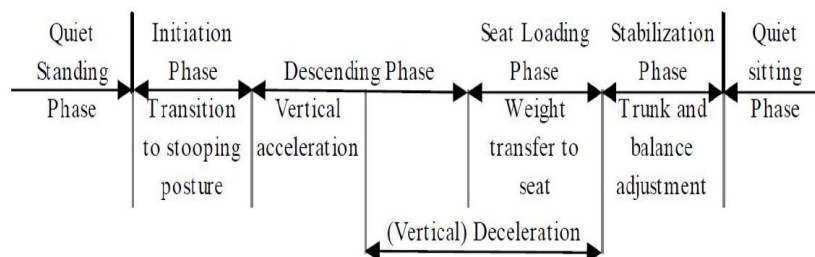


Figure 6.2: Cycle of sitting down motion (Kralj and Bajd, 1989)

6.3 Closed-loop PID control implementation

The main objective of this chapter is to investigate the implementation of assistive exoskeleton system that supports the humanoid in standing up and sitting down movements. Developing and implementing a control method is also considered in this chapter, to control the exoskeleton active joints that deliver the necessary torque to support the hemiplegic patient in performing the movement. It is essential to examine the system torque profiles to understand the level of torque needed for the actuation system before carrying out experimental trials. Therefore, the humanoid model was simulated to evaluate the torque profile before applying the exoskeleton system.

6.3.1 Assessment of humanoid behaviour and torque profiles

Humanoid model was simulated in MSC.vN4D to perform the movement task without support of the exoskeleton. Joints orientation data shown in Figure 3.12 were used as reference in the closed-loop PID controller developed in MATLAB Simulink. In this work, parallel joints of the humanoid lower limb receive the same orientation reference, as left and right legs motions are assumed to be synchronised in the sagittal plane. Humanoid feet were fixed and rigidly attached to the ground during simulation in the virtual environment.

Humanoid hip and knee joints settings in MSC.vN4D were defined as revolute motors, controlled by torque as input signal and measured with orientation meter as output signal. Ankle joints were represented with passive revolute motors with specified range of motion to comply with movements of humanoid legs during simulation. Joints settings were defined in MSC.vN4D software, then integrated with the controller loop through vNplant block in MATLAB Simulink. The implementation of closed-loop reference tracking PID control in MATLAB Simulink is shown in Figure 6.3. The hip and knee joints were controlled independently with two sets of PID controllers. The difference between the

desired joint angle position and the corresponding angle position measured during simulation, i.e. error is used as the PID controller input to generate the required control action that drives the revolute motor to the desire position. Saturation blocks of 150 Nm for the hip controller and 250 Nm for the knee controller were included in the control loop to restrict the output torque within admissible limits.

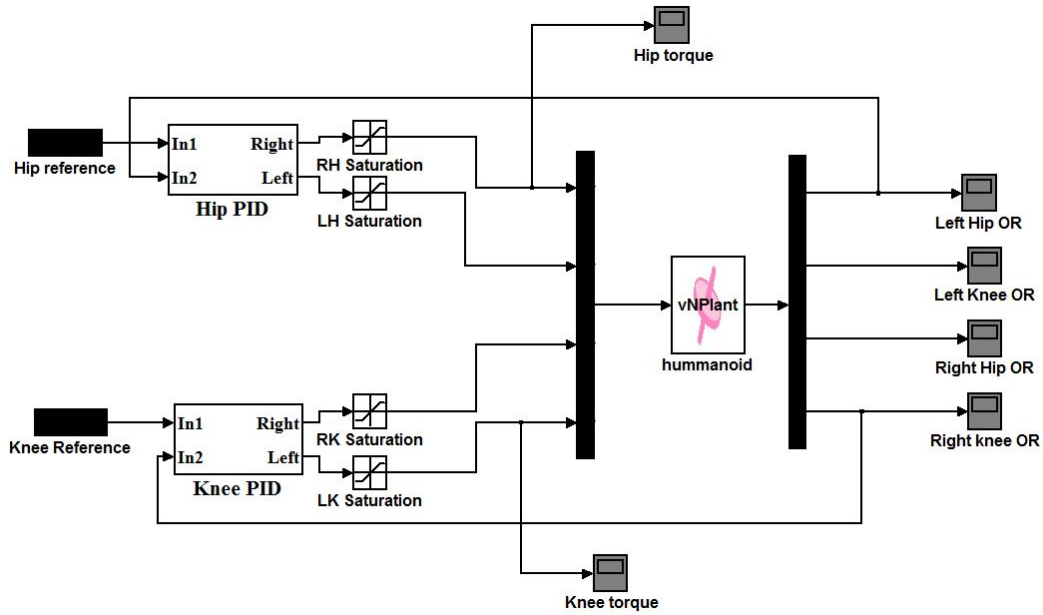


Figure 6.3: Humanoid model PID control scheme

The objective in this section is to evaluate the torque generated to actuate the revolute motor of each joint and the tracking of the predefined joints trajectories of standing up and sitting down movements. Therefore, several simulations were implemented using different combinations of gains for the PID controllers. PID gains were tuned through trial and error and SDA optimisation.

Initially, PID control parameters were tuned based on predefined set of distributed gains; 5 to 100 for K_p , 1 to 20 for K_i and 0 to 10 for K_d . The gain values were deduced from simulation tests carried out to obtain reasonable system behaviour. Thereafter, PID gains with reasonable overall behaviour obtained through trial and error tuning are used for further tuning with SDA optimisation.

SDA optimisation can improve the tuning process by implementing systematic search for the optimal solutions and covers wider range of gains with less computational time compared to trial and error method. For this test, 50 searching points with 10 iterations were considered to obtain the optimal solutions. A total of 6 parameters (K1-K6) of the hip and knee PID controllers were assigned in the optimisation algorithm to be optimised. Table 6.1 shows the PID parameters with smallest RMSEs obtained through trial and error and SDA optimisation tuning methods. RMSE was calculated using equation (5.1). Orientation and output torque simulation results of hip and knee joints with smallest RMSE value obtained are shown in Figure 6.4 and Figure 6.5.

Table 6.1: Trial and error and SDA tuned control parameters with RMSE values

Joint	PID parameters	Trial and error	RMSE	SDA	RMSE
Hip	Kp	44	4.94	42.85	1.2
	Ki	3.5		4.09	
	Kd	1.8		1.22	
Knee	Kp	47	4.95	44.87	1.72
	Ki	2.8		3.02	
	Kd	0.3		0.69	

Simulation results show that SDA tuned PID gains have enhanced the performance of the system in terms of reference tracking and output torque over trial and error tuned parameters. Although, reference tracking of hip and knee joints with manually tuned gains were within acceptable level, as joints error margin was less than 10% of the reference amplitude. However, the output torque generated with lower RMSE was smoother and comparatively less, as shown in Figure 6.4(e,f) and Figure 6.5(e,f) where torque consumption frequency was reduced between 1.3 and 2.4 seconds of the movement cycle.

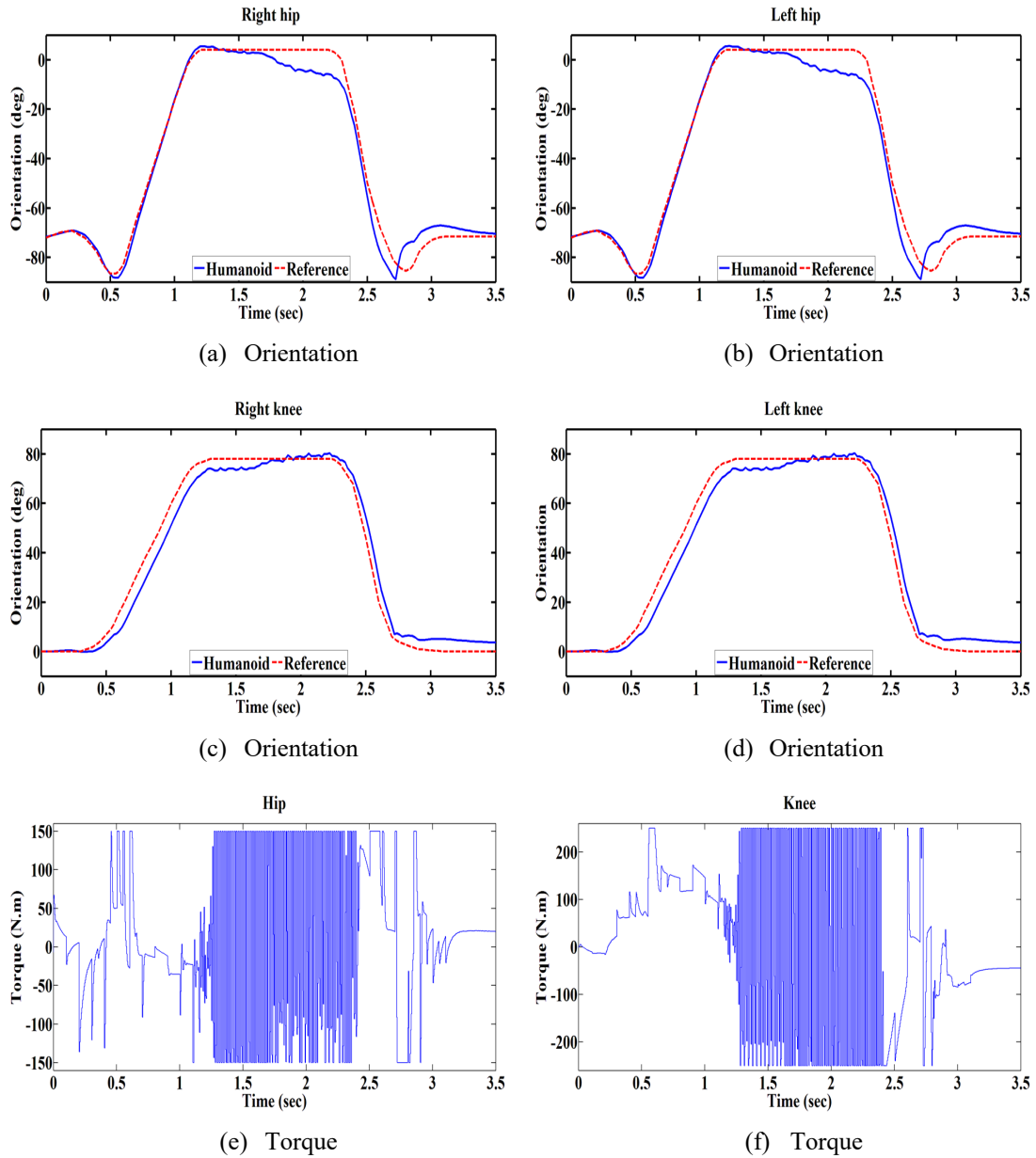


Figure 6.4: Orientation and output torque of hip and knee joints with trial and error tuned parameters

Figure 6.6 shows the control output torque signals before restriction by the saturation blocks. Simulation results show that the output torques generated to actuate the controlled joints reached approximately 300Nm for hip and knee joints. Meanwhile, Figure 6.5(e,f) shows that the torque signals after the saturation block as for most of the standing up and sitting down motion cycle remained below maximum level. Therefore, it was essential to add saturation blocks to the controller output as safety measure to protect joint motors from unwanted peak torque signal.

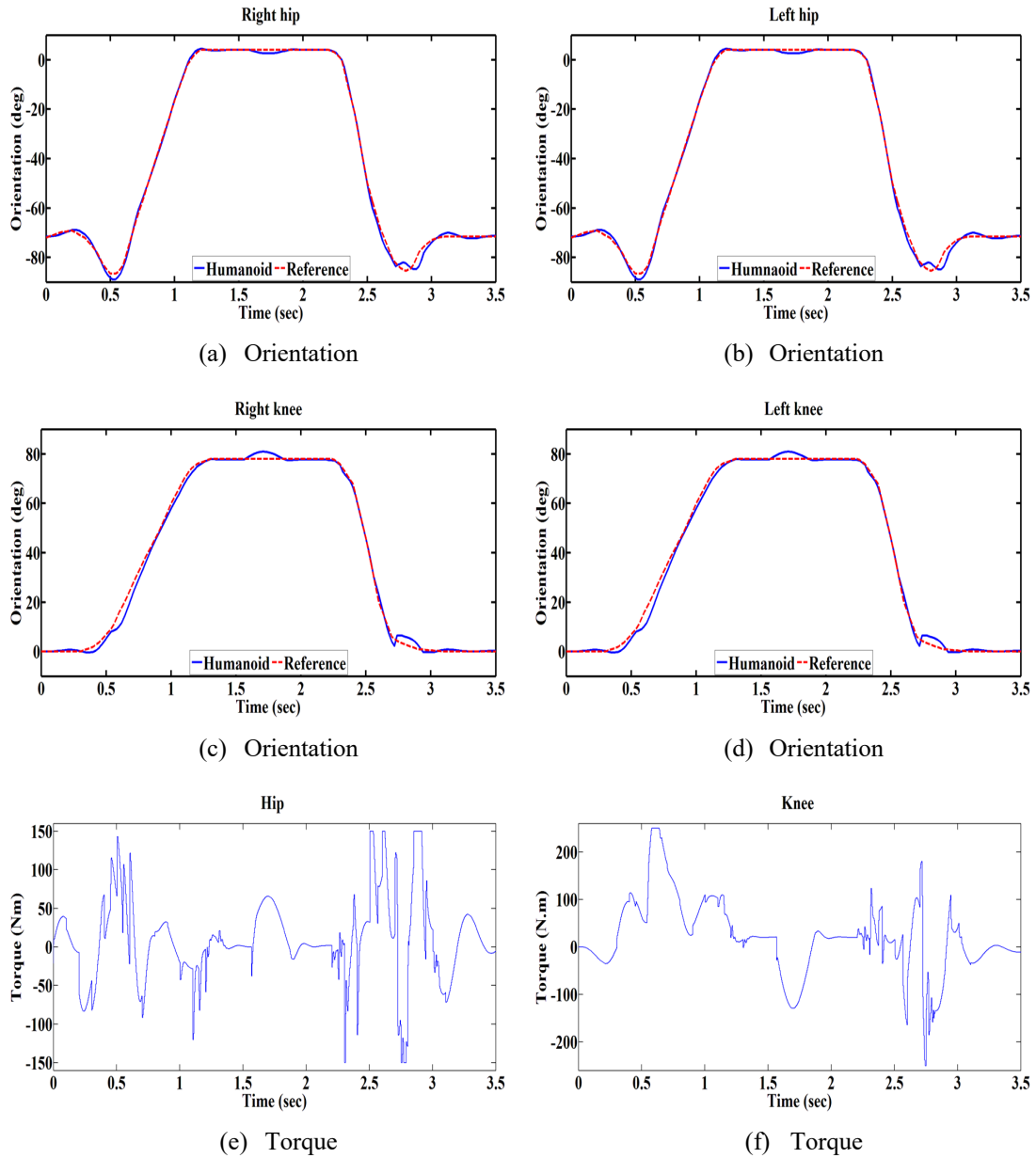


Figure 6.5: Orientation and torque for humanoid joints with SDA tuned PID parameters

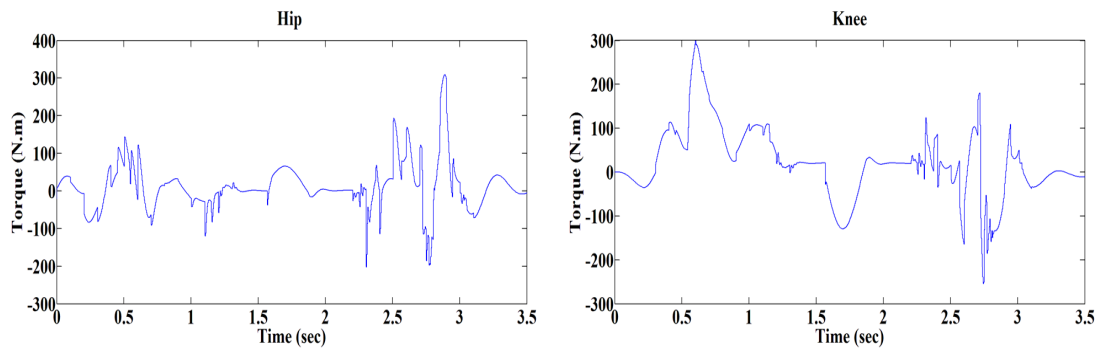


Figure 6.6: Unrestricted output torque of humanoid hip and knee joints

6.3.2 Control of humanoid and assistive exoskeleton

Analysis of the humanoid model carried out in the previous section helped to gain deep understanding of the system behaviour during standing up and sitting down motion cycle. In this section, the humanoid and exoskeleton models are incorporated to carry out investigation of the external assistance mechanism provided by the exoskeleton. The humanoid and exoskeleton joints are configured in MSC.vN4D with revolute motors to actuate in the sagittal plane, where each exoskeleton joint is set in parallel position with the humanoid joints. The exoskeleton is coupled to the humanoid lower limb and collision is allowed between exoskeleton support parts and humanoid thigh, leg and trunk. Collide settings allow the exoskeleton and the humanoid to follow the same predefined trajectory.

The PID controller developed in the previous section to control the humanoid active joints was modified to include the exoskeleton active joints in the control loop. The modification involves the ratio of external torque needed from the exoskeleton to support the humanoid lower limb. Therefore, each controller output was divided to provide 70% to the humanoid joint and 30% to the exoskeleton joint of the overall torque. That signifies a user with 30% deficiency of the required torque to complete standing up and sitting down movements and therefore, compensation is needed to restore mobility disorder. The configuration of a single joint PID controller shown in Figure 5.8 shows the configuration of humanoid and exoskeleton single joint PID controller. Whereas, the overall system control includes all humanoid and exoskeleton active joints as shown in Figure 6.7.

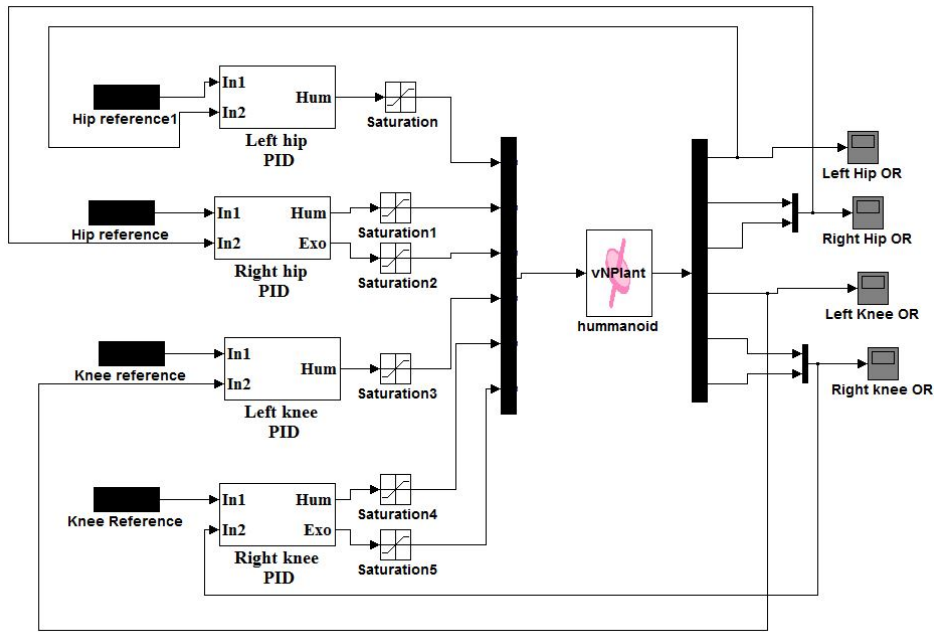


Figure 6.7: Simulink diagram of humanoid and exoskeleton joints PID control

During the simulation exercise, the combined humanoid and exoskeleton dynamic behaviour became more complex compared with the dynamics of the humanoid alone as investigated in the previous section. This was due to interactions between the collided bodies of the humanoid and exoskeleton models. Therefore, trial and error tuning was not considered in this section and SDA optimisation was implemented in the control loop to tune the PID parameters.

In the SDA process, 50 searching point with 10 iterations were considered to obtain the optimal solution. The best solution was evaluated by the smallest cost function, which is the sum of the four PID controllers RMSE values calculated using equation (5.2). Twelve parameters (K1-K12) were assigned in the optimisation algorithm to represent the parameters of the exoskeleton and humanoid lower limb joints PID controllers. At each iteration, the optimisation algorithm highlights the potential optimal solutions, and at the end of the process the most optimal parameters are presented based on the smallest cost function. Several SDA optimisation processes were executed with different range gains and

the smallest cost function obtained was 6.92 with the optimal solutions of PID parameters and their RMSE values shown in Table 6.2.

Table 6.2: SDA tuned control parameters with RMSE values

Joint	PID parameters	SDA	RMSE
Right hip	Kp	43.29	3.12
	Ki	7.18	
	Kd	0.41	
Left hip	Kp	39.39	3.6
	Ki	2.82	
	Kd	1.32	
Right knee	Kp	49.42	4.07
	Ki	2.97	
	Kd	3.65	
Left Knee	Kp	30.05	3.05
	Ki	4.64	
	Kd	4.27	

Simulation of the humanoid with support of the exoskeleton to complete standing up and sitting down cycle was carried out using SDA tuned PID parameters shown in Table 6.2. Figure 6.8 and Figure 6.9 show the orientation and output torque of the humanoid and exoskeleton hip and knee joints throughout the motion cycle. The simulation results show that the humanoid right-side joints were augmented with the required torque from the exoskeleton based on the predefined torque proportion between humanoid and exoskeleton joints. The exoskeleton provided the humanoid with a compensation torque of nearly 45 Nm for the right hip and 75 Nm for the right knee. Meanwhile, hip and knee of the humanoid left leg were actuated without external support, however, symmetric motion was achieved between both lower limbs.

Figure 6.8(b,d) and Figure 6.9(b,d) illustrates that the output torques generated were excessively high in frequency at some phases during standing up and sitting down movements, due to the control effort to maintain the tracking signal closer to the reference. The aforementioned issue is considered one of the drawbacks of implementing PID controller in this work. Therefore, this issue will be addressed in the following section.

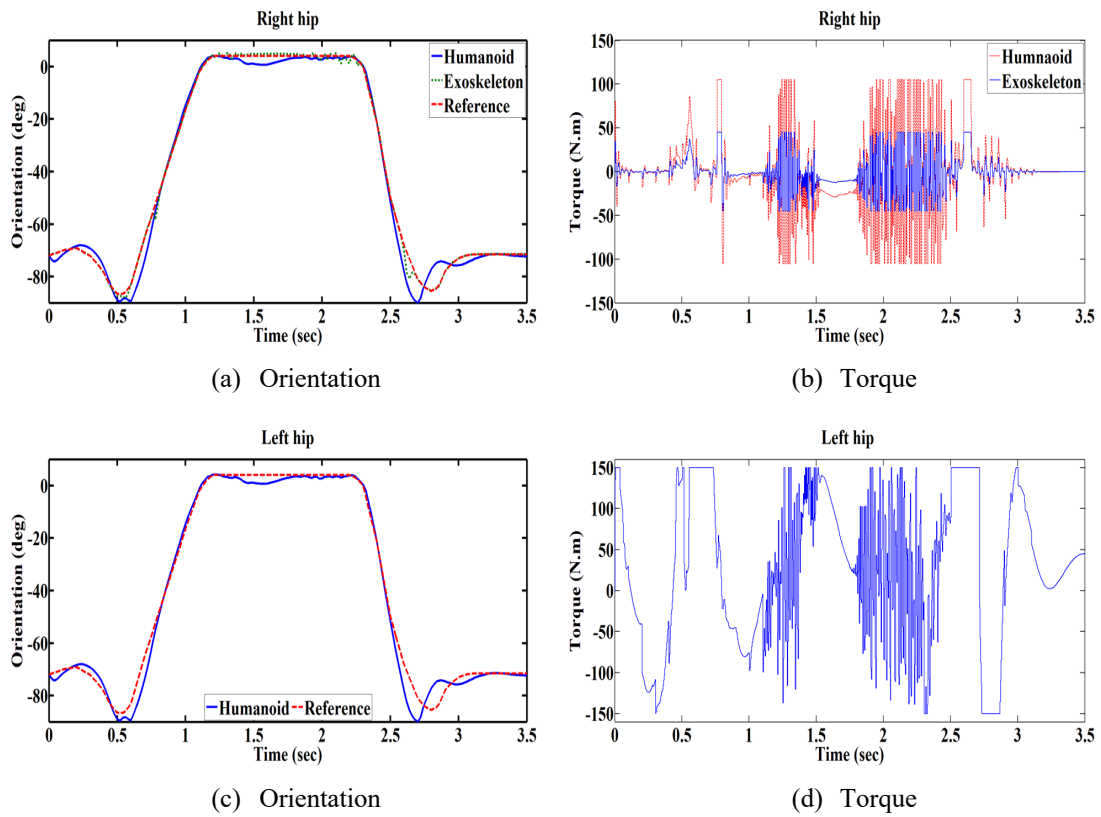


Figure 6.8: Simulation results of humanoid and exoskeleton hip joints

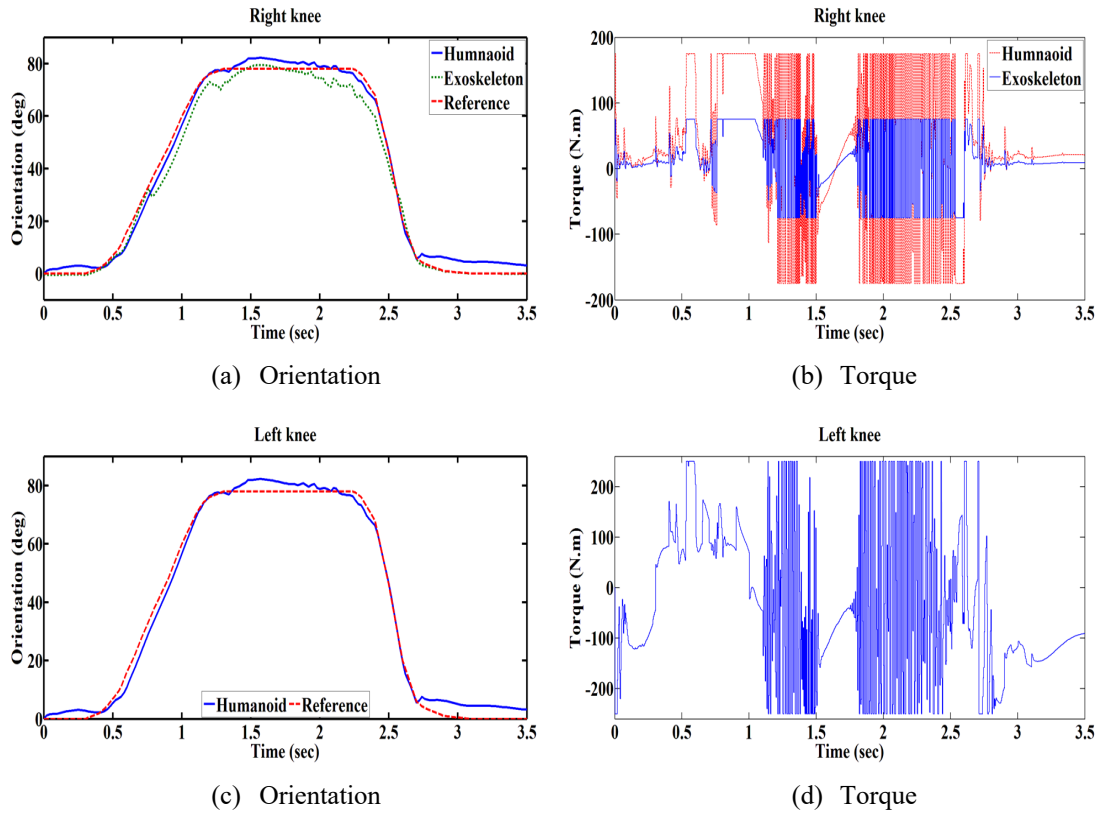


Figure 6.9: Simulation results of humanoid and exoskeleton knee joints

6.4 Fuzzy-based PD controller implementation

Due to the benefits discussed in section 4.2.2 of implementing FLC, fuzzy-based PD controller with MISO Mamdani type was selected in this work to control the active joints of the humanoid and exoskeleton.

Five linguistic terms of membership functions shown in Table 5.4 were used to develop the fuzzy rules set. Standard fuzzy rules set shown in Table 4.1 were modified by evaluating the system performance during standing up and sitting down movements through simulation trials with different fuzzy rules. Table 6.3 shows the set of fuzzy rules developed for this work. Gaussian membership functions implemented in the previous chapter were used for the FLC inputs and outputs, as it demonstrates steady and smooth response to the system. Figure 5.13 shows the five levels of Gaussian membership with 50% crossing between them. FLC input and output used normalised membership function values with the

range of [-1, 1]. The five levels of membership function terms result in $5 \times 5 = 25$ fuzzy rules for each FLC.

Table 6.3: Fuzzy rules set

$e \setminus \Delta e$	NB	NS	Z	PS	PB
NB	PB	PB	PS	PS	Z
NS	PB	PS	PS	Z	NS
Z	PS	PS	Z	NS	NB
PS	PS	Z	NS	NS	NS
PB	Z	NS	NS	NB	NB

Humanoid and exoskeleton control system consist of six independent subsystem FLC controllers that control the hip and knee revolute motors to achieve the desired angle position. While in operation, there is no connection or interaction between the subsystem controllers. However, the humanoid and exoskeleton parallel joints share the same orientation reference in order to follow the motion trajectories. The FLC incorporates two inputs: error (e) and change of error (Δe). Error is the measured variance between actual and required joint position, while change of error is the derivative of the error. FLC output is the torque generated to actuate revolute motors of the joints to the desired position.

Figure 6.10 shows the complete control system implemented in MATLAB Simulink using fuzzy logic toolbox facility. Scaling factors were assigned to the FLC inputs and output in order to adapt the normalised inputs and output membership functions to the system. P and D gains were added to the FLC inputs, and fuzzy gain was also added to the FLC output. Saturation blocks were inserted after the FLC output to restrict the output torque sent to the actuators within acceptable range. The saturation blocks were configured at ± 150 Nm for the hip controllers and ± 250 Nm for the knee controllers.

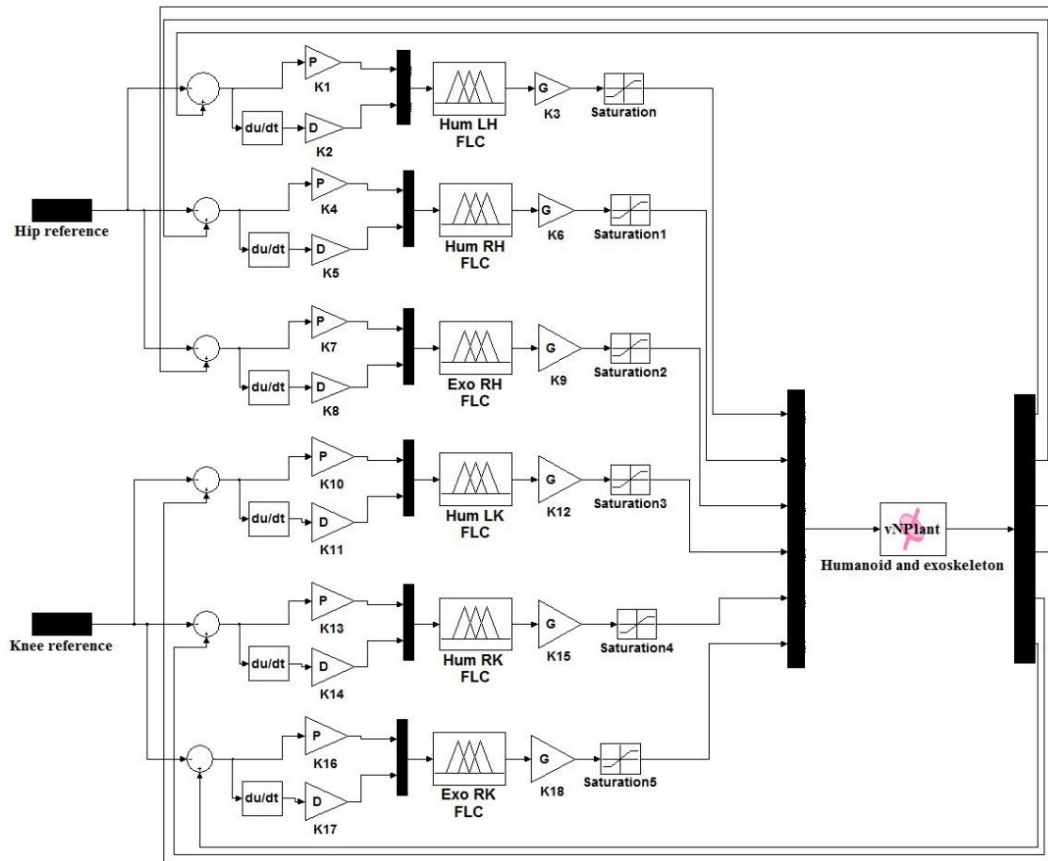


Figure 6.10: Humanoid and exoskeleton PD-fuzzy control scheme

The humanoid and exoskeletons models were integrated with the control scheme in MATLAB Simulink through MSC.vN4D plant block. During simulation, joints positions were measured in real-time by position sensor in MSC.vN4D environment and fed back to the controller, to generate the necessary torque to drive the hip and knee joints to the desired angle position.

A total of 18 gains (K1-K18) were used for the overall control system, represent scaling parameters of the FLCs. Trial and error tuning method for tuning the scaling parameters was considered inefficient and time consuming due to the large number of gains used in the overall system control. Moreover, the dynamics of the humanoid and exoskeleton are interdependent during simulation which makes it more difficult to use manual tuning. However, SDA optimisation proved to be efficient and achieved improved system performance with fuzzy-based PD controller as demonstrated in the previous

chapter. Therefore, SDA optimisation was used to tune and achieve best possible inputs output scaling factors for the FLCs.

In the SDA process, 50 searching points with 10 iterations were considered to obtain the optimal solution. Control system parameters (K1-K18) were assigned in the optimisation algorithm to be optimised. The objective of the optimisation process is to locate the lowest cost function based on hip and knee joints angle position error while performing standing up and sitting down movements. Each PD-fuzzy controller was evaluated by RMSE calculated as in equation (5.1). The overall control system performance was evaluated by the minimum cost function obtained in the optimisation process.

The minimum cost function achieved with SDA optimisation process was 6.58. Table 6.4 shows the optimal FLC scaling factors obtained with SDA optimisation along with their RMSE values. The humanoid and exoskeleton were simulated in MSC.vN4D to complete standing up and sitting down movements for 3.5 seconds through PD-fuzzy controller with SDA tuned scaling factors. Orientation and output torque results of the controlled joints obtained through the simulation are presented in Figure 6.11 and Figure 6.12. In general, implementation of fuzzy-based PD controller showed notable improvements in the performance of the humanoid and exoskeleton system while simulating standing up and sitting down movements compared with the PID controller implemented in the previous section. Joints orientation results showed smooth tracking towards the trajectory reference with less RMSE values. Moreover, simulation results show that the output torque frequency of the controlled joints were reduced significantly and did not reach the maximum torque level set by the saturation blocks. The output torque ranges for the controlled joints were within the admissible level recommended by Low (2011).

Figure 6.11b and Figure 6.12b show that the exoskeleton managed to compensate for the humanoid joints with the necessary assistive torque required to complete the motion

task for 3.5 seconds. For the right hip joint, the exoskeleton supported the humanoid with approximately 45 Nm, while the humanoid joint was actuated with approximately 95 Nm. Meanwhile, the exoskeleton right knee joint supported the humanoid right knee with approximately 65 Nm, while the humanoid joint was actuated with approximately 140 Nm. The humanoid healthy lower limb joints were actuated without external support, therefore, hip joint was actuated with a maximum torque of 140 Nm and the knee joint with 205 Nm. Simulation results showed that a symmetric motion between right and left joints was achieved throughout standing up and sitting down movements with the assistance of the exoskeleton fitted on the right side of the humanoid lower limb.

Table 6.4: SDA tuned FLC scaling parameters

Joint controllers	FLC parameters			RMSE
Left hip	K1	K2	K3	1.83
	0.97	0.24	160	
Right hip	K4	K5	K6	1.75
	0.72	0.34	100	
Exoskeleton hip	K7	K8	K9	1.68
	0.45	0.89	60	
Left knee	K10	K11	K12	2.16
	0.45	0.01	250	
Right knee	K13	K14	K15	2.15
	0.44	0.86	170	
Exoskeleton knee	K16	K17	K18	3.6
	0.49	0.6	80	

It was noted that the hip and knee joints had the most tracking error margin at seat loading phase during sitting down movement, due to the inclusion of gravity factor during the simulation, which makes the humanoid and exoskeleton models rebound after attaching

the virtual seat implemented in MSC.vN4D. However, the control system kept the humanoid and exoskeleton models stable during the stabilisation phase while the upper body of the humanoid was adjusting its stability.

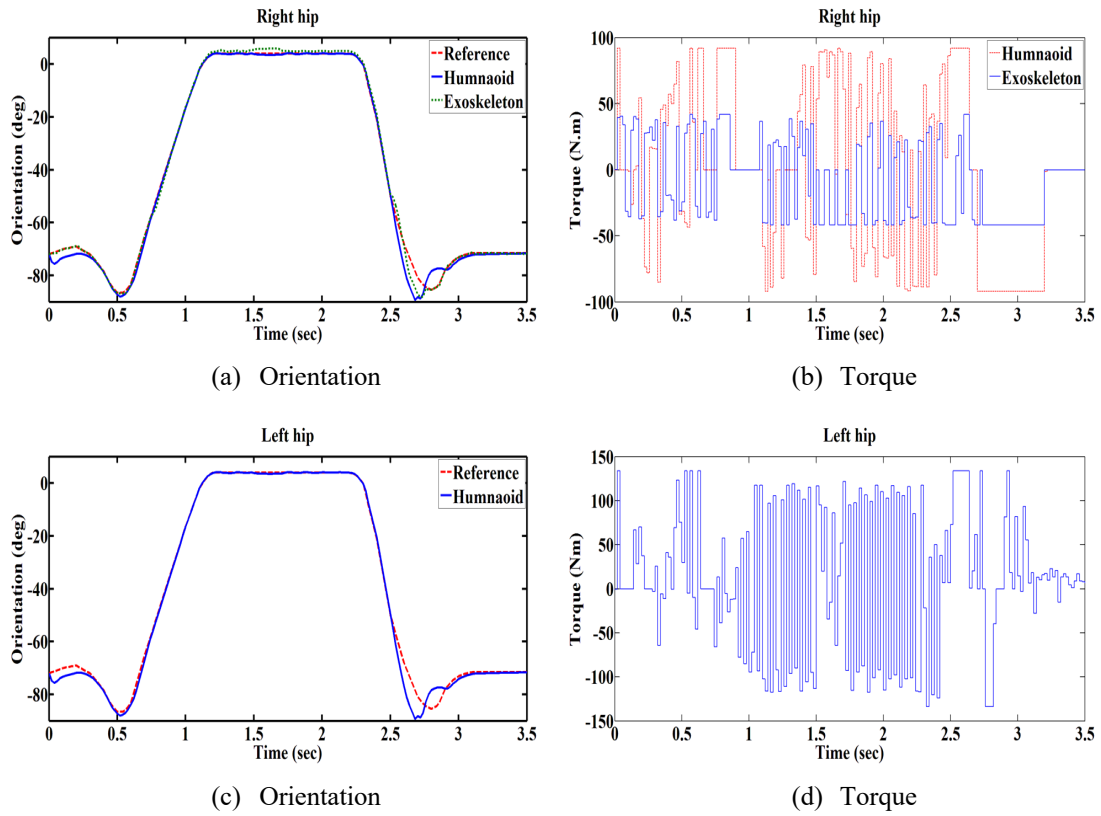


Figure 6.11: Orientation and output torque results for humanoid and exoskeleton hip joints

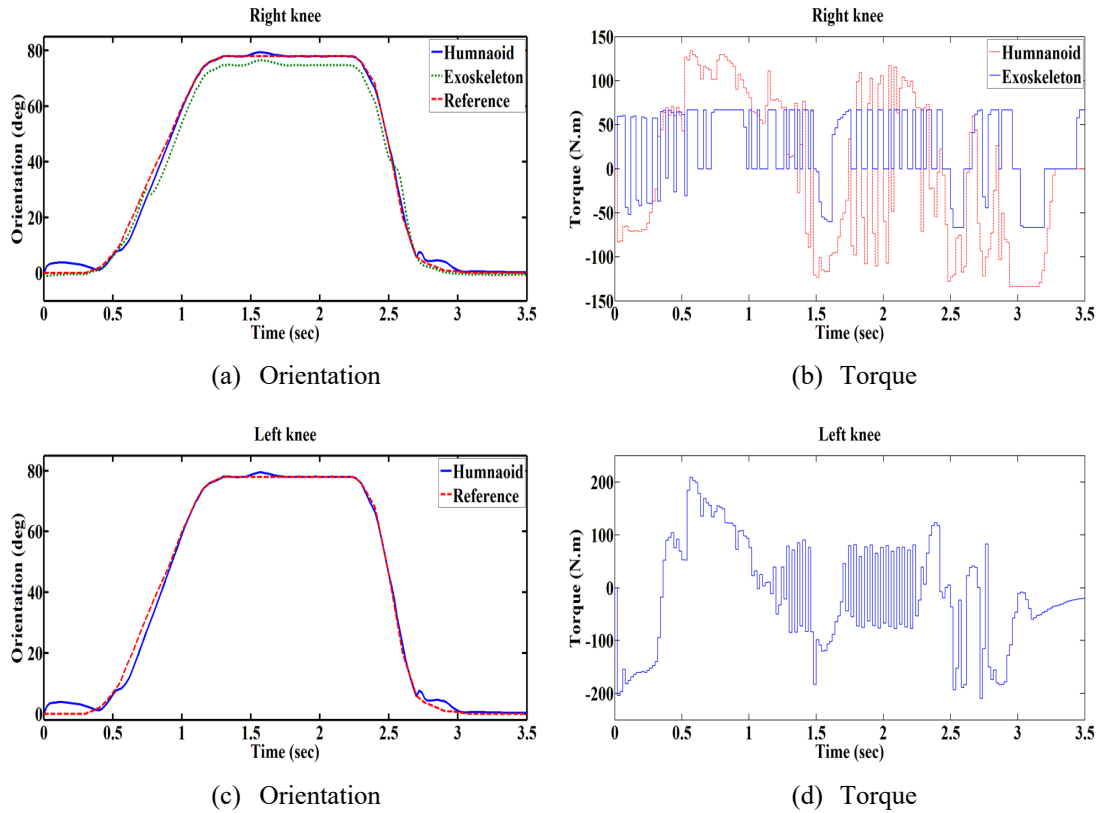


Figure 6.12: Orientation and output torque results for humanoid and exoskeleton knee joints

6.4.1 Tests with different standing up and sitting down cycle speeds

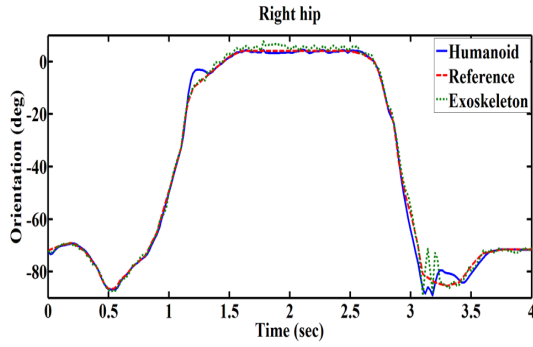
In order to validate the efficiency of the humanoid and exoskeleton control system while performing standing up and sitting down manoeuvres, several simulation tests were carried out using different motion cycle speeds. The hip and knee orientation reference shown in Figure 3.12 was modified to develop two sets of joint trajectories with different time scales of complete standing up and sitting down movements cycle. The motion cycle with a duration of 4 seconds was used to define slow speed manoeuvre, while a motion cycle with a duration of 3 seconds was used to define fast speed manoeuvres.

The configurations of fuzzy-based PD controller employed in the previous section were used to simulate the humanoid and exoskeleton models with different standing up and sitting down cycle speeds using the modified joint trajectories as reference. The optimised fuzzy scaling factors obtained with SDA optimisation were also used as the control

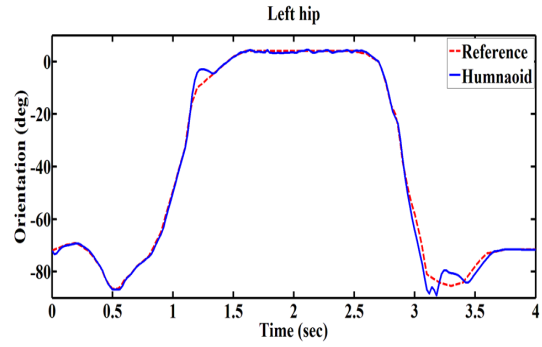
parameters. This investigation was focused on examining the control action in terms of joint trajectory tracking and output torque in different motion conditions.

The humanoid and exoskeleton models were simulated to complete standing up and sitting movements for 4 seconds using slow speed trajectories reference. Figure 6.13 and Figure 6.14 show the simulation results of hip and knee joints position tracking and output torque with low-speed cycle. The RMSE values obtained for the hip joints of the humanoid and exoskeleton were 2.2 and 2.6 respectively. Meanwhile, RMSE values of the humanoid and exoskeleton knee joints were 2.3 and 3.4 respectively. The RMSE values were higher compared with the values obtained with average speed cycle shown in Table 6.4. However, the tracking trajectories of the controlled joints showed that the system dynamics was still smooth and stable during the simulation with low-speed cycle. The output torques generated to actuate the humanoid and exoskeleton joints conformed to the acceptable levels and did not reach the maximum value set by the saturation blocks.

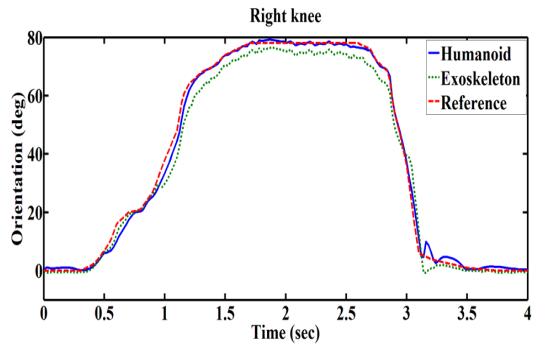
Simulation results of the humanoid and exoskeleton joints with fast standing up and sitting down motion cycle are presented in Figure 6.15 and Figure 6.16. The RMSE values obtained were 3.8 for the humanoid hip and 2.1 for the exoskeleton hip, 3.2 for the humanoid knee and 3.1 for the exoskeleton knee. It was noted that the reference tracking errors of the hip joints were higher during sitting down stabilisation-phase and at quiet-standing phase for the knee joints. Although the error margin was still within the acceptable level which was less than 10 degree of the reference. Nevertheless, simulation results show that the humanoid and exoskeleton performance was smooth and stable during most of the movement cycle. The output torques generated to actuate the humanoid and exoskeleton joints conformed to the acceptable levels and did not reach the maximum values set by the saturation blocks.



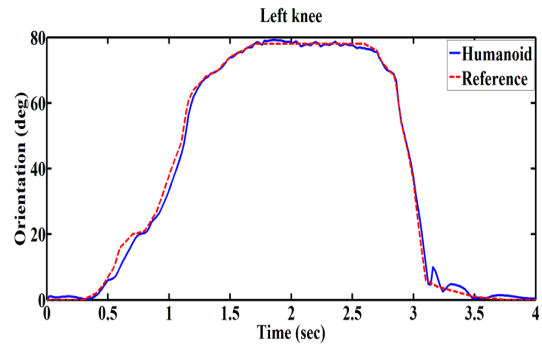
(a) Orientation



(b) Orientation

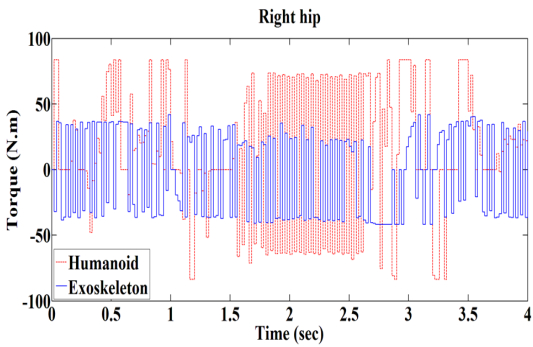


(c) Orientation

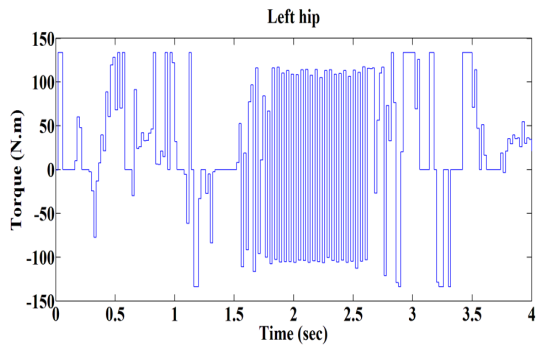


(d) Orientation

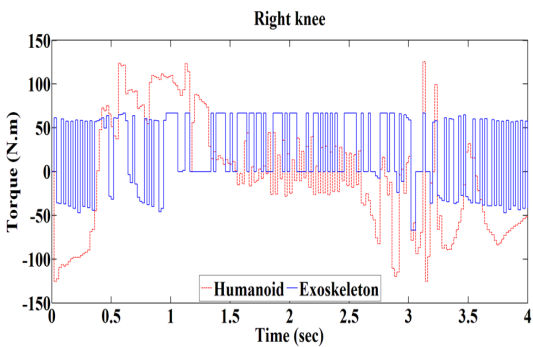
Figure 6.13: Orientation results of the humanoid and exoskeleton joints with slow speed cycle of standing up and sitting down



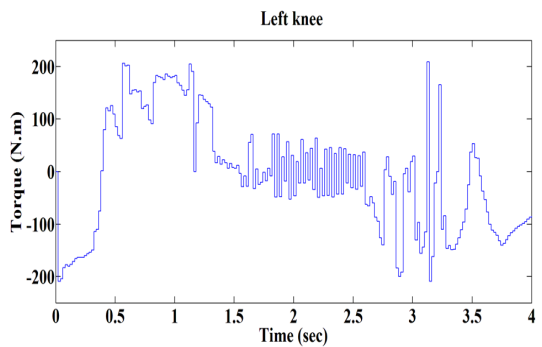
(a) Torque



(b) Torque



(c) Torque



(d) Torque

Figure 6.14: Torque results of the humanoid and exoskeleton joints with slow speed cycle of standing up and sitting down

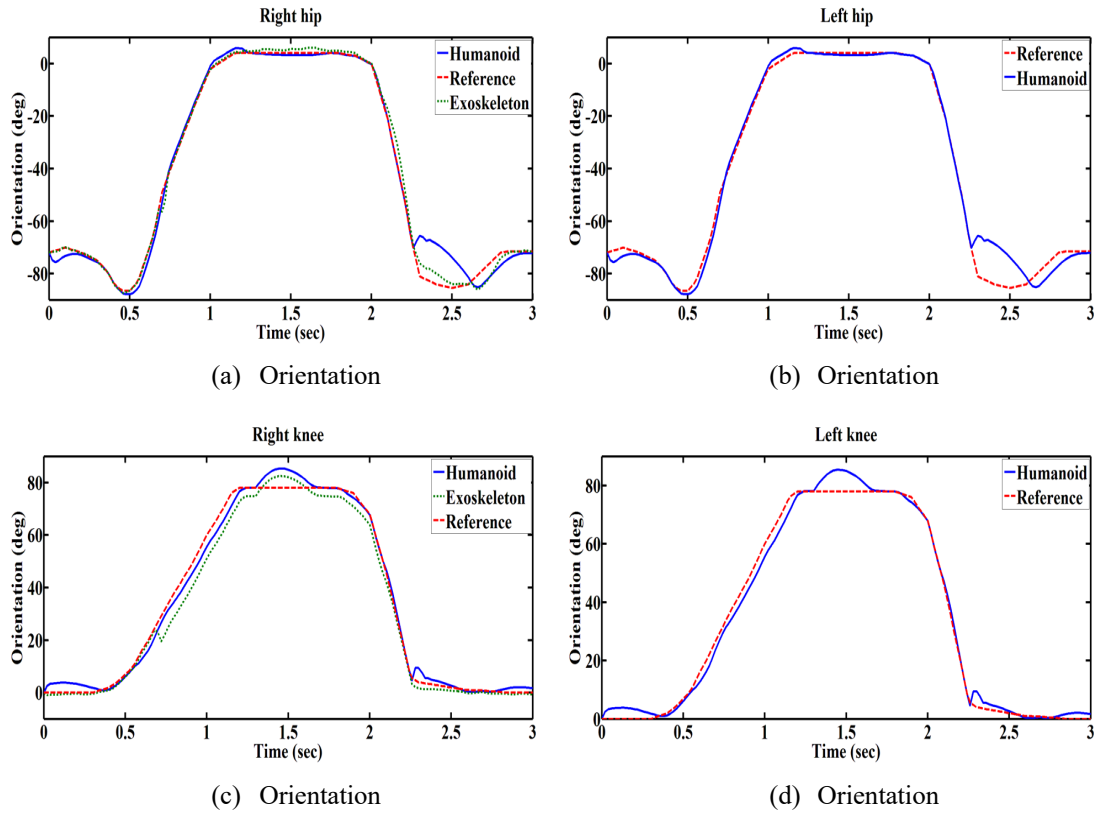


Figure 6.15: Orientation results of the humanoid and exoskeleton joints with fast speed cycle of standing up and sitting down

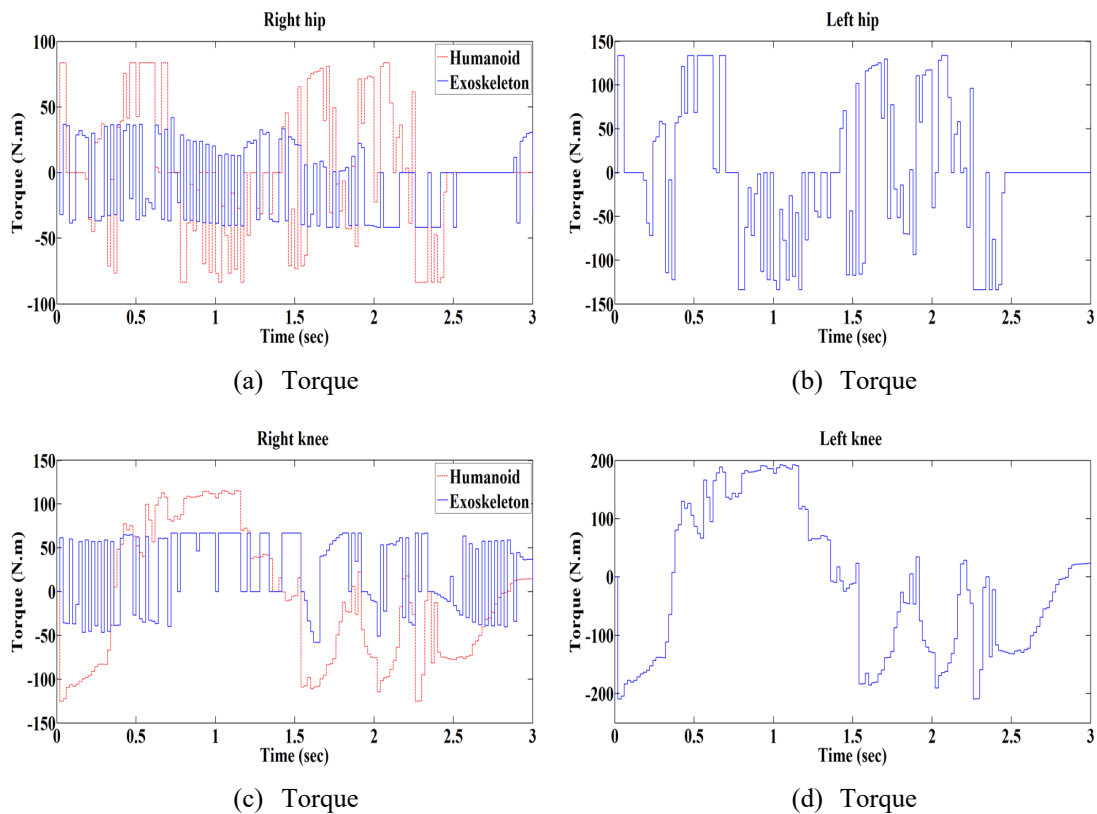


Figure 6.16: Torque results of the humanoid and exoskeleton joints with fast speed cycle of standing up and sitting down

6.4.2 Tests with constant loads and disturbance forces

The control system was tested by subjecting the humanoid and exoskeleton models to various constant loads and external disturbance forces in different simulation attempts, to examine the system behaviour and evaluate the control robustness. Constant loads and disturbance forces were applied at different phases during standing up and sitting down movement cycle. Figure 6.17a shows the positions of the disturbance forces applied on the humanoid model during seat unloading phase while standing up and at the descending phase while sitting down. Figure 6.17b shows the constant load positions applied on the humanoid and exoskeleton model at separate stages of the movement cycle. The positions were selected to examine the response of the controlled joints related to the humanoid right lower limbs and the exoskeleton segments. Three levels of disturbance were applied in both tests; 500N, 1000N and 1500N. Fuzzy-based PD controller with SDA tuned scaling parameters were used during these tests. Constant load and disturbance force tests were carried out separately.

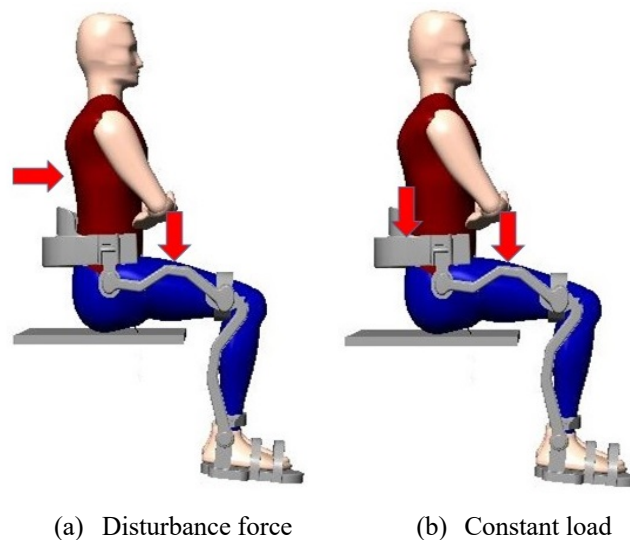


Figure 6.17: Constant load and disturbance force positions on the humanoid and exoskeleton models

For the constant load test, simulation was implemented with force function applied on the humanoid right thigh and exoskeleton back support. During standing up, the constant load was activated on the humanoid right thigh from 0 to 1.5 seconds, thereafter, another load was activated on the exoskeleton back support from 2 to 3.5 seconds during sitting down. Simulations were repeated with different levels of load forces to examine the system behaviour and the control action. Figure 6.18 shows the combined tracking trajectory results of the humanoid and exoskeleton right hip and knee joints with three levels of load forces. With a constant load force of 500N, the system behaviour was stable for most of the motion cycle. However, with 1000N the tracking error increased slightly but the controller kept the system stable throughout the motion cycle. It is noted that the system became unstable when a force of 1500N or more was applied on the system while simulating standing up and sitting down manoeuvres.

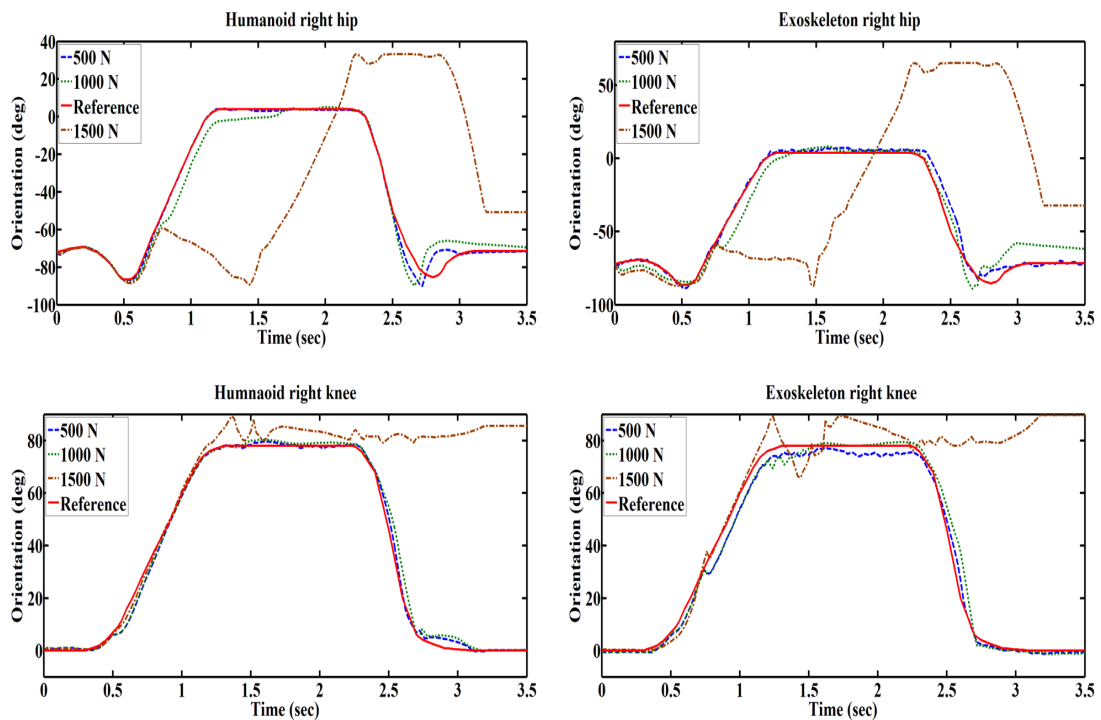


Figure 6.18: Simulation results of the humanoid and exoskeleton right side joints orientation under different constant loads

For the disturbance force test, impulse forces were applied on the humanoid and exoskeleton models during simulation at different stages of the movement cycle, to examine robustness of the controller to external disturbance during transition of standing up and sitting down phases. Impulse force was applied in the opposite direction of the humanoid right thigh movement during standing up from 0.9 to 1 second, thereafter, another impulse force was applied on the humanoid back during sitting down movement from 2.4 to 2.5 seconds. Simulation results of hip and knee joints orientation under the influence of three levels of disturbance forces are shown in Figure 6.19 . For the 500N and 1000N impulse forces, the system was stable throughout the whole cycle. However, when the impulse force of 1500N was applied on the humanoid back during sitting down, the overall system became unstable, meanwhile, the system sustained stability with the same amount of impulse force applied on the right thigh during standing up movement.

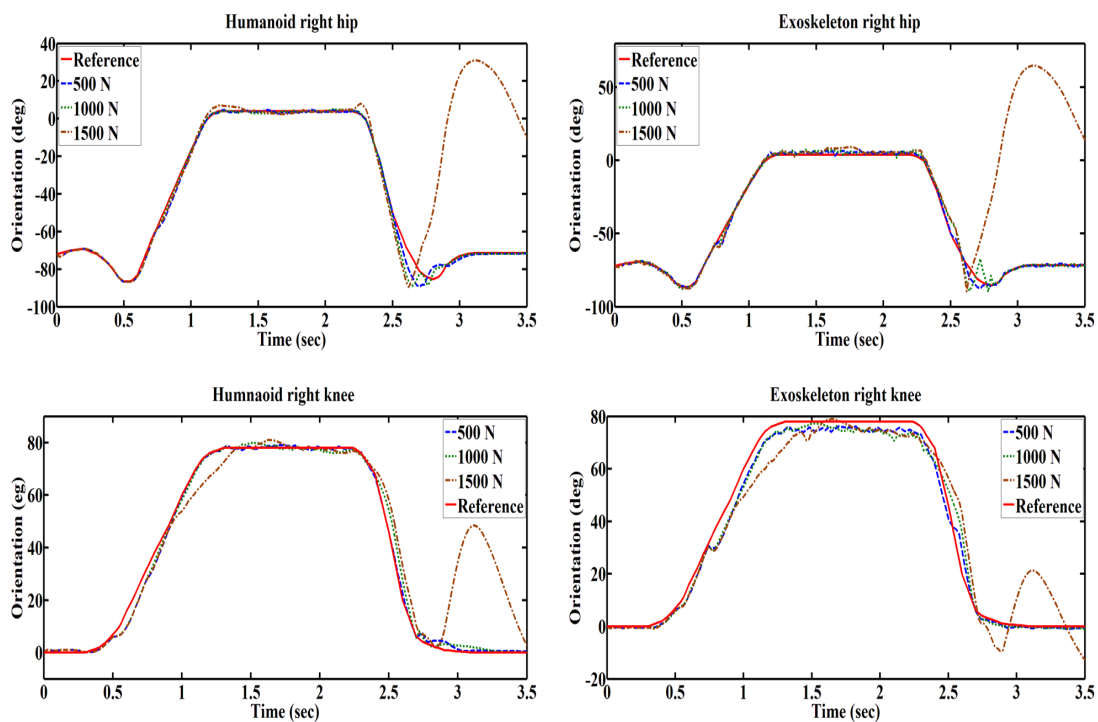


Figure 6.19: Simulation results of the humanoid and exoskeleton right side joints orientation under different disturbance forces

6.5 Summary

Investigations of assisting hemiplegic patient to achieve natural movements of standing up and sitting down with support of single leg exoskeleton have been carried out. Two types of controller, namely PID and fuzzy-based PD, have been developed using MATLAB Simulink to control and simulate the humanoid and exoskeleton models in MSC.vN4D virtual environment. Torque profiles of the humanoid and exoskeleton joints have been examined to achieve safe and stable joints actuation. The performance of the controllers has been evaluated using recorded trajectories and output torque results, through simulations of in MSC.vN4D virtual environment.

Simulation results obtained from the employed controllers have demonstrated that fuzzy-based PD controller enhances the system performance compared with PID controller, in terms of reference tracking by minimising RMSE and reducing torque consumption. Additionally, control parameters tuned with SDA optimisation have shown great advantage in decreasing RMSE values compared to the control parameters obtained with heuristic tuning. Simulation results demonstrate that the controller can provide suitable control action to achieve safe and stable standing up and sitting down movements, by generating the required torque within admissible limits. The output torque results show that the exoskeleton is capable to compensate the humanoid with almost 30% of the total torque required to achieve stable motion. A comparison of the torque root mean square (RMS) values of the exoskeleton joints generated with PID and PD-fuzzy controllers is shown in Table 6.5. The RMS values shows that PD-fuzzy controller reduced the torque consumption of the controlled joints which lead to less energy consumption.

Table 6.5: Comparison of torque RMS values generated with PID and PD-fuzzy controllers for the exoskeleton joints during standing up and sitting down simulations

Joint / torque RMS	Torque RMS with PID controller (Nm)	Torque RMS with PD-fuzzy controller (Nm)	Torque reduction (%)
Hip	39	31	20.5
Knee	49	42	14.3

Finally, two types of tests have been carried out to evaluate the control efficiency and robustness under different conditions. The tests have been carried out using different movement cycle speeds, disturbance forces and constant loads. For all the tests, the controller has shown capabilities to maintain the system stable and recover from external disturbances.

Chapter 7: Conclusion and future works

7.1 Summary and conclusion

A comprehensive literature review has been carried out to gain understanding of what has been achieved in the exoskeleton technology, specifically lower limb exoskeletons. The review has included the biomechanics of human essential movements, exoskeleton design considerations, control strategies and recently developed applications. Several drawbacks and gaps have been highlighted regarding exoskeleton technologies. However, there are no sufficient experimental publications that provide medical and technical assessment for using exoskeleton devices specially for standing up and sitting down movements.

Few publications have been identified that evaluate the lower limb exoskeleton designs using software facilities by simulating CAD prototypes in virtual environments, because majority of the published works is focused on exoskeleton prototypes construction during the experimental period. Therefore, advantages of using software facilities are considered in this research to develop the humanoid and exoskeleton models and test the control implementation in virtual environment. The humanoid model has been designed in a way to replicate dynamics and kinematics of the human body without taking into account its musculoskeletal features. Although, inclusion of more human characteristics to the humanoid model will improve accuracy of the results, but its implementation would have differed the objectives of this study. Additionally, according to the available software resources the humanoid model has been designed taking into account the complexity and computational time during simulations. The exoskeleton model has been structured with active joints that are parallel in position with the humanoid hip, and ankle joints to allow support to the humanoid lower limb segments. The integration between the humanoid and

exoskeleton models presented in this study has been adequate to provide a platform to test the controllers and simulate the designated mobility tasks.

The aim of this research has been to develop a single leg exoskeleton to assist hemiplegic patient in walking, standing up and sitting down movements in a torque compensation manner. Moreover, to develop a suitable control system that is able to control the humanoid and exoskeleton system simultaneously and provide the necessary external torque through the exoskeleton to compensate the humanoid during the designated tasks. The work carried out has shown that the research aims and objectives have been successfully accomplished.

The humanoid model has been simulated to generate and analyse the torque profiles of hip, knee and ankle joints whilst executing walking, standing up and sitting down with the use of PID controller. The analysis has offered important information such as maximum joint torques, range of controller gains, humanoid dynamic behaviour and verification of the motion trajectory reference applied as an input to the controller. This information has been considered when implementing the control and simulation of the exoskeleton model to deliver the required support during walking, standing up and sitting down to the humanoid model.

The humanoid and exoskeleton models have been incorporated to implement the external assistance mechanism during mobility tasks. Based on the torque profile analysis, the level of external compensation needed from the exoskeleton has been estimated to be approximately 30% of the overall torque needed to complete the task. Therefore, the controller output has been configured to provide the humanoid joints with 70% of the output torque and 30% for the exoskeleton joints. PID and fuzzy-based PD controllers have been utilised to control the humanoid and exoskeleton system. The simulation results of the mobility tasks obtained through the two control methods have been compared based on

lowest RMSE in respect of reference tracking and output torque. This study has identified that PID control is not sufficient to control a complex system such as the dynamics of the humanoid and exoskeleton models. However, non-model based intelligent controller such as fuzzy logic control method has been utilised to avoid modelling complexity of the system. Moreover, SDA optimisation has been used to optimise the control parameters. The results obtained with the fuzzy-based PD controller with SDA tuned parameters, have shown the potential advantages in implementing an intelligent control approach to control such a complex dynamic system.

The humanoid and exoskeleton system has been simulated with different conditions such as disturbance forces, constant loads and different motion cycle speeds, to evaluate the control efficiency and robustness. The control system has shown abilities to maintain the humanoid and exoskeleton reasonably stable with different disturbance forces and constant loads between 500N and 3000N, and with different speeds of walking, standing up and sitting down motion cycles.

7.2 Recommendations for future work

In this study, the specified aims and objectives have been successfully achieved. The presented results obtained through simulation of the humanoid and exoskeleton system may be considered for further investigation and analysis. This section highlights a list of recommendations for further enhancement of the system performance and extension of its functionalities for more developed application.

- For the scalability of the exoskeleton structure, further investigations in frame material and mechanical design are required to develop portable lightweight exoskeleton system that works as universal fitting for different user's dimensions.

- Implement advanced mechanism that provides online estimation of the external assistance percentage needed to augment the user's need in order to provide more accurate assistance since paralysis level can vary from person to person.
- More research on actuation system may be carried out to select the most suitable motors in terms of range of torques, RoM and DoF capabilities, to represent the system more accurately during simulation in virtual environment.
- Further investigation is needed to actuate and control the ankle joint during standing up and sitting down movements to add more balance to the humanoid and exoskeleton system.
- Upgrade the control hierarchy to include further control level that automatically detects the transition between walking, standing up and sitting down modes.
- Expand RoM control of the humanoid and exoskeleton active joints in the horizontal axes to add further balance and stability measures for the system.
- Include FLC parameters such as fuzzy rules and membership functions in the optimisation process to enhance the system performance and obtain optimal results.

Finally, alternative software facilities may be considered to overcome the limitation of MSC.vN4D software such as high computational time and limited simulation tools of complex model dynamics. The AnyBody modelling system software provided by (AnyBodyTechnology, 2017) could be efficient alternative, due to its advanced capabilities of calculating joint forces and momentum, contact forces, metabolic cost and system equilibrium.

References

- Aissaoui, R., and Dansereau, J. (1999). Biomechanical analysis and modelling of sit to stand task: a literature review. In *IEEE SMC'99 Conference Proceedings. 1999 IEEE International Conference on Systems, Man, and Cybernetics* (Vol. 1, pp. 141–146).
- Akkizidis, I. S., Roberts, G. N., Ridao, P., and Batlle, J. (2003). Designing a fuzzy-like PD controller for an underwater robot. *Control Engineering Practice*, 11(4), 471–480.
- Aliman, N., Ramli, R., and Haris, S. M. (2017). Design and development of lower limb exoskeletons: A survey. *Robotics and Autonomous Systems*, 95, 102–116.
- Almeshal, A. M., Goher, K. M., Nasir, A. N. K., Tokhi, M. O., and Agouri, S. A. (2013). Fuzzy logic optimized control of a novel structure two-wheeled robotic vehicle using HSDBC, SDA and BFA: A comparative study. In *2013 18th International Conference on Methods & Models in Automation & Robotics (MMAR)* (pp. 656–661).
- AnyBodyTechnology. (2017). The AnyBody modeling system. Retrieved March 20, 2017, from <https://www.anybodytech.com/software/>
- Army-Technology. (2010). Raytheon XOS 2 Exoskeleton, Second-Generation Robotics Suit. Retrieved June 20, 2017, from <https://www.army-technology.com/projects/raytheon-xos-2-exoskeleton-us/>
- Benasla, L., Belmadani, A., and Rahli, M. (2014). Spiral optimization algorithm for solving combined economic and emission dispatch. *International Journal of Electrical Power & Energy Systems*, 62, 163–174.
- Bierman, W. (1946). Hemiplegia. *The American Journal of Nursing*, 46(2), 115–118.
- Bjornstrup, J. (1995). *Estimation of human body segment parameters-historical background[report]*. Retrieved from <http://citeseerx.ist.psu.edu/viewdoc/summary?doi=10.1.1.21.5223>
- Bogue, R. (2015). Robotic exoskeletons: a review of recent progress. *Industrial Robot: An International Journal*, 42(1), 5–10.
- Bogue, R. (2018). Exoskeletons – a review of industrial applications. *Industrial Robot: The International Journal of Robotics Research and Application*, 45(5), 585–590.

- Cao, J., Xie, S. Q., Das, R., and Zhu, G. L. (2014). Control strategies for effective robot assisted gait rehabilitation: The state of art and future prospects. *Medical Engineering & Physics*, 36(12), 1555–1566.
- Cardero, C. (2012). Articulated human body.grabcad. Retrieved October 1, 2015, from <https://grabcad.com/library/articulated-human-body-2>
- Cenciarini, M., and Dollar, A. M. (2011). Biomechanical considerations in the design of lower limb exoskeletons. In *2011 IEEE International Conference on Rehabilitation Robotics* (pp. 1–6).
- Chen, B., Ma, H., Qin, L.-Y., Gao, F., Chan, K.-M., Law, S.-W., Qin, L., and Liao, W.-H. (2016). Recent developments and challenges of lower extremity exoskeletons. *Journal of Orthopaedic Translation*, 5, 26–37.
- Chen, G., and Pham, T. T. (2000). *Introduction to fuzzy sets, fuzzy logic, and fuzzy control systems*. CRC Press.
- Cheong, F., and Lai, R. (2007). Designing a hierarchical fuzzy logic controller using the differential evolution approach. *Applied Soft Computing*, 7(2), 481–491.
- Choi, J., Na, B., Jung, P. G., Rha, D. w., and Kong, K. (2017). WalkON Suit: A Medalist in the Powered Exoskeleton Race of Cyathlon 2016. *IEEE Robotics & Automation Magazine*, 24(4), 75–86.
- Crowell III, H. P. (1995). Human engineering design guidelines for a powered, full body exoskeleton. *U.S. Army Research Lab, Aberdeen Proving Ground, Md, ARL-TN-60*.
- Crowell III, H. P., Boynton, A. C., and Mungiole, M. (2002). Exoskeleton power and torque requirements based on human biomechanics. *U.S. Army Research Lab, Aberdeen Proving Ground, Md, ARL-TR-276*.
- Cyberdyne Inc. (2011). Hybrid assistive limb. Retrieved April 16, 2018, from <https://www.cyberdyne.jp/english/products/HAL/index.html>
- Dassault Systèmes SolidWorks. (2016). Solidworks standard. Retrieved March 1, 2016, from <https://www.solidworks.com/category/3d-cad>
- Dawe, E. J. C., and Davis, J. (2011). (vi) Anatomy and biomechanics of the foot and ankle. *Orthopaedics and Trauma*, 25(4), 279–286.

- de Looze, M. P., Bosch, T., Krause, F., Stadler, K. S., and O'Sullivan, L. W. (2016). Exoskeletons for industrial application and their potential effects on physical work load. *Ergonomics*, 59(5), 671–681.
- Dollar, A. M., and Herr, H. (2008). Lower extremity exoskeletons and active orthoses: Challenges and state-of-the-art. *IEEE Transactions on Robotics*, 24(1), 144–158.
- Engelbrecht, A. P. (2007). *Computational intelligence an introduction* (Second). John Wiley & Sons Ltd.
- Esquenazi, A., Talaty, M., Packel, A., and Saulino, M. (2012). The ReWalk powered exoskeleton to restore ambulatory function to individuals with thoracic-level motor-complete spinal cord injury. *American Journal of Physical Medicine & Rehabilitation*, 91(11), 911–921.
- Farris, R. J., Quintero, H. A., and Goldfarb, M. (2012). Performance evaluation of a lower limb exoskeleton for stair ascent and descent with Paraplegia. In *2012 Annual International Conference of the IEEE Engineering in Medicine and Biology Society* (pp. 1908–1911). IEEE.
- Fontana, M., Vertechy, R., Marcheschi, S., Salsedo, F., and Bergamasco, M. (2014). The body extender: A full-body exoskeleton for the transport and handling of heavy loads. *IEEE Robotics & Automation Magazine*, 21(4), 34–44.
- Gálvez-Zúñiga, M., and Aceves-López, A. (2016). A review on compliant joint mechanisms for lower limb exoskeletons. *Journal of Robotics*, 2016(Article ID 5751391), 9.
- Ghoussayni, S., Stevens, C., Durham, S., and Ewins, D. (2004). Assessment and validation of a simple automated method for the detection of gait events and intervals. *Gait & Posture*, 20(3), 266–272.
- Government Publishing Office. (2015). Federal Register Volume 80, Number 36. Retrieved February 1, 2016, from <http://www.gpo.gov/fdsys/pkg/FR-2015-02-24/html/2015-03692.htm>
- Grosu, V., Guerrero, C. R., Brackx, B., Grosu, S., Vanderborght, B., and Lefeber, D. (2015). Instrumenting complex exoskeletons for improved human-robot interaction. *Instrumentation & Measurement Magazine, IEEE*, (October), 5–10.
- He, H., and Kiguchi, K. (2007). A study on EMG-based control of exoskeleton robots for human lower-limb motion assist. In *2007 6th International Special Topic*

- Conference on Information Technology Applications in Biomedicine* (pp. 292–295). IEEE.
- Hoffmann, F. (2001). Evolutionary algorithms for fuzzy control system design. *Proceedings of the IEEE*, 89(9), 1318–1333.
- Hogan, N. (1985). Impedance control: An approach to manipulation: Part II—implementation. *Journal of Dynamic Systems, Measurement, and Control*, 107(1), 8.
- Hsu, J. D., Michael, J., and Fisk, J. (2008). *AAOS Atlas of orthoses and assistive devices* (4th ed.). Elsevier Health Sciences.
- Jansen, J. F. (2000). *Exoskeleton for soldier enhancement systems feasibility study*. United States. <https://doi.org/10.2172/885757>
- Jezernik, S., Colombo, G., Keller, T., Frueh, H., and Morari, M. (2003). Robotic orthosis lokomat: a rehabilitation and research tool. *Neuromodulation: Technology at the Neural Interface*, 6(2), 108–115.
- Karlin, S. (2011). Raiding Iron Man’s closet [Geek Life]. *IEEE Spectrum*, 48(8), 25.
- Kawamoto, H., Hayashi, T., Sakurai, T., Eguchi, K., and Sankai, Y. (2009). Development of single leg version of HAL for hemiplegia. *Proceedings of the 31st Annual International Conference of the IEEE Engineering in Medicine and Biology Society: Engineering the Future of Biomedicine, EMBC 2009, 2009*, 5038–5043.
- Kawamoto, H., Kandone, H., Sakurai, T., Ariyasu, R., Ueno, Y., Eguchi, K., and Sankai, Y. (2014). Development of an assist controller with robot suit HAL for hemiplegic patients using motion data on the unaffected side. *36th Annual International Conference of the IEEE Engineering in Medicine and Biology Society*, 3077–3080.
- Kazerooni, H. (2006). The Berkeley lower extremity exoskeleton project. *Experimental Robotics IX. Springer Tracts in Advanced Robotics*, 21, 291–301.
- Kerr, K. M., White, J. A., Barr, D. A., and Mollan, R. A. B. (1997). Analysis of the sit-stand-sit movement cycle in normal subjects. *Clinical Biomechanics*, 12(4), 236–245.

- Kerr, K., White, J., Barr, D., and Mollan, R. (1994). Standardization and definitions of the sit-stand-sit movement cycle. *Gait and Posture*, 2(3), 182–190.
- Kirtley, C. (2005). Normative gait database. Retrieved October 20, 2015, from <http://www.clinicalgaitanalysis.com>
- Kong, K., and Jeon, D. (2006). Design and control of an exoskeleton for the elderly and patients. *IEEE/ASME Transactions on Mechatronics*, 11(4), 428–432.
- Kopp, C. (2011). Exoskeletons for warriors of the future. *Defence Today*, 9(2), 38–40.
- Kralj, A. R., and Bajd, T. (1989). *Functional electrical stimulation: standing and walking after spinal cord injury*. CRC press.
- Kralj, Jaeger, R. J., and Munih, M. (1990). Analysis of standing up and sitting down in humans: Definitions and normative data presentation. *Journal of Biomechanics*, 23(11), 1123–1138.
- Kranzl, M. A., and Kopf, D. A. (1997). 65 year old man with hemiplegia, right side. Retrieved from <http://www.clinicalgaitanalysis.com>
- Kuan, T.-S., Tsou, J.-Y., and Su, F.-C. (1999). Hemiplegic gait of stroke patients: The effect of using a cane. *Archives of Physical Medicine and Rehabilitation*, 80(7), 777–784.
- Laporte, D. M., Chan, D., and Sveistrup, H. (1999). Rising from sitting in elderly people, Part 1: Implications of biomechanics and physiology. *British Journal of Occupational Therapy*, 62(1), 36–42.
- Lawson, B. E., Shultz, A. H., and Goldfarb, M. (2013). Evaluation of a coordinated control system for a pair of powered transfemoral prostheses. In *2013 IEEE International Conference on Robotics and Automation* (pp. 3888–3893). IEEE.
- Li, N., Yan, L., Qian, H., and Wu, H. (2015). Review on lower extremity exoskeleton robot. *The Open Automation and Control Systems Journal*, 441–453.
- Low, K. H. (2011). Robot-assisted gait rehabilitation: From exoskeletons to gait systems. In *Defense Science Research Conference and Expo (DSR), 2011* (pp. 1–10). Singapore: IEEE.
- Luu, T. P., Low, K. H., Qu, X., Lim, H. B., and Hoon, K. H. (2014). Hardware development and locomotion control strategy for an over-ground gait trainer: NaTure-Gaits. *IEEE Journal of Translational Engineering in Health and Medicine*, 2, 1–9.

- Mackenzie, B. (2004). Range of movement (ROM). Retrieved April 21, 2016, from <http://www.brianmac.co.uk/musrom.htm>
- Maeshima, S., Osawa, A., Nishio, D., Hirano, Y., Takeda, K., Kigawa, H., and Sankai, Y. (2011). Efficacy of a hybrid assistive limb in post-stroke hemiplegic patients: a preliminary report. *BMC Neurology*, *11*(1), 1–6.
- Mamdani, E. H., and Assilian, S. (1975). An experiment in linguistic synthesis with a fuzzy logic controller. *International Journal of Man-Machine Studies*, *7*(1), 1–13.
- Marinov, B. (2016). 2015 Year in review: Exoskeletons and wearable robotics. Retrieved October 9, 2018, from <http://exoskeletonreport.com/2016/01/2015-year-in-review-exoskeletons-and-wearable-robotics/>
- Mauritz, K.-H. (2002). Gait training in hemiplegia. *European Journal of Neurology*, *9 Suppl 1*, 23–29; dicussion 53-61.
- Mertz, L. (2012). The next generation of exoskeletons: Lighter, cheaper devices are in the works. *IEEE Pulse*, *3*(4), 56–61.
- Moore, K. L., and Dalley, A. F. (1999). *Clinically oriented anatomy*. Williams and Wilkins.
- MSC Software. (2003). MSC Visual Nastran 4D Desktop. Retrieved October 1, 2015, from <http://www.mssoftware.com/>
- MSC Software. (2004). integrated motion and stress analysis within Windows based 3D CAD systems. Retrieved October 1, 2015, from http://www.mssoftware.com/assets/3080_vn4d2004sepzzzldat.pdf
- Mudi, R. K., and Pal, N. R. (1999). A robust self-tuning scheme for PI- and PD-type fuzzy controllers. *IEEE Transactions on Fuzzy Systems*, *7*(1), 2–16.
- Neuhaus, P. D., Noorden, J. H., Craig, T. J., Torres, T., Kirschbaum, J., and Pratt, J. E. (2011). Design and evaluation of Mina: A robotic orthosis for paraplegics. In *2011 IEEE International Conference on Rehabilitation Robotics* (pp. 1–8).
- Novak, D., and Riener, R. (2015). A survey of sensor fusion methods in wearable robotics. *Robotics and Autonomous Systems*, *73*, 155–170.
- Nuzik, S., Lamb, R., VanSant, A., and Hirt, S. (1986). Sit-to-Stand movement pattern: A kinematic study. *Physical Therapy*, *66*(11), 1708–1713.
- Ogata, K. (2010). *Modern control engineering* (Fifth). Pearson Education, Inc.

- Okamoto, T., and Okamoto, K. (2007). *Development of gait by electromyography : application of gait analysis and evaluation*. Walking Development Group.
- Olney, S. J., and Richards, C. (1996). Hemiparetic gait following stroke. Part I: Characteristics. *Gait & Posture*, 4(2), 136–148.
- Önen, Ü., Botsalı, F. M., Kalyoncu, M., Tınkır, M., Yılmaz, N., and Şahin, Y. (2014). Design and actuator selection of a lower extremity exoskeleton. *IEEE/ASME Transactions on Mechatronics*, 19(2), 623–632.
- Passino, K. M., and Yurkovich, S. (1998). *Fuzzy Control*. California: Addison Wesley Longman, Inc.
- Physiopedia. (2016). Gait. Retrieved December 2, 2016, from <https://www.physiopedia.com/index.php?title=Gait&oldid=203095>
- Pngkey. (2018). Conventional method to treat a spinal cord injury - paraplegia quadriplegia and hemiplegia. Retrieved November 30, 2018, from <https://www.pngkey.com/>
- Polygerinos, P., Correll, N., Morin, S. A., Mosadegh, B., Onal, C. D., Petersen, K., Cianchetti, M., Tolley, M. T., and Shepherd, R. F. (2017). Soft robotics: review of fluid-driven intrinsically soft devices; manufacturing, sensing, control, and applications in human-robot interaction. *Advanced Engineering Materials*, 19(12).
- Pons, J. L. (2008). *Wearable Robots: Biomechatronic exoskeletons*. *Wearable Robots: Biomechatronic Exoskeletons*.
- Quinlivan, B. T., Lee, S., Malcolm, P., Rossi, D. M., Grimmer, M., Siviyy, C., Karavas, N., Wagner, D., Asbeck, A., Galiana, I., and Walsh, C. J. (2017). Assistance magnitude versus metabolic cost reductions for a tethered multiarticular soft exosuit. *Science Robotics*, 2(2).
- Rewalk, R. (2016). Rewalk robotics. Retrieved March 1, 2016, from <http://rewalk.com>
- RexBionics. (2011). Rex Bionics. Retrieved March 1, 2016, from <http://www.rexbionics.com>
- Ross, T. J. (2010). *Fuzzy logic with engineering applications* (3rd ed.). John Wiley & Sons.
- Rovekamp, R. N., Francisco, G. E., Chang, S.-H., and Beck, C. E. (2017). Wearable robotic approaches to lower extremity gait systems. In V. Tepe & C. M. Peterson (Eds.),

Full Stride: Advancing the State of the Art in Lower Extremity Gait Systems (pp. 75–97). New York, NY: Springer New York.

- Sahin, Y., Botsal, F. M., Kalyoncu, M., Tinkir, M., Önen, Ü., Lmaz, N., and Çakan, A. (2014). Mechanical design of lower extremity exoskeleton assisting walking of load carrying human. In *Advanced Materials, Mechanics and Industrial Engineering* (Vol. 598, pp. 141–145). Trans Tech Publications.
- Salzman, B. (2010). Gait and balance disorders in older adults. *American Family Physician*, 82(1), 61—68.
- Sankai, Y. (2010). HAL: hybrid assistive limb based on cybernics. *Springer Tracts in Advanced Robotics*, 66(STAR), 25–34.
- Sanz-Merodio, D., Cestari, M., Arevalo, J. C., and Garcia, E. (2012). Control motion approach of a lower limb orthosis to reduce energy consumption. *International Journal of Advanced Robotic Systems*, 9, 1–8.
- Schenkman, M., Berger, R. A., Riley, P. O., Mann, R. W., and Hodge, W. A. (1990). Whole-Body movements during rising to standing from sitting. *Physical Therapy*, 70(10), 638–648.
- Sg robotics. (2017). WalkON Suit. Retrieved April 10, 2018, from <http://sg-robotics.com/en/walkon-suit/>
- Shaari, N. L. A., Md Isa, I. S., and Jun, T. C. (2015). Torque analysis of the lower limb exoskeleton robot design. *ARPN Journal of Engineering and Applied Sciences*, 10(19), 9140–9149.
- Sinha, R., Paredis, C. J. J., Liang, V.-C., and Khosla, P. K. (2000). Modeling and simulation methods for design of engineering systems. *Journal of Computing and Information Science in Engineering*, 1(1), 84–91.
- Spinalcord. (2017). Types of Paralysis. Retrieved April 12, 2017, from <https://www.spinalcord.com/types-of-paralysis>
- Stratasys. (2016). GrabCAD. Retrieved February 1, 2016, from <https://grabcad.com/library>
- Strausser, K. a., and Kazerooni, H. (2011). The development and testing of a human machine interface for a mobile medical exoskeleton. *2011 IEEE/RSJ International Conference on Intelligent Robots and Systems*, 4911–4916.

- Sugar, T., Veneman, J., Hochberg, C., Shourijeh, M., Acosta, A., Vazquez-Torres, R., Marinov, B., and Nabeshima, C. (2018). Hip exoskeleton market - review of lift assist wearables [white paper]. Retrieved April 12, 2018, from <http://www.wearablerobotics.com/industry-news-education/>
- Sung, S. W., Lee, J., and Lee, I. (2009). *Process identification and PID control*. John Wiley & Sons (Asia) Pte Ltd.
- Takagi, T., and Sugeno, M. (1985). Fuzzy identification of systems and its applications to modeling and control. *IEEE Transactions on Systems, Man, and Cybernetics, SMC-15*(1), 116–132.
- Tamura, K., and Yasuda, K. (2011a). Spiral dynamics inspired optimization. *Journal of Advanced Computational Intelligence and Intelligent Informatics, 15*(8), 1116–1122.
- Tamura, K., and Yasuda, K. (2011b). Spiral multipoint search for global optimization. In *2011 10th International Conference on Machine Learning and Applications and Workshops* (Vol. 1, pp. 470–475).
- Tamura, K., and Yasuda, K. (2011c). Spiral optimization -A new multipoint search method. In *2011 IEEE International Conference on Systems, Man, and Cybernetics* (pp. 1759–1764).
- Tao, W., Liu, T., Zheng, R., and Feng, H. (2012). Gait analysis using wearable sensors. *Sensors*.
- Tran, H. T., Cheng, H., Rui, H., Lin, X., Duong, M. K., and Chen, Q. (2016). Evaluation of a fuzzy-based impedance control strategy on a powered lower exoskeleton. *International Journal of Social Robotics, 8*(1), 103–123.
- Tsukahara, A., Kawanishi, R., Hasegawa, Y., and Sankai, Y. (2010). Sit-to-Stand and Stand-to-Sit Transfer Support for Complete Paraplegic Patients with Robot Suit HAL. *Advanced Robotics, 24*(11), 1615–1638.
- Tucker, M. R., Olivier, J., Pagel, A., Bleuler, H., Bouri, M., Lamercy, O., Millán, J. del R., Riener, R., Vallery, H., and Gassert, R. (2015). Control strategies for active lower extremity prosthetics and orthotics: a review. *Journal of NeuroEngineering and Rehabilitation, 12*(1), 1–30.

- Vaughan, C. L., Davis, B. L., and O'Connor, J. C. (1999). *Dynamics of human gait* (second). Kiboho.
- Veale, A. J., and Xie, S. Q. (2016). Towards compliant and wearable robotic orthoses: A review of current and emerging actuator technologies. *Medical Engineering and Physics*, 38(4), 317–325.
- Viteckova, S., Kutilek, P., de Boisboissel, G., Krupicka, R., Galajdova, A., Kauler, J., Lhotska, L., and Szabo, Z. (2018). Empowering lower limbs exoskeletons: state-of-the-art. *Robotica*, 1–14.
- Viteckova, S., Kutilek, P., and Jirina, M. (2013). Wearable lower limb robotics: A review. *Biocybernetics and Biomedical Engineering*, 33(2), 96–105.
- Wang, L.-. (1993). Stable adaptive fuzzy control of nonlinear systems. *IEEE Transactions on Fuzzy Systems*, 1(2), 146–155.
- Wang, L.-. (1997). *A course in fuzzy systems and control*. Prentice-Hall International, Inc.
- Webber, S. C., Porter, M. M., and Menec, V. H. (2010). Mobility in older adults: A comprehensive framework. *The Gerontologist*, 50(4), 443–450.
- Wehner, M., Quinlivan, B., Aubin, P. M., Martinez-Villalpando, E., Baumann, M., Stirling, L., Holt, K., Wood, R., and Walsh, C. (2013). A lightweight soft exosuit for gait assistance. In *2013 IEEE International Conference on Robotics and Automation* (pp. 3362–3369).
- Whittle, M. W. (1996). Clinical gait analysis: A review. *Human Movement Science*, 15(3), 369–387.
- Winter, D. A. (2009). *Biomechanics and motor control of human movement*. Hoboken, N.J. : Wiley, c2009.
- Woolley, S. M. (2001). Characteristics of gait in hemiplegia. *Topics in Stroke Rehabilitation*, 7(4), 1–18.
- World Health Organization. (2013). Spinal cord injury. Retrieved from <http://www.who.int/mediacentre/factsheets/fs384/en/>
- Wyss Institute. (2017). Soft exosuit economies: understanding the costs of lightening the load. Retrieved March 14, 2018, from <https://wyss.harvard.edu/soft-exosuit-economies-understanding-the-costs-of-lightening-the-load/>

- Yan, T., Cempini, M., Oddo, C. M., and Vitiello, N. (2015). Review of assistive strategies in powered lower-limb orthoses and exoskeletons. *Robotics and Autonomous Systems*, 64(JANUARY), 120–136.
- Yang, C.-J., Zhang, J.-F., Chen, Y., Dong, Y.-M., and Zhang, Y. (2008). A review of exoskeleton-type systems and their key technologies. *Proceedings of the Institution of Mechanical Engineers, Part C: Journal of Mechanical Engineering Science*, 222(8), 1599–1612.
- Ying, H. (2000). *Fuzzy control and modeling: Analytical foundations and applications* (1st ed.). Wiley-IEEE Press.
- Young, A. J., and Ferris, D. P. (2017). State of the art and future directions for lower limb robotic exoskeletons. *IEEE Transactions on Neural Systems and Rehabilitation Engineering*, 25(2), 171–182.
- Zadeh, L. A. (1965). Fuzzy sets. *Information and Control*, 8(3), 338–353.
- Zang, H., Zhang, S., and Hapeshi, K. (2010). A review of nature-inspired algorithms. *Journal of Bionic Engineering*, 7(4), S232–S237.
- Zoss, A., and Kazerooni, H. (2006). Design of an electrically actuated lower extremity exoskeleton. *Advanced Robotics*, 20(9), 967–988.
- Zoss, A., Kazerooni, H., and Chu, A. (2006). Biomechanical design of the berkeley lower extremity exoskeleton (BLEEX). *IEEE/ASME Transactions on Mechatronics*, 11(2), 128–138.
- ZurichETH. (2016). Cybathlon 2016. Retrieved April 1, 2018, from <http://www.cybathlon.ethz.ch/cybathlon-2016.html>